Balder Beamline

MAX IV beamline review report

The Balder beamline team

Kajsa Sigfridsson Clauss, Konstantin Klementiev, Justus Just,
Susan Nehzati, Mahesh Ramakrishnan, Dörthe Haase, Stefan Carlson, Stuart Ansell

2023-11-16

Table of content

1 General introduction

The Balder beamline is dedicated to X-ray absorption and emission spectroscopy in the medium to hard X-ray energy range (2.4 to 40 keV) and is located at the 3 GeV ring. This is the only spectroscopy beamline in the hard X-ray energy range at MAX IV, while several soft X-ray spectroscopy beamlines exist. A wiggler insertion device is the source for Balder's broad energy range and fast energy scanning characteristics, thus allowing the probing of the chemistry of all elements from Sulphur to heavier atomic number elements in the periodic table. Hard X-rays offer the possibilities to measure samples under realistic conditions, i.e. no need for *in vacuo* sample environment, ample space for specialized sample environments to follow reactions (in situ/operando) or to measure natural unmodified samples. This defines the two user communities Balder was specially designed to cater for: operando catalysis, and "natural" samples in the bio/geo/environmental area.

X-ray absorption spectroscopy (XAS) is the main technique at Balder with steady user operation since fall 2019. With XAS the X-ray absorption coefficient μ(E) is measured as a function of the incident X-ray energy. The information is element- and orbital-specific, and provides information on the local atomic and electronic structure of the element of interest. Two regions of the XAS spectrum are analyzed separately; X-ray Absorption Near Edge Structure (XANES) ~100 eV around the absorption edge providing information about the absorbing atom, and Extended X-ray Absorption Fine Structure (EXAFS) from 50 to 1000 eV above the edge providing information about the neighboring atoms (i.e. the local structure surrounding the absorbing atom). Users especially appreciate the ability to quickly change edges several thousands of eV apart, making it suitable for multi-element materials. Another beamline strength and design goal were to have a stable intense beam to quickly measure high *k* EXAFS (better resolved local structure) with sub-second time resolution. The resolution of XANES is achieved with two sets of DCM crystals that are of excellent quality together with source properties and the collimating mirror.

X-ray emission spectroscopy (XES) is the second main technique of Balder open for user operation since spring 2023. XES is a photon-in/photon-out spectroscopic technique, where both the incoming X-rays from the monochomator and the emitted X-rays detected by the spectrometer crystals are resolved using perfect crystal Bragg optics. XES gives access to information about the electronic structure from the occupied states and can be non-, as well as resonantly (RXES), excited. The spectrometer can also be used as a high energy resolved fluorescence detector for XAS (HERFD-XAS). The Balder emission spectrometer, SCANIA-2D, is conceptionally designed by K. Klementiev and functions in backscattering mode with three large Johansson crystals active for the same energy on a 1.5 m Rowland circle geometry with a 2D detector and sample. This geometry makes the spectrometer compatible with almost any sample environment. The commissioning time has been long due to limited time to focus on XES with a full user operation program running. The spectrometer is continuously being improved to develop it to its full capacity.

As secondary techniques, to be combined with XAS/XES, Balder offers X-ray diffraction (XRD) and X-ray fluorescence (XRF) for almost simultaneous measurements. The implementation of a 2D detector for XRD was initially financed by Chalmers in order to boost the capacity for the in situ/operand catalytic studies. Today it is a popular complementary technique to additionally follow the development of the crystalline structures. This capability, together with our newly implemented hardware based sub-sec scanning of EXAFS producing highest quality data, makes Balder superior in operando research.

For inhomogeneous samples, our solid-state detectors can be used for XRF detection in combination with the focused beam spot (50-100 micrometers) to offer elemental 2D mapping of larger areas, fitting, for example, the rings of a tree and the varve of lake sediments. Importantly we are developing the possibility to do fast and efficient XANES mapping to probe the speciation of a selected element.

User needs, grants and collaborations have driven developments of specialized sample environments in many research fields, for example, the SSF financed AdaptoCell and in-FORM projects, dome cell for catalytic surface

studies, liquid jet (*in kind* contribution Uppsala University), and several user defined electrochemistry and battery cells and more. The beamline staff are often part of, driving, or supporting, these developments.

Balder's broad user community covers many areas like energy materials, catalysis, environmental sciences, life sciences and many more. To get awarded beamtime the proposal must be very competitive. Numerous proposals to the beamline are of high quality (accepted average grade 4.4 of 5) resulting in a high oversubscription factor (3.6 average for every year of operation). However, measurements of standard samples can be very quick. In order to increase user accessibility, productivity, and guarantee highest quality of the experiments and publications, we have introduced a fast access mode since 2022 (feasibility test and standard measurement service).

To finalize the scope of the Balder project, we will focus our next steps on delivering down to Sulphur K-edge to users. Today Balder is offering X-ray energies down to 4 keV corresponding to Calcium K-edge.

2 Technical description

2.1 Beamline design

This section explains the rationale for the main beamline elements, see Figure 1, their main features and performance figures.

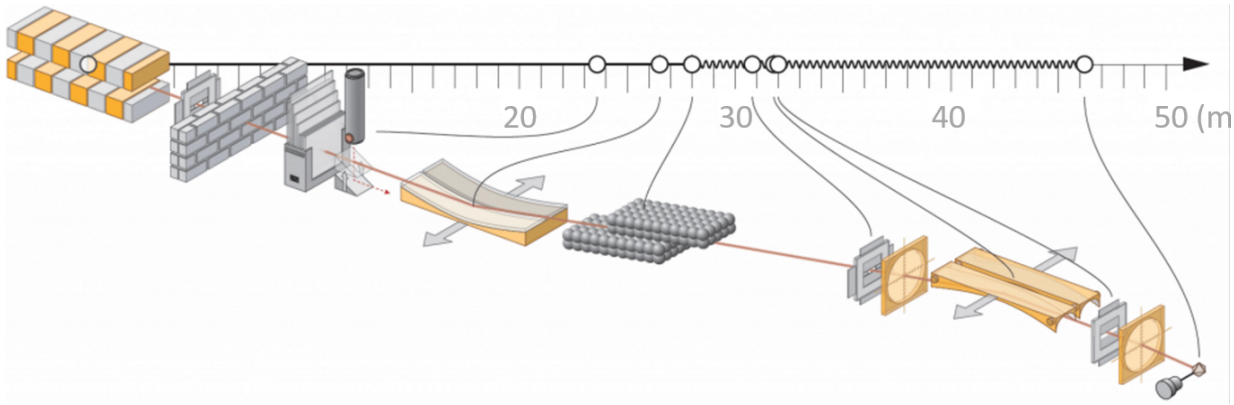

Figure 1. Balder beamline layout. Elements from left to right: in vacuum Wiggler, Front end mask, wall of the ring building, low energy filters, insertable alignment laser, collimating mirror (VCM), double crystal monochromator (DCM), slits, fluorescent screen, vertical focusing mirror (VFM), slits, fluorescent screen, sample.

Insertion Device

It was known from several older XAFS beamlines that high quality EXAFS spectra could be measured in about 15 min with a monochromatic flux of $10^9 – 10^{10}$ ph/s. Therefore, purely based on statistics, one could measure EXAFS within one second with a flux $10^{12} – 10^{13}$ ph/s. The prospect of one second EXAFS became the main driving argument in the beamline design. However, there exists a quandary - on the one hand, the required high flux value excludes a bending magnet or a few-pole wiggler as a possible source type; on the other hand, the high scanning speed of ~1 keV/s advocates for a broad band source – a wiggler, thus excluding an undulator.

The Balder's IVW50 wiggler was built at Soleil, see Figure 2, and is an updated version of their previous wiggler with an added extra possibility of gap tapering. This is a 2m-long device with 2.4 T magnetic field at the formal minimum gap 4.2 mm.[1] The operationally reached minimum value is 4.7 mm.

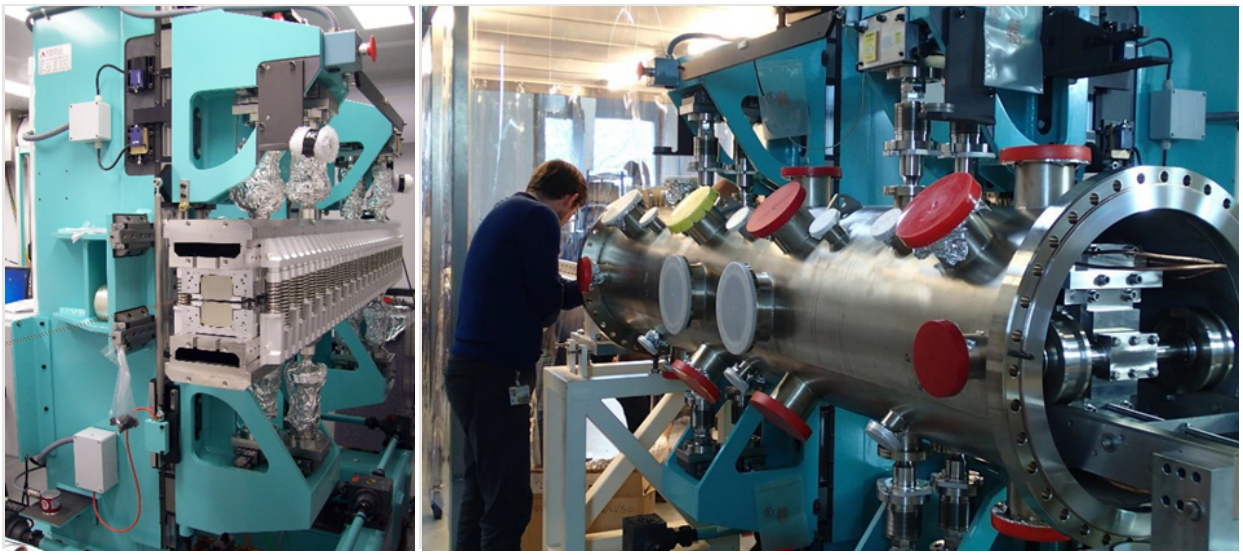

Figure 2. Balder's wiggler during manufacturing at the Soleil synchrotron in 2015–2016. Left: the assembled girders ready for magnetic measurements. Right: insertion of the girders into the ID vacuum chamber.

Earlier computational studies[2] showed that at low energies the wiggler spectrum has well separated undulator harmonics. At higher energies, the interference effects become weaker and the spectrum eventually becomes smooth and similar to that of a bending magnet. It was believed at the beamline design time that introducing a large enough magnetic gap taper would introduce sufficient smoothing to the low energy end of the spectrum. Unfortunately, the effect of taper is not so simple and it even creates some detrimental beating effect that increases in amplitude at large taper values. In our recent paper[3] we systematically studied various factors affecting the ripple amplitude and its effect on the quality of EXAFS spectra. In addition to taper, undulator ripples in the wiggler spectrum also depend on the electron beam inclination, see Figure 3. The nature of the intensity ripples can be understood by examining the transverse intensity distribution through the incoming aperture of the beamline, see Figure 4. This distribution is non-uniform and has a periodic energy dependence. One important conclusion from that paper is that the ripples do not significantly spoil the EXAFS for reasonably good (homogenous) samples. A second important conclusion is that the spectrum can be completely smoothed by introducing large enough magnetic errors at the assembly time and thus be better suited also for bad (non-uniform) samples. Our wiggler was built too perfectly for its purpose and in a possible future project we can probably downgrade its magnetic uniformity.

[1] doi.org/10.1063/1.5084590

[2] Walker, R. (2003). In Undulators, Wigglers and Their Applications, edited by H. Onuki & P. Elleaume. Taylor & Francis

[3] doi.org/10.1107/S1600577521012844

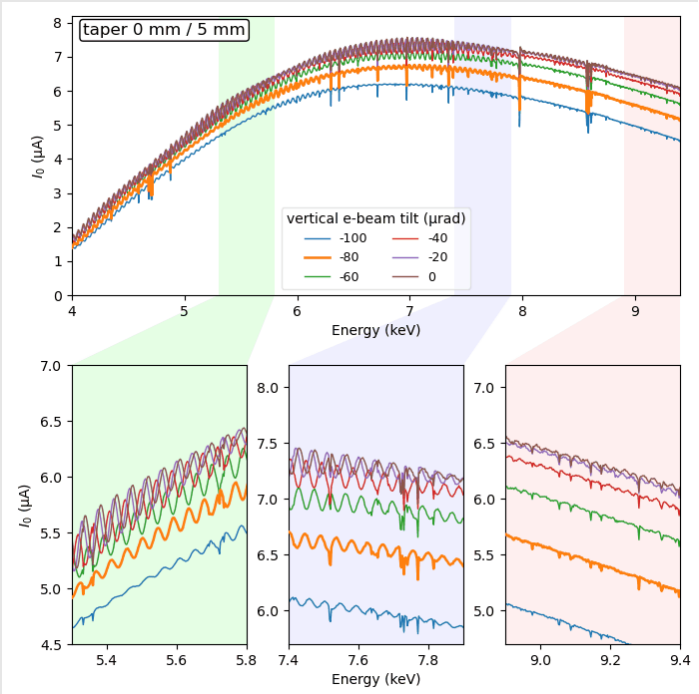

Figure 3. (animated in Wiggler-taperExp-ani.gif) Experimental wiggler spectra measured as intensity upstream of the sample (I0) during quick energy scans at various e-beam inclination and taper values of the magnetic gap. The typical operational inclination value is −80 µrad, shown by a thicker orange line.

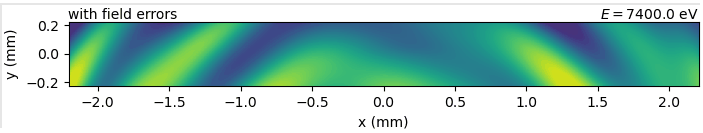

Figure 4. (animated in Wiggler-transverseWithErrors-ani.gif) Calculated transverse intensity distribution at the front-end movable mask at ca. 18 m from the source. The e-beam was tilted by −80 µrad (typical operational tilt) and the taper was set to 0.25 mm (typical operational taper). The field of view corresponds to 250h × 25v µrad². Energy is monochromatic and scanning over one ripple period of 45.6 eV.

In our user operation at energies below ~8 keV, we vary the electron beam inclination by contacting the MAX IV control room. When the beam is inclined away from the nominal storage ring plane, the spectrum ripples become weaker at the expense of flux and focus size, although the flux loss can typically be minimized, see section Front End.

Front End

The standard front end devices are the fixed and movable masks, heat absorber, safety shutter and vacuum equipment. When inclining the beam we rely on the storage ring BPMs (beam position monitors), without direct measurements of our X-ray beam, since the two dedicated X-ray BPMs are unreliable. It is possible to upgrade the existing X-ray BPMs (a prototype is ready) thus making the inclination measurements verified and calibrated. The upgrade will be manageable after the BPM commissioning at two other beamlines at MAX IV.

The maximum front end acceptance was designed to be 400h × 100v µrad². Our most typical movable mask opening is ~max/2 in horizontal and max/4 in vertical, which yields ~$2 \cdot 10^{12}$ ph/s at 9 keV. The two main practical reasons for reducing the flux are (1) a longer lifetime for the Kapton windows of I_0 ionization chamber and the exit window of the flight tube close to the sample and (2) a better level of linearity of I_0 and I_t ionization chambers. During XES sessions, acceptance is usually increased.

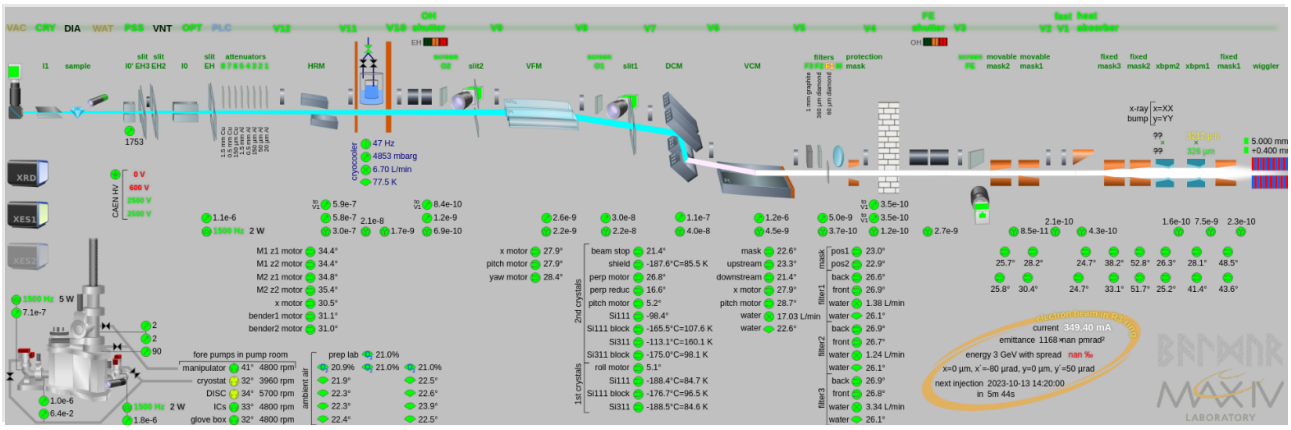

Figure 5. Balder Synoptic application showing the status of R3 storage ring and various beamline systems. The beam propagates from right to left, first as a polychromatic (so called white) beam up to the VCM, as a low-pass filtered (so called pink) beam up to the DCM and then as a monochromatic beam down to the sample.

X-ray Optics

The optical scheme of Balder, see Figure 5, comprises a flat-bent VCM (Vertically Collimating Mirror), a fixed-exit DCM (Double Crystal Monochromator) with two pairs of flat Si111 and Si311 crystals and a VFM (Vertically deflecting Focusing Mirror) consisting of two cylinder-bent mirrors mounted in a single bender. The VFM focalizes in 2:1 ratio, which helps minimize a few important aberrations. This scheme was first proposed at ALS[4] and since then has been implemented at many beamlines worldwide, becoming a standard design for hard X-ray beamlines that perform energy scanning. Other alternative schemes were considered in that paper, including a sagittal focusing second crystal, with the conclusion that the mirror-focused solution offers greater simplicity and robustness.

While the adopted optical scheme is quite standard, the solutions for mirror coatings and possible additional HRM (Harmonic Rejecting Mirror) can vary depending on the required energy range and the available optical adjustments. Having in mind that both Si111 and Si311 do not reflect in the second order (reflectivity ~10^{-30}), the required cut-off energy should lie below the *triple* value of working energy. There exist solutions with three coating materials that cut off the third harmonic for each working energy in the range $2.3 < E < 50$ keV[5]. However, those solutions require a variable pitch angle in a large range and, correspondingly, a large variation in the height of all beamline elements starting from VFM. We have proposed and implemented a solution with (1) only two mirror materials: (a) bare silicon or glass and (b) platinum coating, (2) a fixed exit beam height at VFM that is achieved by adjusting the DCM fixed exit as a function of the mirror angle, see Figure 6, and (3) a possibility to keep the mirror pitch angle fixed when changing between the VFM toroids if no horizontal defocusing is required. The latter feature allows us to minimize the need to realign the beamline and is achieved by having two VFM toroids (uncoated and Pt-coated) equal in shape. There are certain disadvantages in this solution: (1) the pitch angles are relatively small, which restricts the vertical acceptance for reasonably long VCM and VFM (and which defines the 100 µrad front end acceptance), (2) the DCM fixed-exit offset has a slightly larger range than usual and (3) the energy range $2.3 < E < 5$ keV requires an additional pair of HRMs because the cut-off energy of bare silicon/glass is too high for this energy range, see Figure 7,

[4] doi.org/10.1107/S0909049504024835

[5] doi.org/10.1080/23311940.2016.1231987

allowing the third harmonic to be reflected by VCM and VFM. These drawbacks are considered minor as compared to the offered benefits.

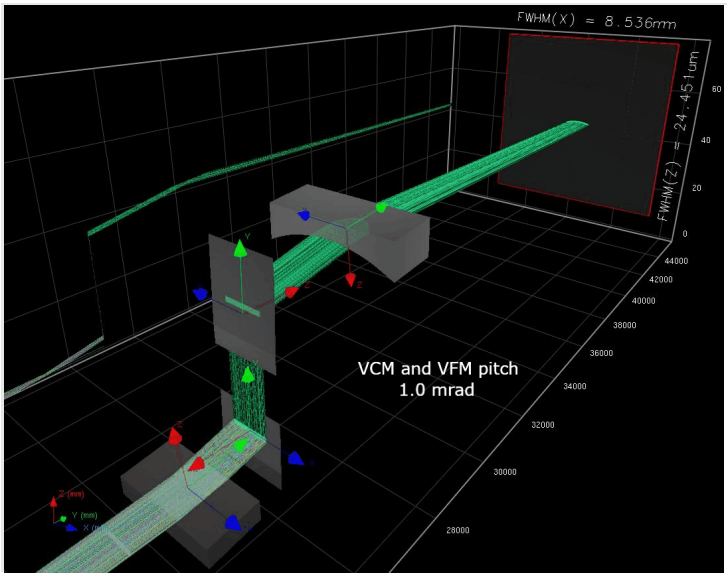

Figure 6. (animated in Mirror-pitch-ani.gif) The functioning of fixed-exit concept relative to the second (focusing) mirror demonstrated at varying pitch angle from 1 to 3 mrad. The vertically moving gray plates are two DCM crystals; they look vertical due to a strongly anisotropic scaling of the scene, with a very strong compression along the beamline. The propagated beams are side projected onto the wall for better visibility of the variable beam kick at the DCM. In this simulation, the sagittal radius of the focusing toroid mirror is optimal at 2 mrad pitch angle.

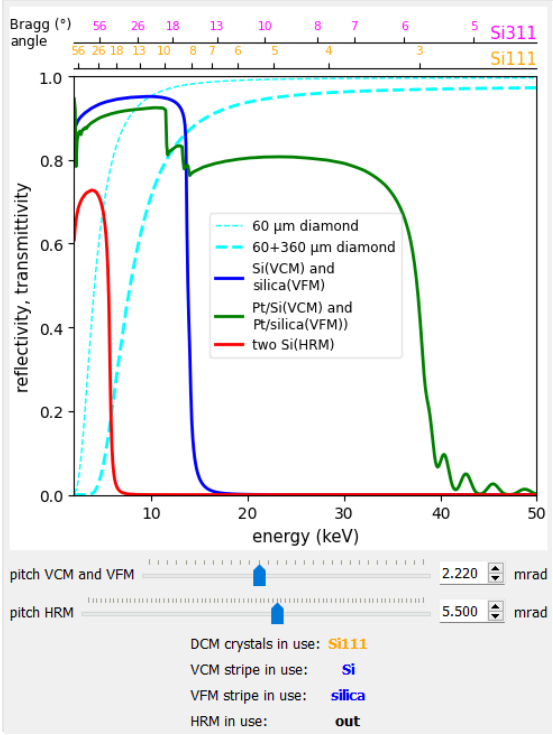

Figure 7. Reflectivity of mirrors at certain incidence angles and transmittivity of filters. This widget is a part of the Balder's user interface and helps the user decide on the required optical settings.

Heat Load and Cooling

The total generated power in the wiggler radiation is about 18 kW. Most of it is absorbed by several front end masks. The beamline optics receive 1 kW of power that is distributed among three devices: 1) up to 3 water-cooled diamond and carbon filters of different thickness, 2) water-cooled VCM and 3) liquid-nitrogen-cooled DCM. The cooling of VCM is done by means of deep grooves carved in the mirror along its two sides and filled with a liquid metal. Two metal fins brazed to water cooling pipes are inserted into the grooves. This cooling scheme provides an efficient thermal contact without applying any force to the mirror. It also defines the orientation of the first mirror as reflecting upward.

Liquid nitrogen cooling of the DCM is fairly robust and does not require much attention. One related vibrational effect is worth mentioning. When we scrutinize the focal beam position, we sporadically see some vertical beam movement by less than 1/10 of the spot size. In searching for the possible source of this motion, we have read the DCM Bragg angle encoder at high frequency and discovered a leading vibration band at 4 Hz. These oscillations had a beating character with a much longer envelope period of a minute scale. Because the liquid nitrogen cryo-lines induce some torque along the Bragg axis, we tried to modify the cryogen flow and pressure. It did influence the beating envelope but the carrying 4 Hz band was unchanged and present even when the flow was completely shut off at the cryo cooler! Only when the cryogen was drained from the lines, the 4 Hz band disappeared, which proves that this band does come from the cryogenic cooling. The present explanation for this effect is the following: the cryo-lines consist of two long coaxial bellows with insulating vacuum between them and a few distributed spacers that hold the inner bellows centered in the outer bellows. The bellows are flexible and therefore are easily vibrationally excited. The outer bellow has steel wire armoring and its friction damps all possible eigen oscillations. The inner one is free to move and all excitation sources, including cryo-stream, cavitation bubbling and cryogen boiling, excite all possible eigen modes, one of them being at 4 Hz. We have proposed to make new cryo-lines with the inner bellow in a tight ceramic sleeve that would damp the eigen modes. Finally, this effect is not strong but it seems to be the strongest remaining one that affects the beam spot stability. As we perfect Balder, we would like to remove this instability.

The cold parts inside our DCM are thermally insulated from the rest of the mechanics by PEEK parts. Additionally, FMB-Oxford implemented heating pads in four places: two at the crystal cages and two at the brackets holding the cryo-lines. We discovered that these heating pads affected the beam stability and have never used them since 2019. As a result, some motors get chilled down to 5–10°C, which is still far from their specified -30°C freezing point. We do not see any long term drift associated with the absent thermal stabilization.

Optional Second Monochromator

The optical scheme has a reserved 1-m-long space after the DCM for a possible second monochromator. This could possibly be a quick scanning monochromator, a high-resolution monochromator or something else. A real need for a second device is presently not identifiable. In the original application was a QEXAFS monochromator of “Frahm-type” suggested, a channel cut mono with cam-driven rotation mechanism that would enable resolution down to 12.5 ms, exists at SOLEIL and SLS. However, the continuous scan performance of the Balder DCM (down to 2 Hz EXAFS, 2.1.1) is currently satisfying the user needs.

Vacuum System

Balder is a windowless beamline down to the entrance window of I_0 ionization chamber in the Experimental Hutch. As a safety measure for protecting the storage ring vacuum, Balder has a fast-acting valve in the front end with four feeding pressure gauges: two right after the ratchet wall of the storage ring, one at the end of the Optics Hutch and one at the entrance to the Experimental Hutch. The last one triggered several unwanted storage ring dumps and was eventually disconnected from the fast-acting valve. The beamline was accidentally vented once up to VFM. As a counter measure we have implemented the automatic closure of the last vacuum valve upon the photon shutter closure. This solution has proven to be practical and reliable.

Radiation Safety

The fact that the deflection at the VCM and DCM is vertical, away from the storage ring orbit, makes the requirements for radiation shielding much easier as compared with the horizontal deflection. We did not have to implement tungsten collimators for the white and the monochromatic beams that would put certain

restrictions on alignment procedures. Our Bremsstrahlung radiation shield is simply a block of tungsten situated downstream of the DCM that we easily overcome with the monochromatic beam.

Balder has a monochromatic shutter at the end of the Optics Hutch to allow access to the Experimental Hutch. Thus the DCM is kept under the white beam illumination to maintain thermal stabilization.

Performance of the Optics

The energy resolution of Si111 DCM is close to the theoretically predicted value, as demonstrated in Figure 8. The resulting angular width transforms to 1.95 10^{-4} relative energy resolution as FWHM. The flux is also close to the expected value, and is user-selectable in a wide range, reaching a few units of 10^{13} ph/s at the sample.

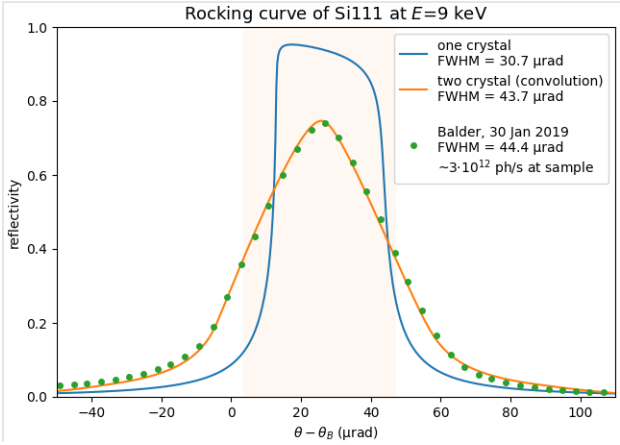

Figure 8. Rocking curve of Si111 DCM at 9 keV compared with calculated reflectivity curves. The storage ring current was ~250 mA (presently 400 mA, eventually 500 mA).

A typical focal spot is shown in Figure 9. Depending on the front end acceptance it can be made smaller or bigger. With two additional slits upstream of the focal position the beam can be slitted down ~10 µm. Defocusing vertically can be quickly done either by VFM unbending or by VFM yawing; the latter alternative is more frequently used in practice. Defocusing horizontally can also be done but requires detuning of the VCM and VFM pitch angles and adjusting the DCM fixed exit offset and, therefore, is done rarely.

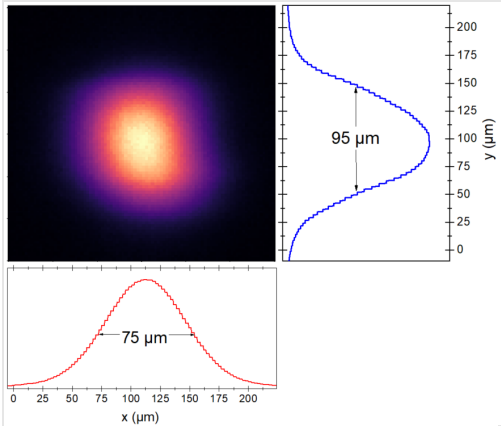

Figure 9. Typical focused beam as visualized by beam viewer – a normal incidence Ce-dopped YAG disk viewed by a macro camera.

2.1.1 Fixed-exit fast scanning monochromator

The purpose of the DCM is to select and transmit X-ray radiation of the desired photon energy from an incident white synchrotron beam. The monochromator employs 2 sets of crystal optics – Si111 and Si311

mounted side-by-side – to cover different energy ranges. To select between the crystal sets a translation of the whole DCM stage is provided. The desired energy is selected by rotating the crystal set, thereby varying the Bragg angle, whilst keeping the crystals parallel to one another. It is possible to translate the 2nd crystal relative to the 1st to achieve the fixed offset of the monochromatic beam with respect to the white beam. This requires a translation of the 2nd crystal in a direction perpendicular to its diffracting surface. The crystals are indirectly cooled via liquid nitrogen cooled copper plates.

Motion Control

The two axes, which are used for energy scanning (Bragg angle and perpendicular motion of the second crystal - x2perp) are driven by a high-precision and high-dynamic range dedicated motion control system (Figure 10). Motions are controlled by an EtherCAT master motion controller (ACS SPiiPlusEC) with a motion control update frequency of 5kHz. It (i) checks motion and provides necessary safety features, (ii) synchronizes the (slave) motion of the x2perp axis to the (master) motion of the Bragg axis for keeping a fixed exit height, (iii) implements arbitrary motion trajectories for energy scans and (iv) provides scan status information to the data acquisition system. A challenge for the control loop is the changing pre-load conditions due to the flexible cryogenic cooling lines. The implemented control loop therefore uses a proprietary observer based algorithm ServoboostTM to adapt the control parameters to the dynamic load conditions. The applied system achieves a control bandwith of 40 Hz and can, to some good extent (~70%), dampen the aforementioned 4Hz vibrations originating from the cryogenic lines. With fixed exit synchronized motion of the two axes, several motion trajectories can be executed up to an energy scan repetition frequency of 2 Hz. However, so far, linear (in angle) motion profiles with scan times down to 10s are given as standard to users.

As an upgrade, quicker scans, up to 2 Hz repetition rate, proper EXAFS motion profiles (slowing down with *k*-weight) and special multimodal and multi-edge scans are currently in commissioning. To this extent, a motion sequence is compiled from different motion profiles for subsequent scanning of different absorption edges and X-ray diffraction acquisitions at fixed energies. This sequence is then executed in loops by the motion controller. More details can be found in the following chapter as well as in 2.2.5 (Multimodal in-situ XAS-XRD). These recently developed features have already been tested by a small number of user groups and are foreseen to become standardly available within the next operation cycle.

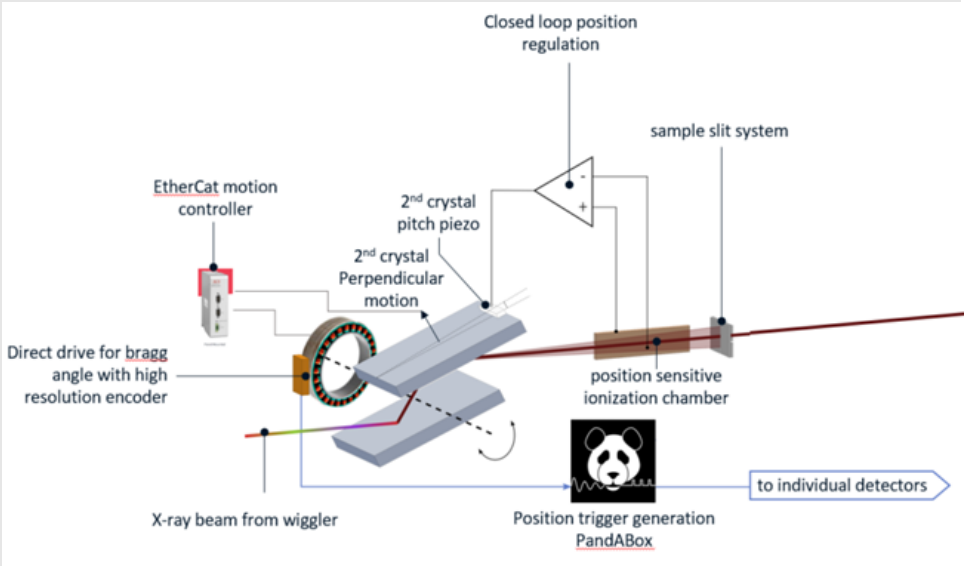

Figure 10. Overview schematics of main components used for quick energy scanning and data acquisition.

Closed loop beam-height regulation

For inhomogeneous samples and whilst using fine sample slit systems (as needed for combined XAS-XRD, flow cell and mapping experiments), it is of high importance that the beam position does not vary during energy scanning. Even with simultaneously driving the Bragg angle and the perpendicular translation of the second crystal, it is not possible to fix the beam position to less than 100 µm vertically during long energy scans. Considering the beam size of the focused beam of 100 µm vertical, we consider a beam stability of approximately ± 10 µm as sufficient.

To achieve the above accuracy, the beamline is equipped with a closed loop regulation of the beam height. The beam height is measured by a position sensitive ionization chamber (I_0) with two channels, see 2.2.1. The difference signal of these two channels is interpreted by a MoCo (Monochromator Controller) which essentially consists of an integrative control loop which controls a piezo drive to fine adjust the pitch angle of the 2nd monochromator crystal.

With this feedback loop we achieve a beam stability during energy scanning of several keVs of approximately ± 10 µm. While this regulation works excellently for slow scanning, we reach limitations with the recent developments of fast scanning capabilities for scans quicker than a couple of seconds. Additionally, we observe that fast beam vibrations, which are induced by the above discussed vibrations of the cryogenic monochromator cooling lines, cannot be reduced effectively with the current system. One aspect of further improving spectral quality, especially for non-homogenous samples, is therefore to improve this feedback loop.

2.1.2 Data acquisition system

The main design principles for the data acquisition system at Balder are: i) Detector based averaging is preferred over oversampling and software averaging and ii) the master of all data acquisition for energy scans is the energy axis position rather than time. Key components of the data acquisition system hardware are: 1) a high resolution incremental encoder, reading the Bragg axis position, 2) an FPGA based gate generation and distribution system (PandABox)[6] developed in a collaboration between SOLEIL and DIAMOND) and 3) the individual detectors.

For energy scans, data acquisition is realized as follows, see Figure 11. An arbitrary continuous Bragg axis motion is assumed, as configured for an energy scan. 1) The high resolution incremental encoder of the Bragg axis position is read into an *actual position* register in the FPGA hardware. 2) This register is compared to a *trigger positions table*, holding the energy axis grid for data acquisition. When a preconfigured position is passed, a TTL gate of a certain duration (*integration time*) is sent to each of the detectors simultaneously. 3) All detectors individually acquire data during the on-time of this hardware generated gate signal.

The above described procedure is called *trigger mode* and leads to fixed integration times for each point. For this mode, the Bragg axis motion needs to be performed substantially slower than necessary to ensure that the next trigger position is never reached during the ongoing acquisition interval. To overcome this, most scans are performed in a so called *gated mode.* Here, after passing a position of the *trigger positions table,* the gate TTL signal for the detectors is held “low” for a minimal readout time of 10 µs and then kept “high” until the next position is reached. In this mode, the integration time for each point varies depending on the actual profile of performed motion. This scheme allows for optimal use of photons (>99%) with minimal dead

[6] https://ohwr.org/project/pandabox/wikis/home

time between points. The PandABox FPGA system is acquiring the actual integration time and the average position of the Bragg axis during each gate “high” signal sent to the detectors. This provides normalization for counting detectors and the exact energy axis, respectively.

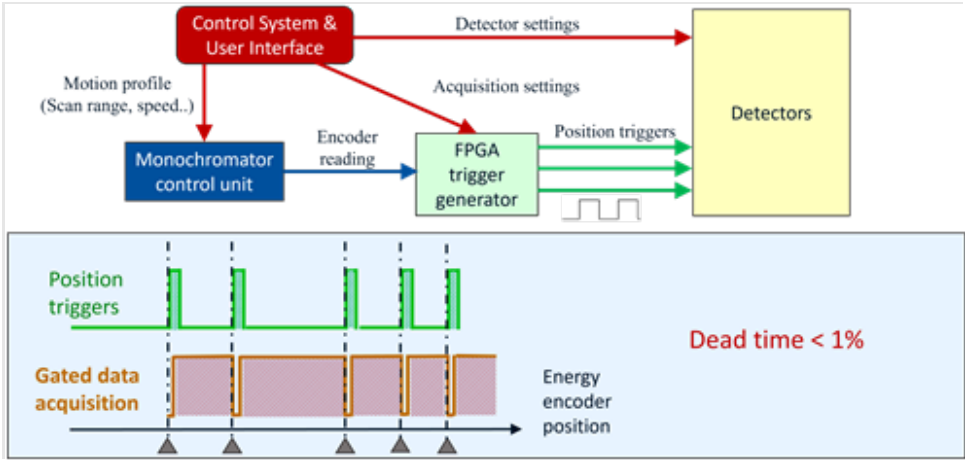

Figure 11. Schematics of the (energy) position based trigger and gate generation for detectors at Balder during energy scanning.

In the current standard implementation, detectors are armed, the trigger table is updated and motion is commanded for each scan and repeat individually by the control system. This configuration time is in the order of seconds and limits the repetition time for scans to above approx. 10 s.

Upgrade: We are currently implementing a new *hardware orchestrated* data acquisition mode (DAQ project), in which the detectors are only armed ones for an entire measurement program consisting of several repeats of a predefined measurement sequence, which can contain multiple absorption edges and diffraction acquisitions (Figure 12). In this mode, the motion controller is the orchestration master for all measurements. It performs a certain motion trajectory repeatedly and transmits a TTL based arm signal to the FPGA trigger unit to activate the *trigger positions table* compare unit before starting a new repeat. Then, similarly as described above the actual position of the motion gates the detectors for all scans comprised in the sequence.

A typical sequence for multi-edge measurements in combination with steady X-ray diffraction is shown in Figure 12.

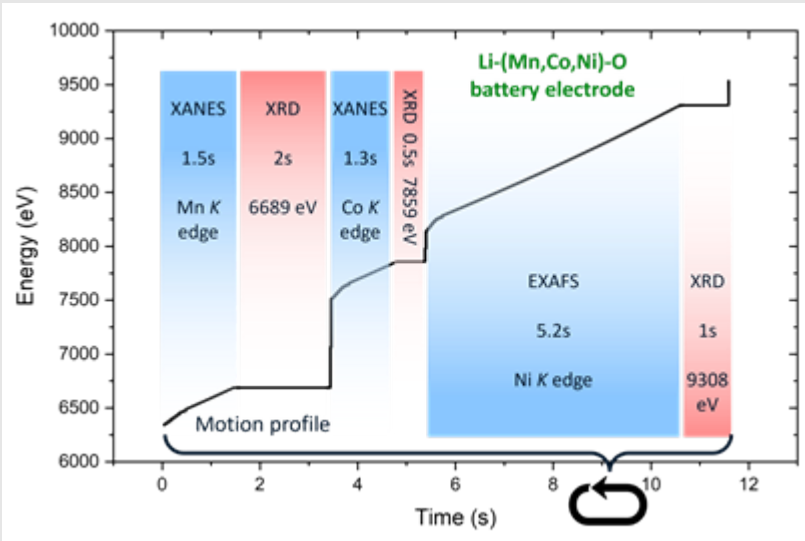

Figure 12. Motion profile recorded during execution of a measurement sequence (comprised of individual scans of multiple absorption edges together with XRD takes at fixed energies) in hardware based orchestration. This sequence is then executed repeatedly.

2.2 Detection techniques

2.2.1 X-ray Absorption Spectroscopy (XAS) in transmission

Transmission detection is the fastest way of measuring absorption coefficient for a given S/N ratio. All reference spectra are exclusively measured in transmission. Low concentration or non-transparent samples require fluorescence detection, and even in these cases, transmission is measured simultaneously with fluorescence for the chance of comparing their quality on the fly during the acquisition.

High Photon Flux Ionization Chambers

The high flux at Balder in the range ~10^{13} ph/s at the sample requires high voltage ionization chambers to sufficiently reduce ion-electron recombination losses. Additionally, our feedback scheme of the scanning DCM relies on the position sensitivity of the primary flux (I_0) ionization chamber in the experimental hutch, so a split collector is required.

We have developed and built a new ionization chamber that meets the above requirements, see Figure 13. It has several appealing features:

- The design enables elevated high voltages applied to the bias electrode. We can reach 5 kV for a chamber open to ambient air.
- Split collector electrode provides two separate signals in either left-right or top-bottom direction and thus position sensitivity for a feedback loop.
- The inner shielding chamber, isolated from the outer body, provides a direct ground return from the signal connectors to the high voltage connector. This shielding serves against external radio frequency pickup and provides improved signal noise.
- There are no plastic parts visible from the beam position. Therefore, there is no charge accumulated on plastic surfaces in such an extremely ionizing environment, which should provide better long-term signal stability.

- All zero-potential surfaces visible from the beam position are connected to one of the two collector electrodes. Therefore, there are no electron losses at the inner walls. The up- and down-stream ends have guard electrodes connected to the inner shielding chamber.
- There are no flexible wires connecting the electric feedthroughs and the electrodes, which minimizes the microphonic effect.

The studies of the main characteristics of the ionization chamber, e.g. I-V curves for different gases and levels of absorption, linearity checks, timing characteristics, were going to be presented at SRI-2021 but due to the pandemic it did not happen. We will wait for the next opportunity.

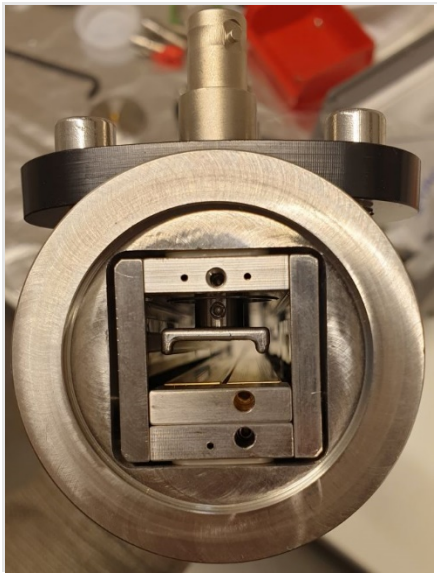

Figure 13. The view of internals of Balder's ionization chamber. The termination flange is KF40. Visible is the rounded rectangular inner shield isolated from the outer body, a split gold-plated collector electrode at the bottom and a bias electrode at the top with a 6 mm distance between them at the center. The length of this chamber is 40 cm; we also have a short version of 10 cm.

Current measurement

The currents of all ionization chambers are measured by an electrometer device, integrating a transimpedance amplifier with a 18 bit ADC and webserver based configuration and visualization (Figure 14). This device is called Em# and was developed at the ALBA Synchrotron.[7] Each device has 4 independent channels with measurement ranges from 100 pA to 1 mA and selectable analogue pre-filters from 3.2 kHz to 1 Hz. Each channel can acquire data based on an external gate signal, which is delivered by the above described FPGA trigger generator and is individually temperature compensated. The minimum time between two consecutive measurements is slightly below 1 ms, which almost fits well to the beamline's capabilities for XAS measurements in the larger sub-second time regime. Additionally, each channel has a DAC generated analogue output which, in the case of the first position sensitive ionization chamber, is used for the above described closed-loop control of the vertical beam position. The webserver based GUI is used for setting up, zero adjustment and live view of the raw currents at the beamline, see Figure 14. Typical currents measured at Balder are in the range of hundreds of nA to several µA, with a signal-to-noise level of typically 10^4 (e.g. dark noise of 100pA in the complete chain with HV on the ionization chambers, compared to a beam induced current of 1µA).

[7] doi:10.18429/JACoW-ICALEPCS2017-TUAPL04

Figure 14. Front and rear view and web-based GUI of the Em#.

Resulting data quality

We typically get exceptionally high quality of EXAFS scans for metal foils, as seen by good reproducibility and low noise (see examples on copper foil in the next section and in (Figure 58). Data quality is also typically very high on liquid samples unless we see bubble formation due to radiolysis of aqueous solutions (see section 2.4.5, Figure 44). Powders, the most common form of samples, are usually prepared as pressed pellets, and the resulting data quality strongly depends on pellet homogeneity. A good example of EXAFS data on powders is shown in Figure 15.

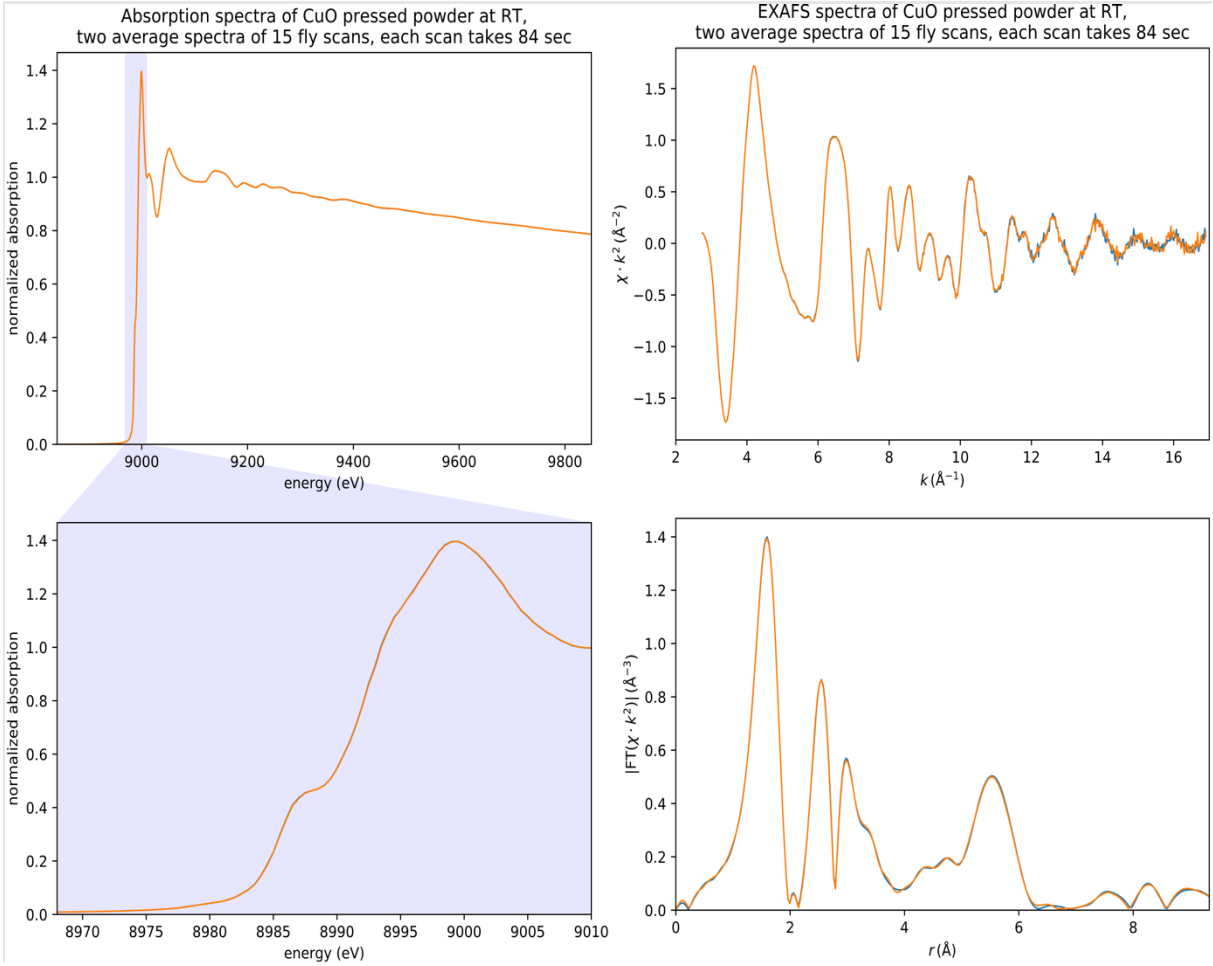

Figure 15. Powder EXAFS. Two averaged XANES and EXAFS spectra of CuO accumulated in a conventional (slow) way of continuous energy scanning.

Sub second scanning and performance

Our recent upgrades in the Bragg axis motion control and the data acquisition system (as described in section 2.1) allow for sub-second XAS measurements. The spectra measured in increasing scanning energy (up) direction as well as measured in decreasing scanning (down) direction can be used. Shows a direct comparison of the edge features, as scanned in up and down directions, at the Cu K-edge of a metal foil. We conclude that sub-second XANES measurements of high quality and reproducibility can be performed for homogenous foil-like samples. The slight shift between up and down measured spectra is anticipated to arise mainly from the response time of the ionization chambers and electrometers used. While this could potentially be optimized, it is sufficiently good for longer sub-second measurements.

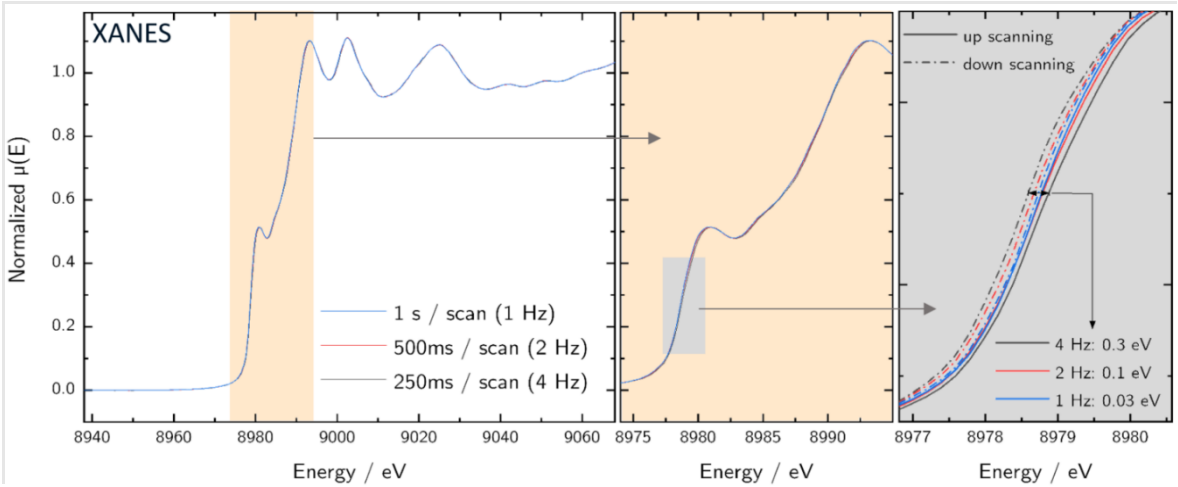

Figure 16. XANES spectra of the K-edge of copper as measured with different scan speeds in energy up and down scanning demonstrating the quick scanning capabilities of the beamline.

The achieved motion quality and signal-to-noise ratios for the whole detection chain are reflected in the higher *k* EXAFS part of XAS measurements. Figure 17 shows the achieved low noise up to k = 18 Å^{-1}, even for sub-second time-resolution.

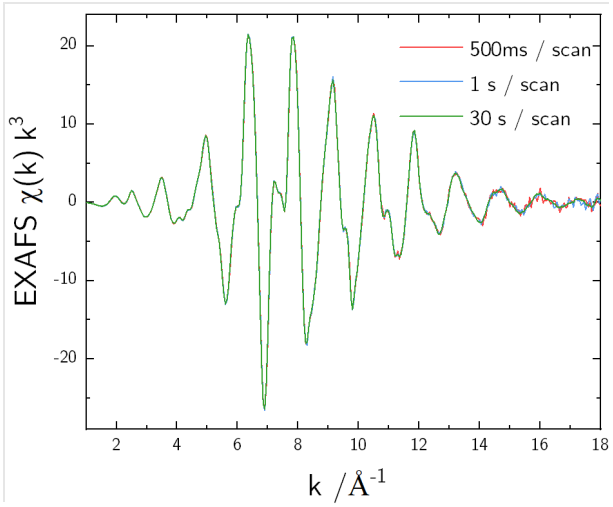

Figure 17. Measured k^3-weighted single EXAFS spectra of a Cu-foil for different scan speeds.

2.2.2 X-ray Absorption Spectroscopy (XAS) in fluorescence

Samples that are of low concentration or highly absorbing in transmission require fluorescence detection to record the X-ray absorption process. For this Balder is equipped with three fluorescence detectors. Two energy-dispersive solid-state detectors used for XAS and X-ray fluorescence imaging (XRF) are the 7-element silicon drift detector (SDD, X-PIPS™, Mirion Technologies Inc., USA), and the 7-element germanium detector (HPGe, Mirion Technologies Inc., USA). The third fluorescence detector is a passively implanted planar silicon (PIPS) diode used for total fluorescence yield (TFY).

Energy-dispersive detectors

The SDD has seven detector elements in a focused geometry (focal point 50 mm), while the Ge detector elements are flat, and both detectors have beryllium windows. These detectors are cooled by closed cycle cooling. The energy-dispersive detectors are fixed inbound and horizontally 90° to the incoming beam on detector the table and can only be used one at the time (Figure 18). These detectors are on individual

translation stages with a distance range of 50-290 mm away from the sample position. Adapted Z-1 fluorescence filters are available to preferentially absorb the elastic scatter signal with standard 3- and 6-absorption lengths, as well as one thin Kapton-film to protect the detector nose when no filter is in use. Currently only one filter frame can be inserted at a time. During cryostat operations either detector can translate directly adjacent to the cold zone and be inserted to the isolating vacuum of the cryostat (See section 0 2.4.3). Each detector is equipped with an Xspress3 digital signal processor.

Both detectors have been inoperative for some time in the last 5 years (2019-2023). The 7-element Ge detector had from the start trouble with signal quality and was away for service/repair of internal cooling and channel tuning. This was returned into operation in fall 2020. The 7-element SDD was the “work horse” detector for low concentration samples, but unfortunately experienced a broken Be window and has since November 2021 been out for repair with the manufacturer (Mirion). The expected return has been delayed several times and is currently estimated in November 2023. It required a full exchange of the seven detector elements and their support structures.

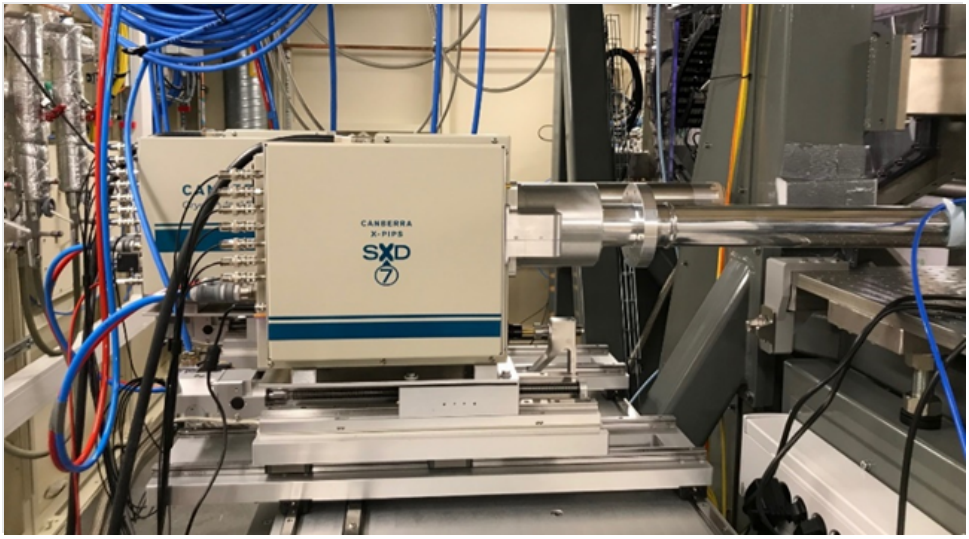

Figure 18. Two solid state detectors on the detector table at Balder side by side. Each of them can slide into the measuring position while the other is parked to the side. Ge detector in the back and SDD in the front.

PIPS diode

The PIPS diode is 900 mm^2 in diameter and enclosed in black Kapton. During user operation the PIPS is typically mounted onto the experimental table using Thorlab accessories and clamps dependent on the complete experimental setup.

Flexible detector (future)

The large fixed 7 element solid state detectors are not ideal for minimising the sample to detector distance for XANES mapping and lower absorber concentrations or lower energy, since they are fixed in distance and orientation towards the sample. To optimize the capability, we are in the process of purchasing a small beryllium-free SDD detector with umbilical cord allowing for a fully flexible set up. This detector will be important for fluorescence detection in complex (in situ/operando) sample environments. As a demonstration, we successfully tested a similar type of RaySpec, borrowed from NanoMAX.

Table 1. Summary of fluorescence detectors.

Detector	Ideal energy range	Countrate	Extra notes:
7-element SDD	Up to 20 keV	2 mcps/element	Focused sensor arrays
7-element Ge	Up to 40 keV	0.125 mcps/element	
PIPS	unlimited	n/a	
RaySpec SDD (upcoming)	Up to 20 keV	1 mcps/element expected	Be-free, carbon based, umbilical design

Sample orientation

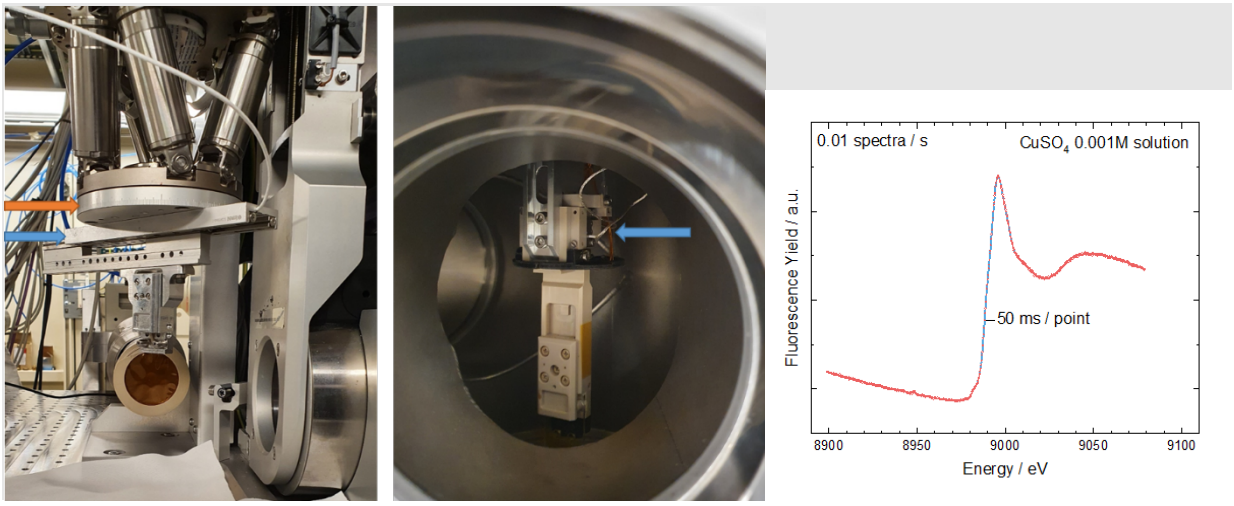

Figure 19. Lateral sample stages in 45° for fluorescence detection. Left photo, ambient stage manual rotation interface (orange arrow), linear SmarAct positioner (blue arrow). Beam is coming from right side in the picture and the Ge detector perpendicular to the beam. You can also see the Supereyes borescope camera (see section 2.4.2) in between the beam and detector pointing at the sample position (sample plate is removed). Mid photo, inside cryostat the manipulator sample rod is rotated to 45º and the linear SmarAct cryo-positioner (blue arrow) can move the sample lateraly. Right panel, example fluorescence spectra at Cu K-edge raw data collected of 0.001 M copper sulphate using the 7-element Ge detector.

Sample orientation to the beam and detector is classical 45º and is set in this geometry by a manual rotation interface holding the lateral positioner of the ambient stage, the x translation axis keeps the detector and beam geometry constant versus the scanning sample. The same is true for the cryostat sample translations, see Figure 19.

2.2.3 X-ray Emission Spectroscopy (XES) with SCANIA-2D

The spectrometer is based on the Rowland circle geometry with three exchangeable sets of crystals: Si(111), Si(220) and Si(400). Each set has 6 crystals which are of Johansson type in the meridional direction and flat in the sagittal direction. The main design ideas and features are summarized in Figure 20. Presently, only one branch has been built. We have another Eiger detector, unassembled crystals and installed motor drives for the second branch.

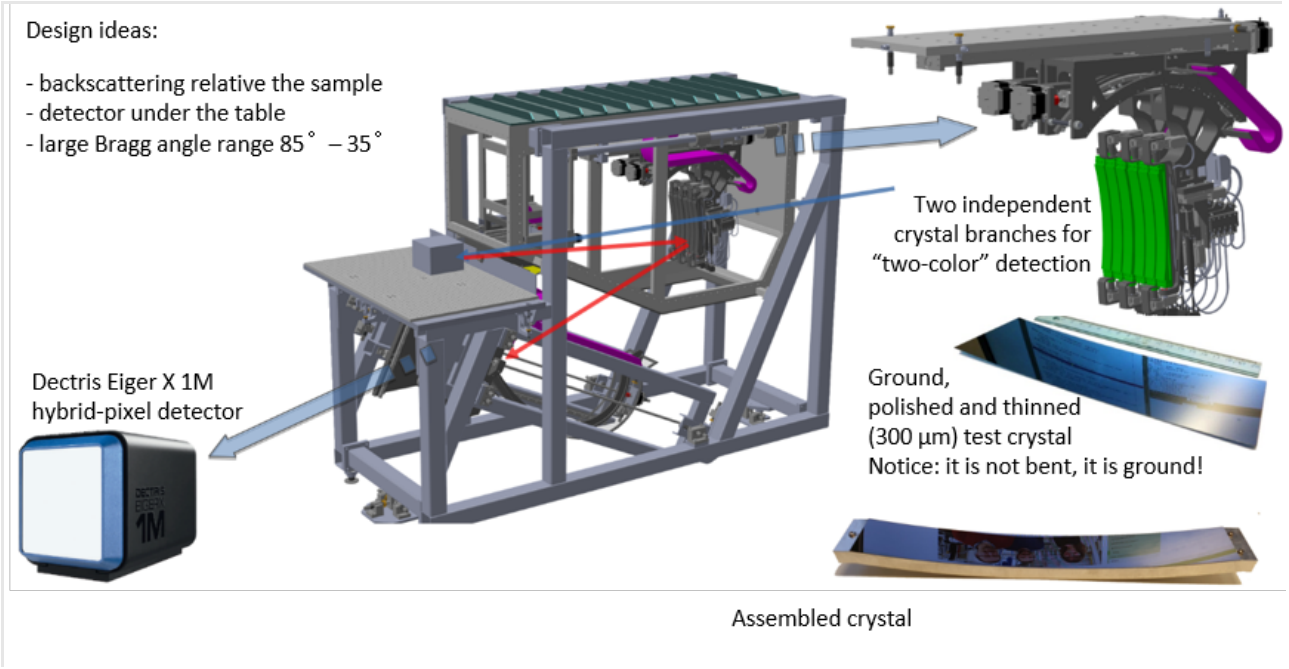

Figure 20. The concept of SCANIA-2D (Segmented Crystal Analyzer with Image Acquisition in 2D) with the main components magnified. The primary monochromatic beam comes from the right through the crystal analyzers down to the sample (a box on the experimental table).

Some technical improvements of the spectrometer are still ongoing. 1) The sagittally narrow flight tube has been modified several times and is now approaching a good implementation. 2) The bottom part of the main spectrometer's vessel, which is a helium-filled volume, represents quite serious restrictions at lower energies and requires modification. 3) The back of the front wall of the spectrometer will get a Soller structure of concentric conical sheets to reduce the scattered background.

The alignment algorithm of the spectrometer is presently well established and can be completed within 30 minutes. Energy resolution charts have been measured for individual crystals and for a combination of three crystals at a specific Bragg angle and a specific reflex. These measurements will be systematically repeated and presented elsewhere.

An XES scan is a theta scan of all three crystals, housed within a single branch, at a fixed position of the detector. During the scan, the diffracted energy band moves over the detector position in the θ–2θ dependence, with θ being the incidence angle and 2θ the deflection angle. There are more detectable bands, not only the anticipated θ–2θ band, which we explain by the Borrmann effect where a dramatic increase in the transparency of the crystal is observed close to a Bragg reflection, and which should be present in every thin crystal analyzer; more on this will be published elsewhere. The tangential detector coordinate is transformed to emission energy by analyzing the elastic scattering at two various incident energies, see Figure 21.

The raw data object is a 3D array of a set of 2D Eiger images stacked along the scanning axis. One such data set may be a few 100 MB in size and after several days of operation, the data folder may be a few TB. Therefore, to overcome the problems of big data transfer and big data analysis, we decided to go for an on-the-fly data reduction along the sagittal detector dimension. The data reduction routine detects the emission band and its inclination on the detector; this inclination is corrected by image skewing using *scikit-image* analysis package. The resulting gain factor in data size is about 1000.

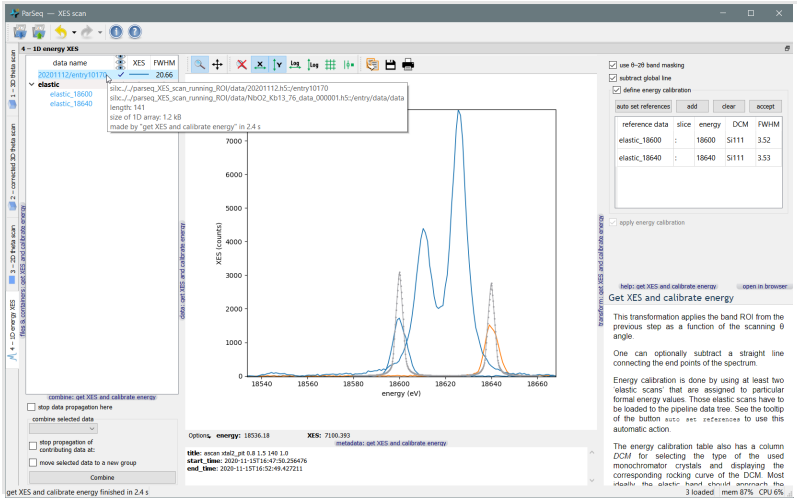

Figure 21. The ParSeq – XES analysis pipeline demonstrated on a dataset of Kβ1,3 of NbO2 nXES.

We anticipate two main use modes of the spectrometer: a) non-resonant XES at a fixed excitation energy and scanning Bragg angle and b) HERFD XANES measured at a fixed spectrometer energy and scanning DCM energy. The mode (a) is exemplified in Figure 21 while the mode (b) is shown in Figure 22. A third mode to use the spectrometer is in resonant XES maps (RXES/RIXS), by scanning both the excitation energy and the spectrometer Bragg angle.

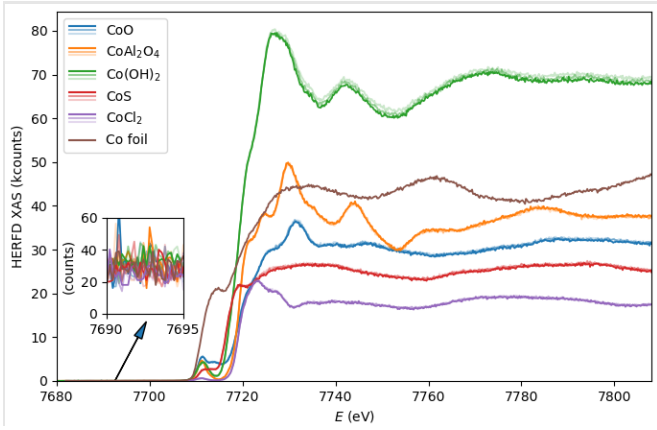

Figure 22. The Co Kα1 HERFD (High Energy Resolution Fluorescence Detected) XANES spectra were collected together with expert commissioning users (A. Jentys group from TU Munich) in July 2022. A full spectrometer branch (3 crystals) was used for the first time. Here, the scanning range had 650 points (rather excessive) at 0.5 sec per point. Note the noise level in the inset plot that would remain much smaller than signal with a sample dilution down to 1wt%.

2.2.4 X-ray Fluorescence (XRF)

X-ray fluorescence imaging (XRF) capabilities have been developed as a secondary technique to enhance the characterization of chemically heterogeneous information. The comparatively small beamspot at Balder has exposed chemical heterogeneity in a number of user cases. The ability to complement standard XAS with mapping capabilities (i.e. spot-XAS, chemical imaging, XANES-mapping) has increased the versatility of measurement strategies to better fit the user's needs. A live XRF mapping viewer, seen in Figure 23, shows binned elements of interest which can be defined by the user to display 2D elemental maps. This serves as a live source to map or spot-XANES and -EXAFS data acquisition, each pixel in the viewer containing x and y sample motor positions to allow the user to easily set up subsequent scans.

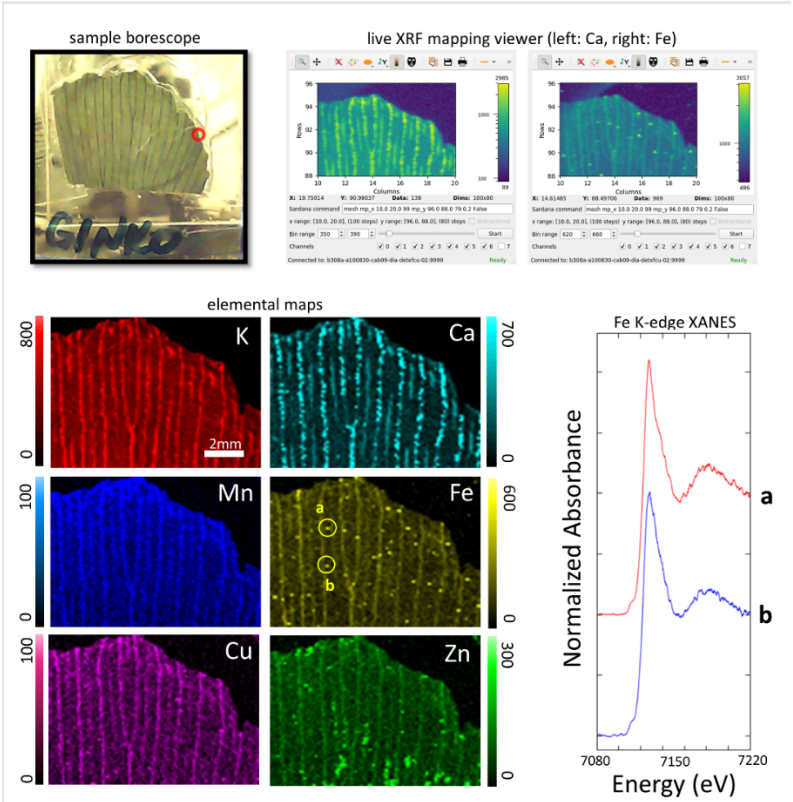

Figure 23. Features of XRF mapping and spot-XANES data collection. Sample borescope is used to set up initial scanning coordinates. The live XRF mapping viewer displays user-defined binned elements. Elemental maps shown are of Ginkgo leaf mapped with 100 µm steps. XANES data collected following XRF mapping. Sample coordinate positions of ensuing scans can be read in the live viewer when hovering over the pixels.

To make full use of Balder's fast and reliable energy scanning, rapid XANES 2D mapping is currently under development. This is a unique measurement strategy of 2D hyperspectral maps. XANES spectra are collected, point by point, as the measurement raster-scans the region of interest. Each energy position of the XANES simultaneously records MCA data. As a whole, the spectra and MCA are stacked in a multidimensional array so that users can construct 2D elemental maps at any energy position along the XANES scan. This strategy exceedingly reduces scanning time and radiation dose while providing better spectral resolution compared to traditional stacking strategies in XANES mapping (Figure 24). Furthermore, compared to XANES mapping, sample or beam drift issues are negligible.

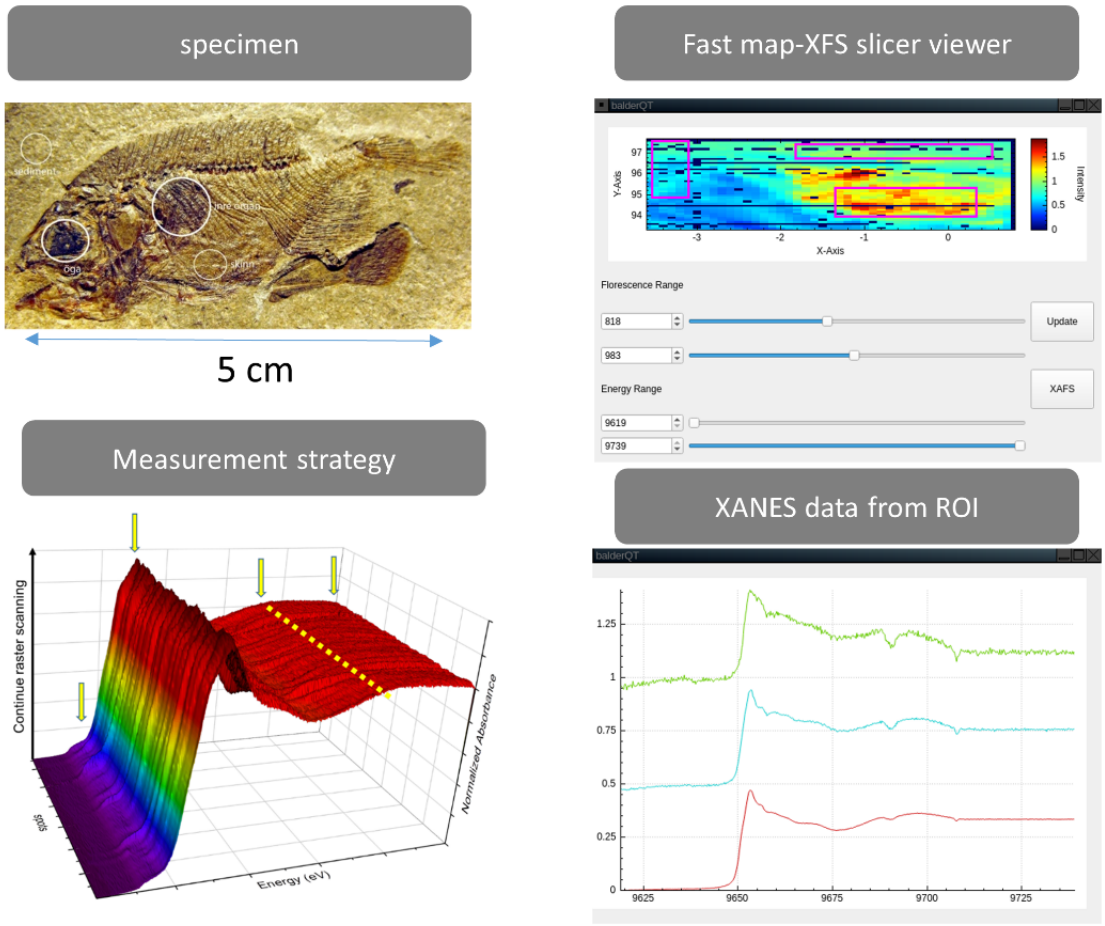

Figure 24. Rapid XANES 2D mapping scheme.

2.2.5 Multimodal in-situ XAS-XRD

X-ray diffraction (XRD) is offered at Balder as a complementary technique to XAFS Figure 25. This is primarily intended to benefit in-situ and operando XAS experiments, giving insight into crystallographic material properties such as lattice constants, crystallographic phase fractions, texture or strain. The small source size, low divergence, small focal size and high positioning stability of the Balder X-ray beam, enables the recording of high quality X-ray diffraction patterns without changing the optical elements defining the beam. Together with the high flux, this allows for a quick (sub-second) and nearly uncompromised combination of XAS scanning and XRD for a variety of processes and sample environments. Typical applications include, but are not limited to, operando catalysis, operando cycling of batteries and in-situ material formation studies.

Usually, when coupled with hard X-ray spectroscopy, XRD is used just to monitor the reaction as a complementary perspective. However, it should be noted that both transmission XAS, as well as XRD, are fully quantitative techniques. By comparing the crystalline phase fraction with the phase fraction measured by linear combination analysis of the XANES, even amorphous phase fractions can be determined quantitatively.

Setup and Methodology

Usually, multimodal XAS-XRD is measured in sequentially repeated acquisitions, such that one or multiple XAS scans are combined with one or multiple XRD acquisitions at fixed energies into one sequence (Figure 12). Depending on the time and q-resolution needed, XRD measurements are usually performed either at the beginning (and/or end) of the sequence or interspersed between the XAS measurements measured by up-

down scanning of the energy. Even the measurement of anomalous diffraction, at an energy close to the absorption edge, can be integrated in a measurement sequence to achieve element selectivity for diffraction patterns. A pre-defined measurement sequence is then repeated with repetition rates up to 2 Hz, depending on the individual acquisition times chosen for XAS scans and XRD takes. We usually record good signal to noise diffraction patterns of crystalline samples within 100 ms to 1 s. The energy chosen for X-ray diffraction takes is just limited by the reflectivity of the chosen mirror set, e.g. below the maximum of 14 keV for the Si/silica mirrors.

The general setup for combined XAS-XRD measurements is depicted in Figure 25. For a reliable measurement of lattice constants by diffraction, the absolute beam, and/or sample, positional stability is of high importance. It is achieved by the closed-loop regulation of the beam height (as detailed in section 2.1.1) in conjunction with additional sample slits, positioned as close as possible to the focal position. These slits are placed approximately 30 cm upstream from the sample position and consist of two pairs of horizontal and vertical slits (JJ X-Ray) placed one behind the other along the beam path. The first pair of slits define the horizontal and vertical size of the X-ray beam while also producing long tails in all directions due to parasitic scattering from the knife-edge. The second pair of slits act as guard slits to cut these tails to produce a clean beam spot. While XRD is measured usually with approximately the full beam (100 µm x 100 µm), the beam can be effectively slitted down to approximately 15 µm vertical x 60 µm horizontal. A short ionization chamber of the type described in section 2.2.1 is present between the guard slit set and the sample and is used to accurately measure the incident intensity for XAS, if the sample slits are in place.

The two-dimensional XRD pattern of the sample is then acquired using an EIGER 1M area detector, which is gated by the FPGA based gate generation system, as described in section 2.1.2.

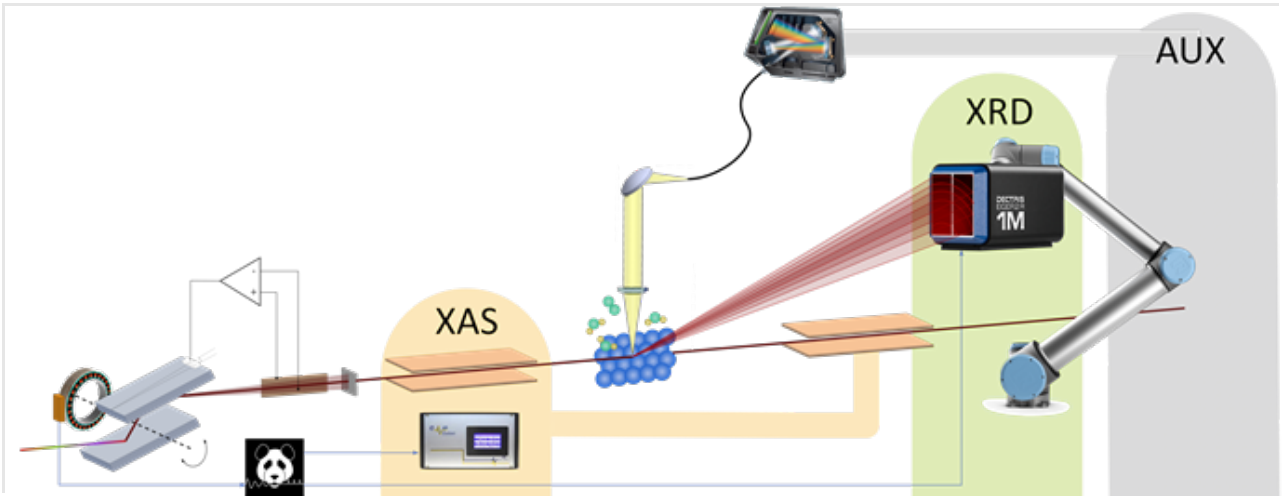

Figure 25. Schematic setup of simultaneously combined XAS-XRD measurements. Sometimes even auxiliary optical measurements are taken simultaneously.

The 2D detector is mounted on a robotic arm which allows flexible positioning for measurements in various experimental geometries and sample environments with the freedom to choose the 2θ-range for the XRD measurements. Currently, the detector is moved manually to a position best suited to the experiment and is kept fixed during the measurements. However, the capability of the beamline to perform quick automated energy changes also enables the measurement of multiple q-ranges with different resolutions without repositioning the detector. Because of the detector size (1M pixel) it has to be decided whether to position the detector very close to the sample (typically 10 - 20 cm), for a large q-range but with a compromise in peak shape resolution, or far from the sample (typically 50 cm - 1 m) for a narrow q-range but high peak resolution.

While the former is useful to identify crystalline phases, morphologies and relative compositions, the latter is used to track lattice parameters with high precision.

The position of the robot arm and the detector are chosen individually for each experiment. A pyQt based graphical simulator has been developed to enable the users to simulate the Debye-Scherrer rings on the 2D detector and customize the detector position and the X-ray energy (Figure 26). After the detector is positioned, prior to making any measurements, Debye-Scherrer rings from a standard calibrant, such as LaB_6 are obtained at a well-defined X-ray wavelength. Calibration is done manually using the graphical tool available in the pyFAI package to obtain the detector distance and the point of normal incidence in the format of a standard *PONI file*. This file is used to perform azimuthal integration of the 2D data. Details of the data reduction and treatment methods used at the beamline are provided in a later section 2.6.

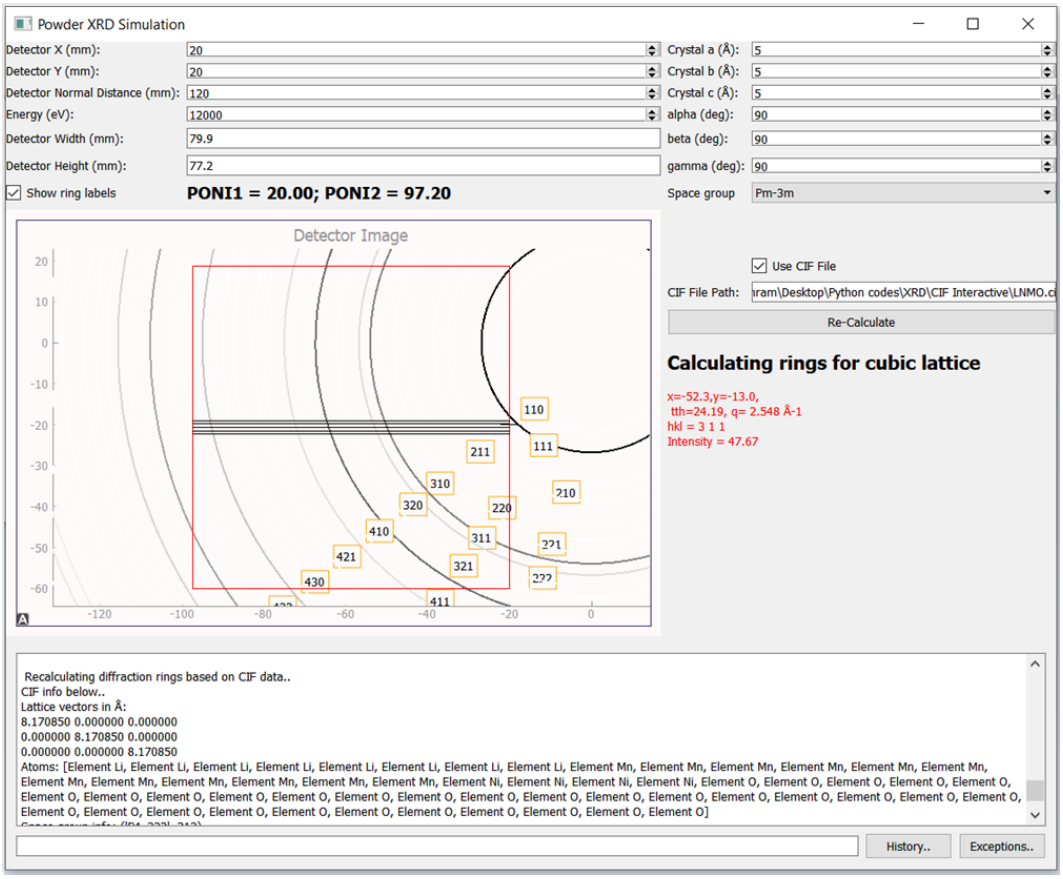

Figure 26. Screenshot of the powder ring simulation GUI developed for XRD at Balder. The user inputs the detector positions and the X-ray energy and can define the crystal lattice either as a set of lattice parameters and the space group or by providing a CIF file as input. Apart from showing the ring pattern within the detector (the rectangular region bounded by red borders), the GUI also provides the HKL indices and intensities (if a CIF file is provided as input) of the rings, the 2θ and $q(\cong(4\pi/\lambda)\sin\theta)$ while hovering over the display widget with the mouse pointer.

Data quality and performance

Taking advantage of the flexible positioning of the detector, one can either obtain an overview diffraction pattern, which covers a large angular range and several diffraction rings, or a smaller angular range with fewer rings. Figure 27 shows the two kinds of patterns obtained for a Si powder peak shape standard. The peak shape obtained also resembles a standard pseudo-Voigt profile.

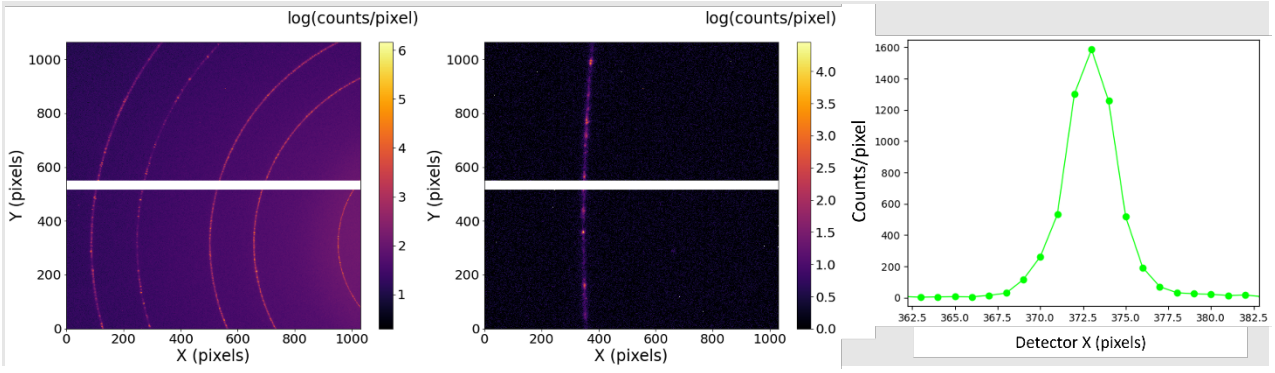

Figure 27. XRD images of Silicon powder measured at a typical detector distance for I) overview pattern (d = 10 cm) and ii) high resolution diffraction (d = 90 cm).

The maximum achievable angular range and the maximum q-range for a typical energy of 10 keV are shown in Figure 28. The range essentially depends on the area of the detector and is often constrained by the sample geometry and environment. The q-resolution, however, depends on several factors, e.g. the beam size, divergence, sample size (both in the longitudinal and lateral directions), scattering angle and size of individual pixels, as well as the detector distance. The best and worst resolutions are at the largest and smallest scattering angles, respectively. An example is shown in Figure 28 for a beam with a vertical size of 20 µm and a sample size of 100 µm in the longitudinal direction.

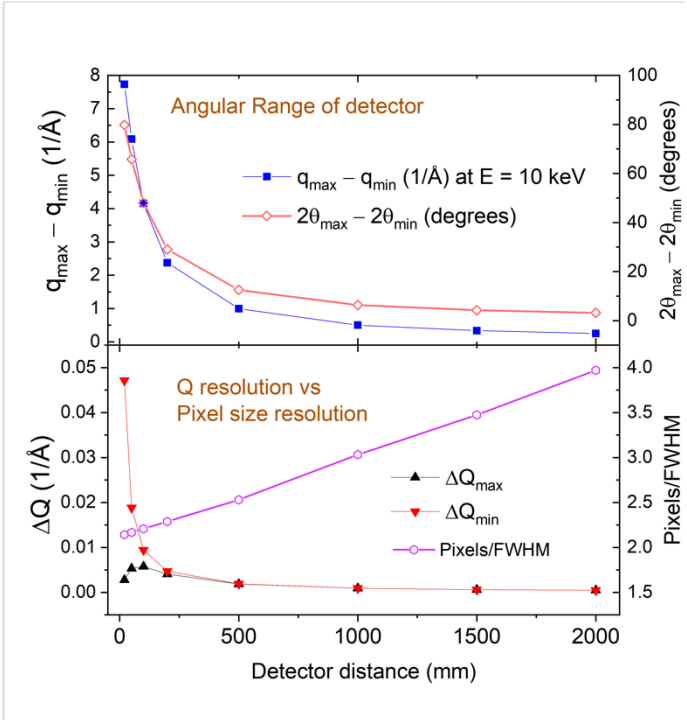

Figure 28. Top: Angular range and q-range covered by the detector at 10 keV for different sample detector distances. Bottom: Achievable q-resolution for different detector distances at 10 keV for a vertical beam size of 20µm and a sample depth of 100 µm.

For combined XAS-XRD measurements in transmission geometry, the sample can be rather thick (often up to 1.5 mm) to achieve a proper edge step in XAS measurements for diluted materials. This is particularly true for samples with low mass loading, such as dispersed nanoparticles in light supports or zeolite-based catalysts with low mass loading of the active element. Such thick samples are usually the main limitation encountered in terms of resolution in X-ray diffraction patterns.

To demonstrate the performance of multimodal combined XAS-XRD in a typical real-world applications, we applied this technique to observe the oxidation and reduction of a Pd catalyst in our capillary reactor (detailed in section 2.4.4) under application of O_2 or H_2 gas, respectively. Sequential XAS and XRD measurements were

performed with a repetition rate > 1 Hz around the K-edge of Pd. The as-measured XAS spectra and azimuthally integrated XRD patterns are shown in Figure 29.

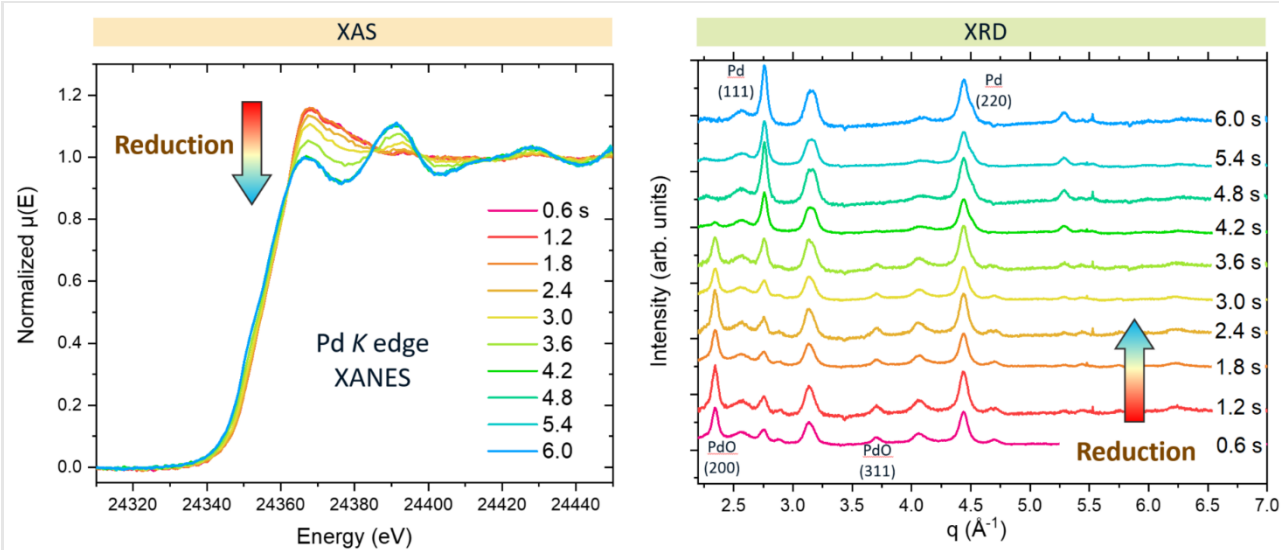

Figure 29. Multimodal in situ XAS-XRD with sub-second time resolution measured during reduction of a Pd- catalyst.

Ongoing and future developments

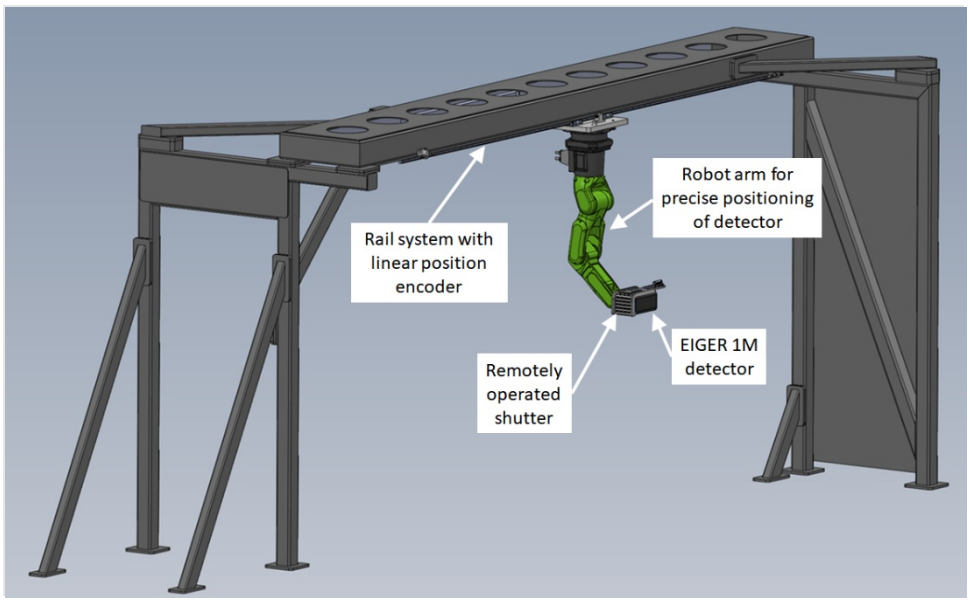

Figure 30. Design concept of the rail and robot positioning system for the XRD detector. (Courtesy - Nils Pistora, MAX IV Design Office).

Whilst it has been possible for general users to record XRD at Balder since 2021, its integration is still to be completed. Major aspects, which are addressed in an ongoing project, are: I) the design of the detector cover which needs to be manually placed is designed in such a way that may result in a high risk for damage II) The position repeatability of the currently installed robot is larger than one pixel. Further, under certain conditions, the robot position is unstable and can vibrate. A new robot with much higher precision is going to be installed soon. III) The position flexibility of the detector is currently limited and experimental sample environments are restricted by the position of the robot on the EH table. To make more space and achieve a high flexibility of q-ranges, the new robot will be held from an above head rail system, as depicted in Figure

30. The new system is currently being developed in collaboration with the internal resource groups within MAX IV (mechanical design, workshop, electronics and software) and is planned to be in operation by the end of 2025.

With the possibility to measure a diffraction image for every energy point during a continuous energy scan we are currently exploring possibilities for in-situ and operando measurements of the diffraction anomalous fine structure (DAFS). This technique in principle enables the measurement of crystallographic site specific XAS and is anticipated to be achievable within a time resolution of minutes. Early achievements are detailed in the later section of in-house projects. This technique makes perfect use of Balder's unique capabilities and has a high potential for groundbreaking research when applied to complex catalysts or battery electrodes.

2.2.6 RefleXAFS

XAFS measurements on two-dimensional systems and surfaces are possible in fluorescence mode but are challenging due to low signal and/or high background from the bulk, the substrate or the support structure. In experiments where the film or surface is atomically flat, specular reflectivity can be observed even at high X-ray energies, which can be used to measure XAFS in reflection mode (RefleXAFS).

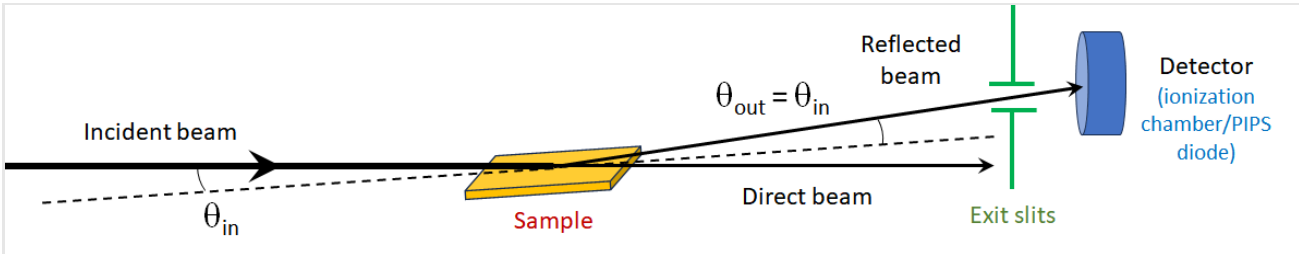

Figure 31. Schematic representation of the typical RefleXAFS setup used at Balder.

Spectra obtained by RefleXAFS include features that arise due to geometric factors and self-absorption. Geometric factors can be modelled based on reflectivity curves obtained at different energies, but not self-absorption. At grazing incidences below the critical angle, total external reflection occurs. In this regime, self-absorption is absent. At grazing incidences, the footprint of a 100 µm wide X-ray beam on the sample can be several millimeters, hence, precision alignment of the sample in all directions is essential. A dedicated sample stage is used for this purpose at Balder (Figure 31) in combination with motorized exit slits to cut out any direct beam leakage, stray scattering or fluorescence which can affect signal quality.

2.3 Radiation damage at 4th generation synchrotron XAS beamline

2.3.1 Beam damage

Balder produces a high flux beam (10^{13} ph/sec) in the focused beam spot of 50 x 50 µm^2 that puts a lot of energy into the sample and the risk of X-ray induced damage to the sample is high. In the first exploration of the new beamline in spring 2019 we observed photon-induced changes, from bubbles formed in aqueous solutions due to radiolysis to degradation of solid samples, making the sample move away from the beam resulting in unusable EXAFS data, see Figure 32.

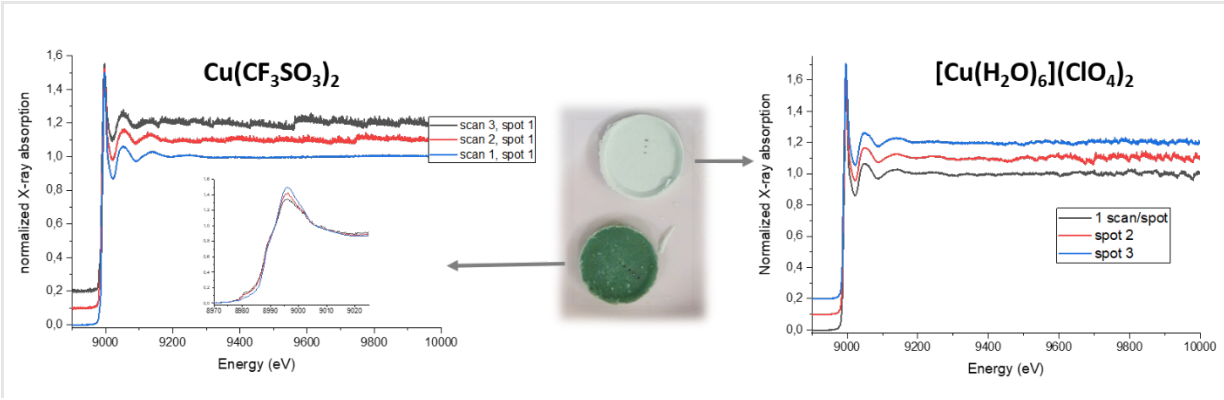

Figure 32. Radiation damage in solid Cu samples from expert commissioning spring 2019. Left panel, dark green pellet was measured in transmission 50 sec/scan. 3 consecutive scans in one spot. EXAFS spectrum degrades already in the second scan. Inset on the XANES region showing Cu^{2+} reduced to Cu^{+} (decrease of white line and increase of pre-edge amplitude). Right panel, pale green pellet, an even more sensitive sample (water coordinated Cu^{2+}), all three scans are on new sample spots and the EXAFS scan degrades halfway.

The most common change is the photo-induced reduction of high valent oxidation states, which we have observed in several materials like ashes, soils and protein solutions. Water containing samples are especially prone to damage, since the water matrix is ionized and resulting radicals can reduce the metal centre, observed as a shift of the absorption edge in XANES, see Figure 33. For an unknown sample a radiation test should be used to assess the sensitivity, by doing quick XANES to observe the edge or by sitting on the edge energy and follow the intensity developed over time (Figure 33, b).

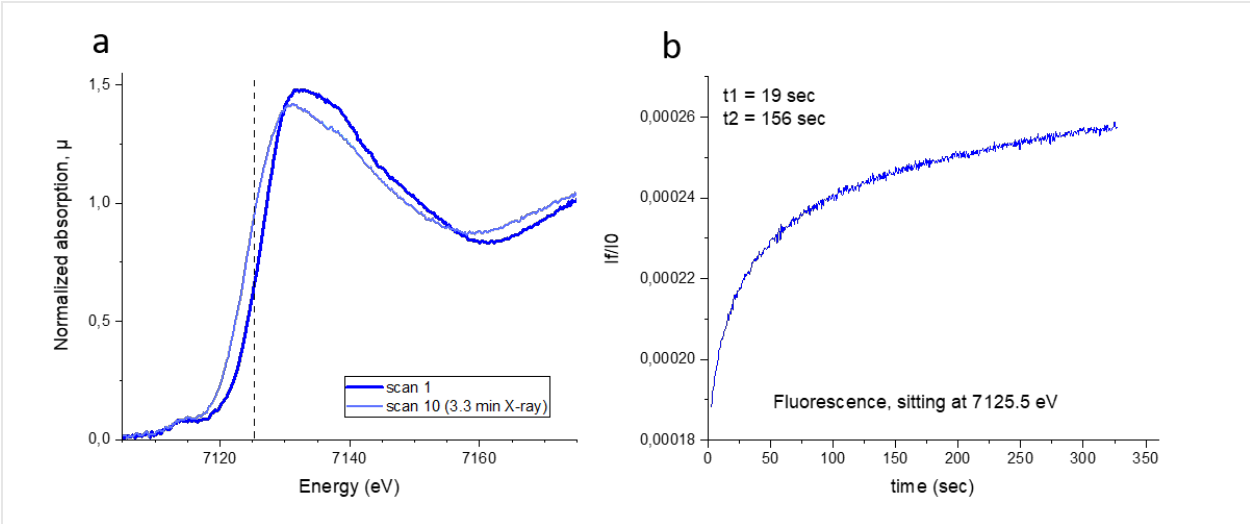

Figure 33. Photo-induced reduction of iron in a soil sample at room temperature with commissioning experts spring 2019. a) Fe K-edge move to lower energy due change in oxidation state scan 1 and 10 (3.3 min later) are displayed. b) The time trace of the reduction process measured by sitting at 7125.5 eV (dashed line in a). The initial reduction is very fast (<19 sec). Future studies of this type of samples used the cryostat to slow the process down.A third example of radiation induced reduction was observed in lyophilized Amyloid-beta fibrils measured at the Cu and Fe K-edges at room temperature. The samples were lyophilized, freeze dried, in order to remove water to protect from water radiolysis. Even so the Cu XANES changed rapidly in the beam by repeating scans on the same

spot, while Fe XANES remained stable for an hour. This change reflected Cu^{2+} reducing to Cu^{+} observed as an increase in the pre-edge peak, see Figure 34, published in Gustavsson et al. (2021).[8]

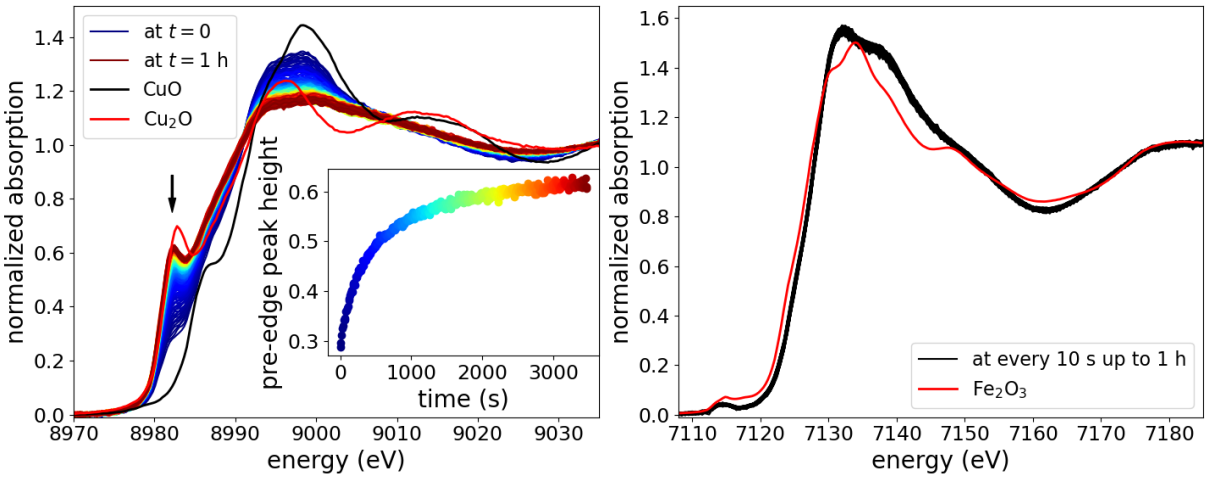

Figure 34. Lyophilized Amyloid-beta fibrils at room temperature. Left: Cu K-edge XANES (rainbow, time 0 dark blue) compared to CuO (black) and Cu_2O (red), inset pre-edge peak height versus time in the beam. Right: Fe K-edge XANES (black) compared to alfa-Fe_2O_3 (red).

2.3.2 Mitigations

In order to avoid or slow down X-ray induced damage, different strategies can be applied. The first strategy is to minimize the effect of the beam by optimizing the time beam is on sample vs data acquisition. Modifications of the flux on the sample can be achieved by defocusing (up to 1 x 0.2 mm^2) and detuning the beamline or use attenuating filters to lower the flux. A fast shutter can be used to only allow beam on the sample while acquiring data. In addition, the data acquisition strategy can be optimized by moving to a new spot between each scan (mesh scan) and scan faster (e.g. fly scans for fluorescence measurements). The new hardware orchestrated scanning method decreases the deadtime at the start of a scan to increase the data quality vs time ratio. Secondly, the sample can be "protected" by using different sample environments. In the case of high water content samples, the sample can be dried to remove water, or measured as a frozen solution in a cryostat to slow down the photo-reduction. If liquid ambient temperature data is required, a flow cell can be used to continuously refresh the sample in the beam. Slow stirring is an option used in some reaction cells. For more details, see Sample environments in section 2.4.

2.4 Sample environments

Balder has several different sample environments available to users, all from the standard pellet holders at ambient or cryo conditions to reactor cells and highly specialized environments developed together with the users.

[8] doi.org/10.1038/s41377-021-00590-x

2.4.1 Standard multiple sample holders

Standard sample holders were developed to fit inside the cryostat as well as the ambient sample stage. The dimension of the sample area is therefore 40 x 20 mm^2. Within the plate, there are a multitude of circular and rectangular sample holders (Figure 35). A special interface with two pins locked in place by a latch for attaching the samples "hanging" into the beam was designed to allow rapid and easy sample changes (see Figure 36 in section 2.4.2). Ideally the sample plates would be exchanged by a gripper equipped robotic arm gripping the two small circles above the sample slots (future upgrade project – the dedicated robot is presently engaged in holding a XRD detector). The cryostat version of the holders is equipped with PEEK clamps to secure the sample from falling off inside the cryostat and exists in two versions for 5 and 13 mm pellets.

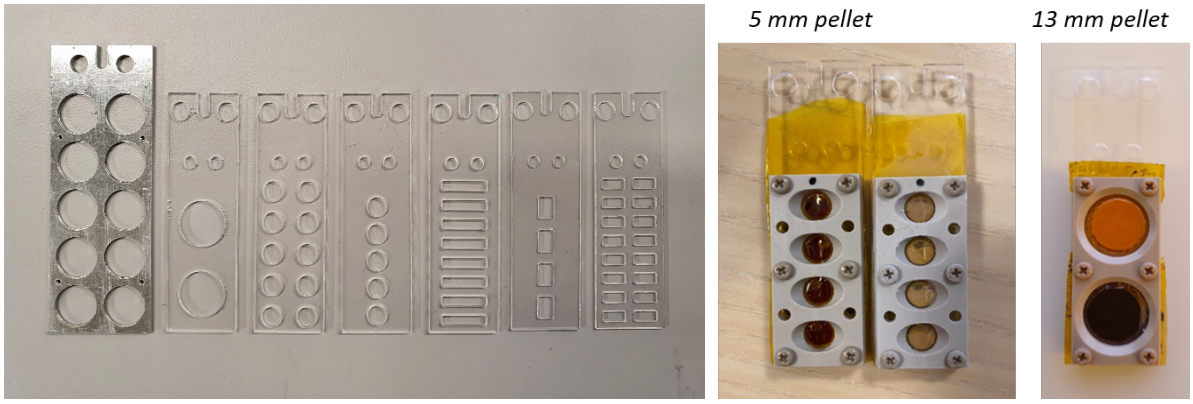

Figure 35. Standard sample holder plates at Blader in acrylic glass or aluminium. The cryostat holders are fitted with peek clamps to secure the samples.

2.4.2 Ambient stage

For ambient conditions, Balder uses a motorized hexapod (PI L.P.) and translational stage (SmarAct) pair giving the user a range of rotational and translational movements of the sample (Figure 36). For simpler sample setups, x and y translation is achieved with the SmarAct and hexapod arm. The travel range is 100 mm in the x-axis and 102 mm in the y-axis. The hexapod allows up to 15 mm axial movements with a rotational range of 10°. The hexapod arm can be rotated 90° outbound for setups that require side-mounting. An additional manual rotational interface between the hexapod and hexapod plate has free rotational range (disregarding SmarAct's and sample range of motion) used when switching between normal (90°) and 45°, or any other configuration.

Samples using in-house sample holders can be mounted on the sample interface. The sample holder is placed on two pins and a latch is placed to secure the sample. Larger sample setups can be directly mounted on the hexapod plate. A sample borescope (Supereyes) is mounted on the table to assist users when setting up sample measurements connected to an in-house viewing software called OrthoView where the user can define beam position and then click and automatically the sample is moved to the desired position.

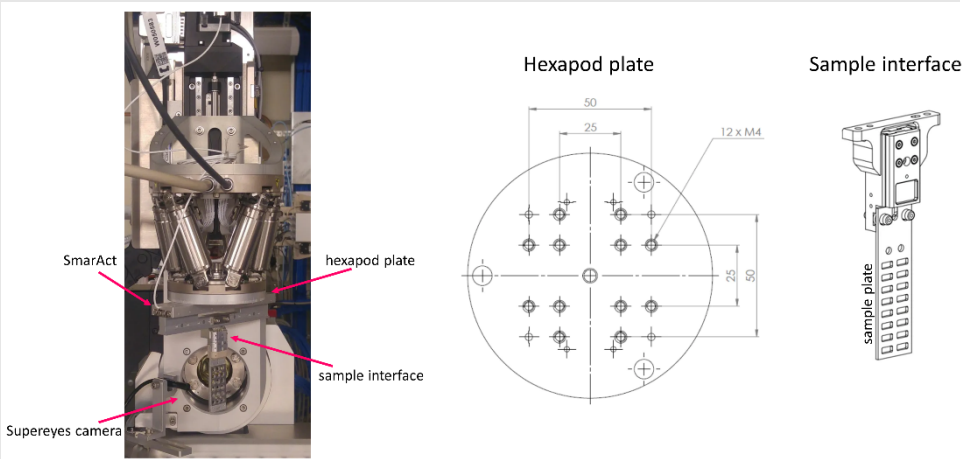

Figure 36. Ambient stage setup with hexapod and translational stage pair. Hexapod plate drawings for users bringing in their own cells.

2.4.3 Temperature stages

Cryostat

Roughly 30% of user beamtime requires cryogenic sample environment. Cryogenic temperatures are achieved at Balder in a closed cycle He cryostat (Figure 37) down to 15 K permanently installed on the experimental table. It is moved to the sample position upon request; the installation time is 30 min, while it takes ~3 hours to reach base temperature. We typically schedule one shift for set up.

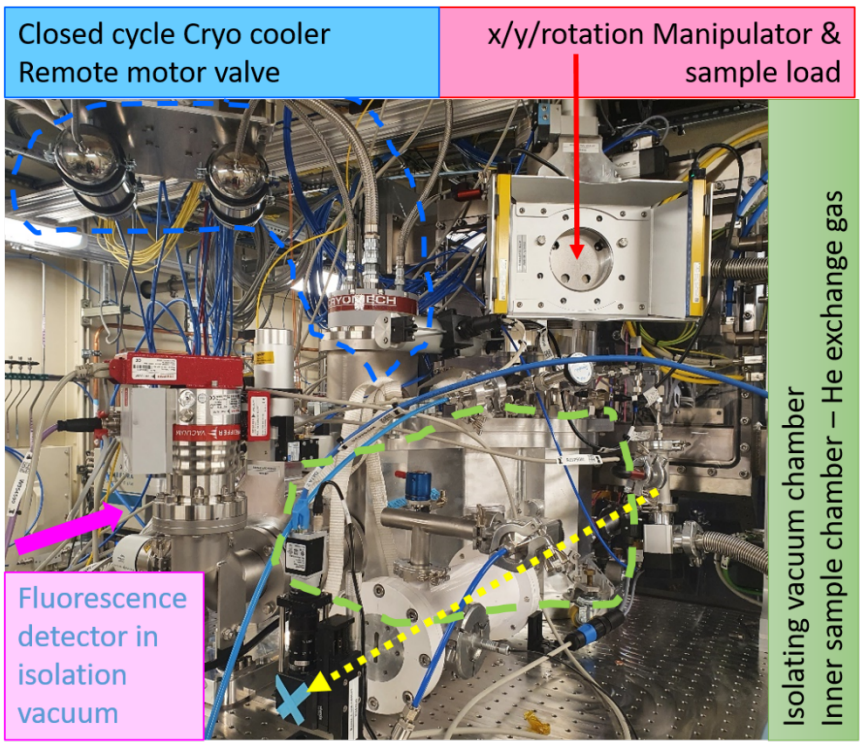

Figure 37. In-house built closed cycle helium cryostat. Remote-controlled valve and pulse tube cryo cooler encircled in blue dashed line. A sample manipulator with x/y/rotation axis moves the sample to the load valve (red arrow). Beam direction (dashed yellow arrow). Isolating vacuum chamber encircled in dashed green line. A fluorescence detector (pink arrow) is attached to the cryostat.

The decision to develop the cryostat in-house was based on the user needs. Special features are the camera for viewing samples inside the cryostat with LED light, manipulator with x/y/rotation of sample in the cold zone, solid state fluorescence detector inside the isolating vacuum, fast and easy sample change (< 10 min back to set temperature) and avoidance of any iron inside the cryostat (to avoid secondary scattering). The cryostat functions are, to a large extent, controlled by PLC logic to avoid mishandling. Typically, samples are mounted frozen and cooled by He (200 mbar) exchange gas inside the sample tail. The cooling capacity is provided by a 2W pulsed tube cryo cooler with a remotely placed motor valve (Figure 37, dashed blue line) to minimize vibrations where the two stages are connected via copper braids to the cold fingers surrounding the sample tail (upper and lower cold fingers) to provide a steep temperature gradient inside. The temperature is controlled with a Lakeshore temperature controller connected to temperature sensors and cartridge heaters on the cold fingers.

To mount or exchange the sample, the manipulator rod is driven up to the load compartment and the cold zone is shut off by a mid-valve (Figure 38). To start the exchange, the upper volume is filled with 1 bar He and the load valve is opened at the same time with a slight overpressure flow of He. The plate containing the sample is manually swapped for a new sample plate stored under LN2 within a dewar. The valve is closed and a semi-automated pump and He purge cycle starts to remove any trace of air, leaving it pumped to the same vacuum kept in the cold zone. The mid valve is then opened, and the manipulator is lowered into the cold. Exchange gas is applied and, if the whole process is completed rapidly, the temperature is back to the set values within a few minutes, typically approximately 10 min. The sample plate is made of acrylic glass and is clamped by two PEEK frames to secure the samples (liquid or solid). We have two large (ø 14 mm) or four small (ø 6 mm) circular windows to choose between within the same plate. Customized holders have been made for special user applications, for example, when mounting varved lake sediments for cryo mapping of Fe speciation.

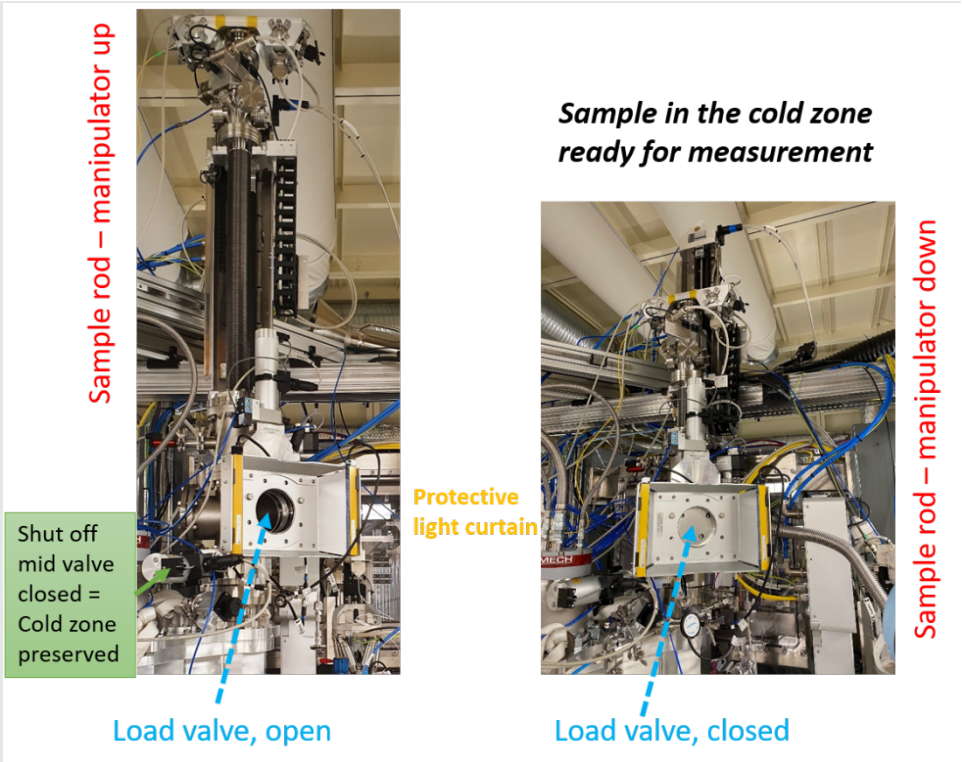

Figure 38. Sample exchange in cryostat via load valve and manipulator y movement.

Linkam Furnace

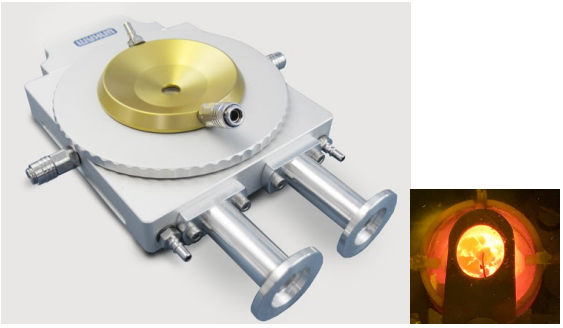

Figure 39. Linkam furnace (left) and its heated sample compartment (right) with a calibration thermocouple placed at the center of the sample. The furnace can be operated in the range RT-1100°C in a protective atmosphere.

The Linkam furnace is used if the users need to heat the sample up to 1000°C (Figure 39). It is interfaced to the PI hexapod and easy to align in the beam in either normal incidence for transmission or at 45° incidence for fluorescence collection. Heating can be controlled remotely with programmable heat rates and hold periods by a Eurotherm temperature controller integrated in the control system.

Upgrades: Vacuum Sample Chamber with Cooling and Moderate Heating (proposal)

Balder beamline aims at building a vacuum chamber with an integrated transverse 2D sample positioning system equipped with a macro camera, LN2 cooling via a retractable cold finger, electrical connections for i) moderate heating, ii) temperature sensors and iii) total electron yield (TEY) measurements. The chamber should be compatible with the two main detection schemes: a) in transmission with a downstream ionization chamber and b) in fluorescence with an orthogonally placed multi-element solid state detector.

In 2022, the in-house design office produced a preliminary design of such a chamber, shown in Figure 40. The design follows the underlying idea of quick sample changes: the cold finger is pulled off the cooling braids and shut off with a vacuum gate valve, the cold parts are heated by heating wires (the same wires provide moderate heating capability) to equilibrate with room temperature, the chamber is vented, and the sample is removed from the top lid (not shown in the design views). The Dewar and the cold finger remain cold and so the next cooling cycle proceeds quickly.

Due to the current budget restrictions the building of this sample chamber was put on hold. In the meantime, we have applied to a private foundation for a grant to finance this project (see section 7.2).

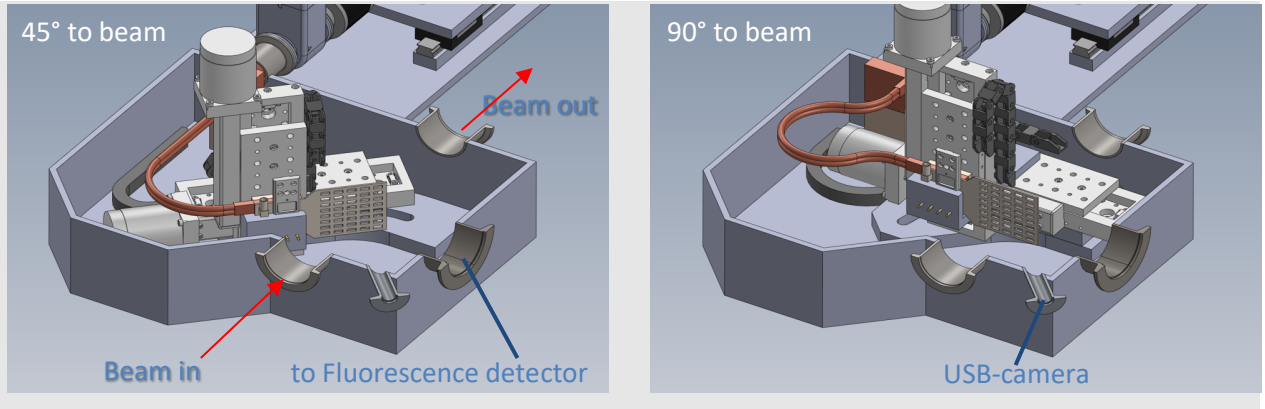

Figure 40. The CAD model of a vacuum sample chamber for LN cooling and moderate heating, shown in two geometries: for fluorescence detection (left) and for transmission detection (right). To get a scale, the beam in and beam out flanges are of KF40 type.

2.4.4 Reactors

SynRAC

The SynRAC liquid reaction cell is available at Balder for transmission mode XAS and XRD on solutions (Figure 41).[9] It is comprised of a glass reaction vessel with stirring and a heating system. Temperatures up to 180°C can be achieved within the liquid in several minutes. The application is currently restricted to energies > 18 keV due to the thick wall glass vessel and the comparably long beam path through the liquid of approximately 1 cm.

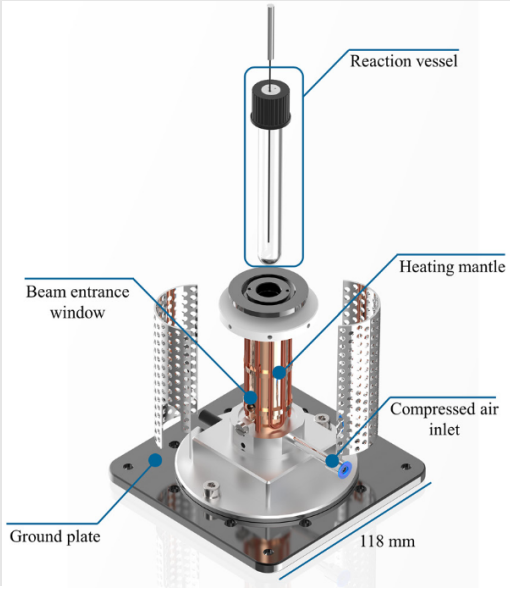

Figure 41. Schematic of the SynRAC reaction cell for liquid reactions.

Capillary Reactor

An in-house designed capillary reactor cell can be used at Balder for combined in-situ XAS-XRD measurements during gas exposure and heating (Figure 42). The cell can operate at temperatures up to 800 °C for capillaries with a diameter of 1.0 or 1.5 mm. Capillaries are held with PTFE ferrules to allow for easy and quick exchange, while being leak tight for back pressures up to 20 bar. At the exhaust connection, a thermocouple can be inserted to read and enable control of the temperature in the immediate proximity to the sample. The effective heat shields and large area silicon nitride radiative heaters achieve an excellent temperature homogeneity < 1°C at 400°C within a range of 4 mm in capillary direction. The heater power can be either regulated by the sample thermocouple or an external thermocouple next to the capillary. A stability of ±1 °C is achieved at 400°C. This cell is very frequently used for catalysis related experiments at Balder. So far, gas mixing and switching systems are provided by the users.

[9] doi.org/10.1063/1.4999688

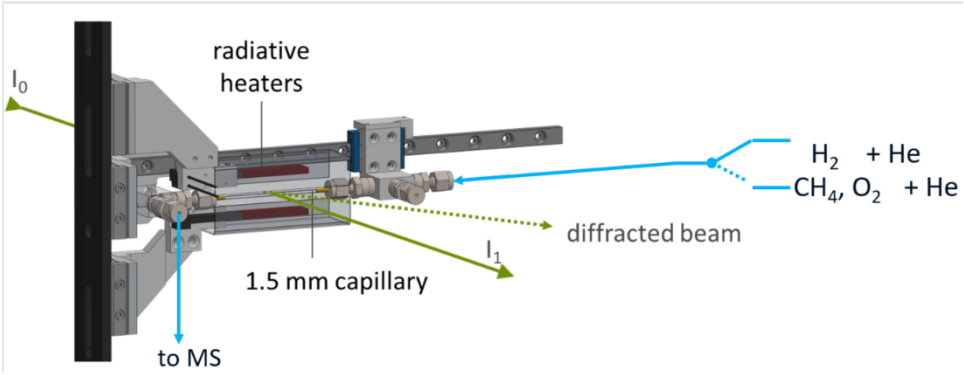

Figure 42. Schematic of the capillary cell available at Balder.

2.4.5 Liquid sample delivery

A liquid sample can be measured successfully in a **static sample cell** if it is not prone to radiation damage, i.e. solution does not contain water (see Figure 43 for an example of high *k* EXAFS of 1 M [$AuCl_4^-$] in biodiesel in a liquid cell with Teflon spacer and Kapton windows).

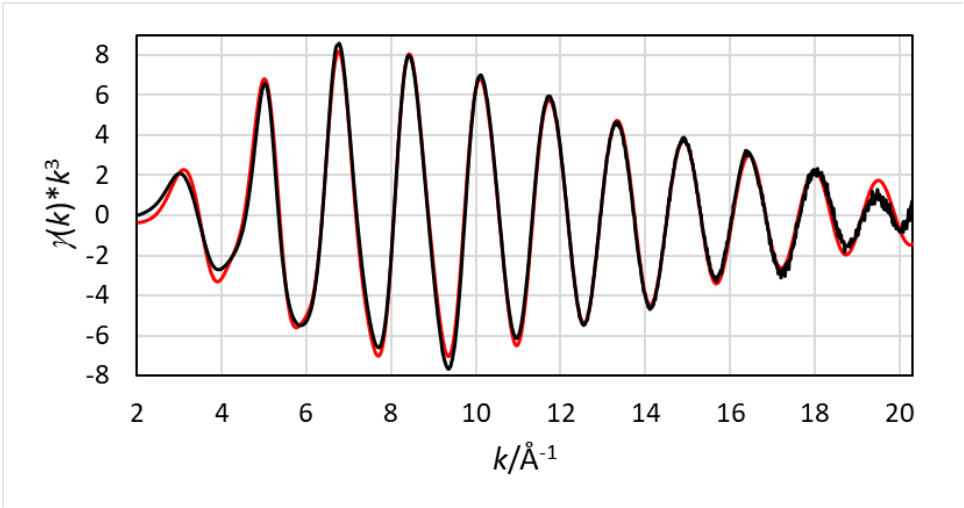

Figure 43. Au L3 EXAFS to k 20 Å-1 of [AuCl4]- complex in biodiesel/malonamide, black line – raw EXAFS data, red line – fit with Au-Cl single scattering and inner-core multiple scattering fitted to k 19 Å-1, measured in a static liquid sample holder in transmission. (FA proposal, I. Persson).

As soon as water is present in the sample mixture, bubbles and radicals are produced via radiolysis, which change the chemistry in the sample. For these types of samples we provide flowing sample environments. Microfluidic flow cells and flow control, developed in a SSF funded project called **AdaptoCell**, are available at Balder. We have several devices of different materials adapted for different X-ray energies and needs available (e.g. COC polymer or Si-glass microfluidic chips). In addition to applying flow to the sample, these cells can be used to mix reactants and observe reactions or changed conditions *in situ*. The time resolution is given by the flow rate (between 1000 and 10 µL/min) and different time points can be probed along the channel length (in the range of tens of sec to tens of ms). In addition, through the Adaptocell project, a specially designed chip for XAS and SAXS with co-flow (hydrodynamic flow focusing) is available at Balder (see Figure 44 for design and test results at Balder).

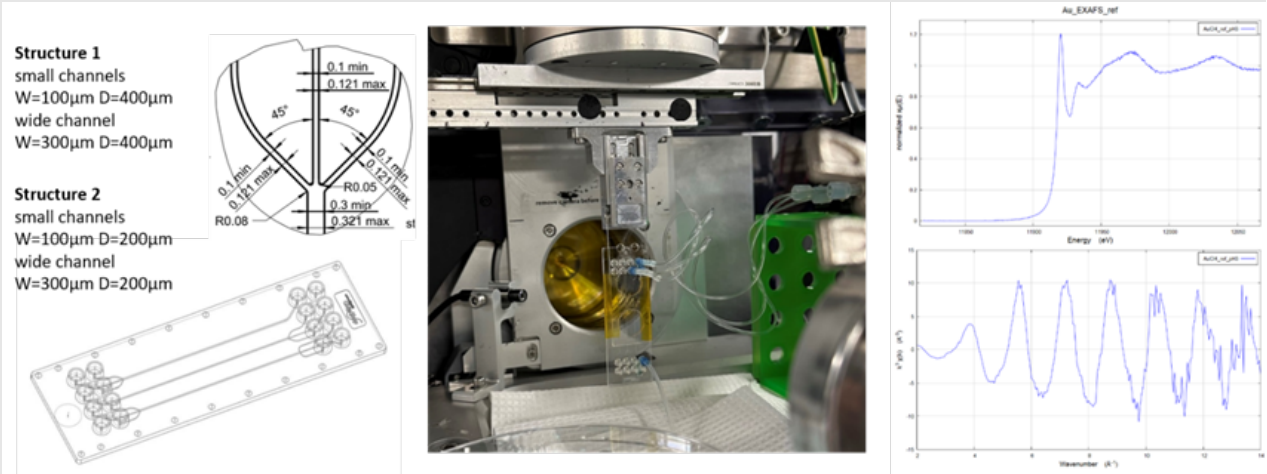

Figure 44. Left panel, AdaptoCell device in COC polymer, in-house design produced by "Microfluidic ChipShop", optimized for XAS/SAXS with co-flow geometry. Three individual observation channels (wide) with flow focusing geometry (three small inlet channels). Mid panel, microfluidics set up at Balder with the same device. Right panel, data collected in "structure 2" of the device at Au L_3 edge on $AuCl_4^-$ in water solution (20 mM) in fluorescence mode with Ge detector. In water, is Au^{3+} sample extremely prone to radiation induced reduction to Au^{1+}. Sample flow was 120 µL/min, 1 min/scan, shown spectrum is average of 15 scans.

The pressure driven flow control system used for the microfluidic chips can also be connected to other liquid flow cells, for example, an electrochemistry cell for small volumes (see Figure 45).

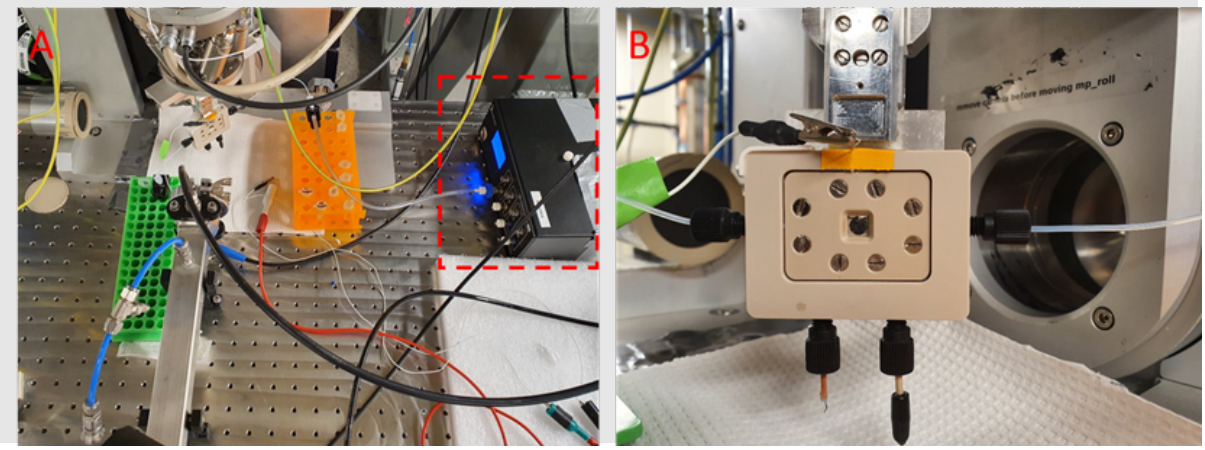

Figure 45. Electrochemistry flow cell for small volumes, here used with an iron protein 1 mM. A) Overview at the beamline, precise control with pressure driven flow controller (OB1, Elveflow, red dashed rectangle). Sample in Eppendorf tubes with special caps for pressure. B) Close up of the cell made in PEEK.

A recent development for liquid sample delivery, provided via an *in-kind* contribution from Uppsala University (P. Wernet group), is the **liquid jet** for windowless sample flow delivery, see Figure 46. The flow speed is much higher than for the microfluidics set up, but the volume dimensions are larger and therefore similar timescales can be probed (10 - 30 mL/min allows timescales of seconds to ms to be achieved depending on the tube volume). It works by jetting the liquid out from a capillary (1 - 1.5 mm diameter) with a catcher below, the liquid being actively pumped by two high power peristaltic pumps, one supplying liquid to the jetting capillary and the other removing the liquid from the catcher. The pump systems are connected so that the liquid is recirculating.

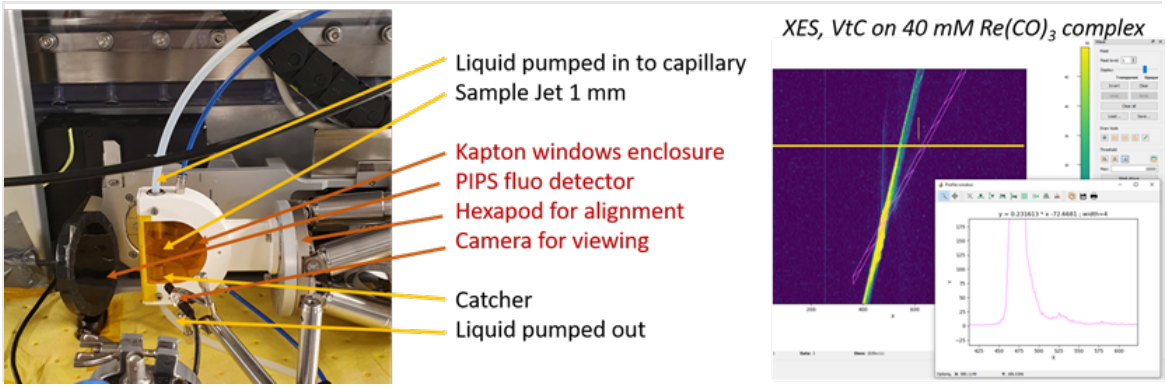

Figure 46. Liquid Jet set up at Balder. It was used together with the XES spectrometer to detect VtC (valence to core) emission bands on Re complexes, example spectrum to the right.

2.4.6 Specialized user sample environments

Many experiments proposed by users require unique sample environments in order to facilitate effective beamtime measurements. This prompts the beamline staff to arrange for, and in some cases design, compatible sample environments that best fit the planned measurement strategy. The sample environment team at MAX IV is able to provide 3D printing of adapters that are used to tailor already existing sample environments (Figure 47).

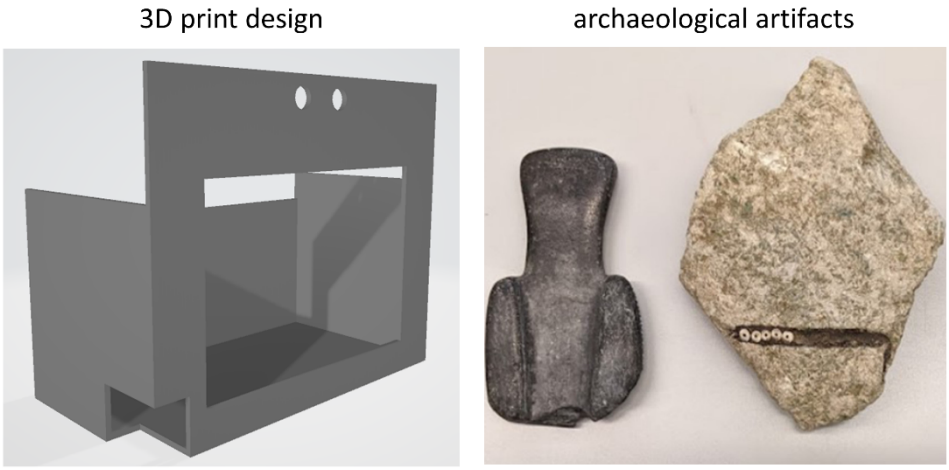

Figure 47. Example of 3D printed sample holder for unique samples.

Below are descriptions of a few other specialized sample environments used during beamtime.

Operando battery full and half-cells

A variety of sample-environments have been used at Balder for operando battery cycling experiments. Some examples are AMPIX[10] and pouch-cell holders[11] which can be used for simultaneous experiments on multiple cells (Figure 48). For operando battery cycling measurements are designed specifically to allow transmission XAS and XRD measurements for both half-cell and full-cell configurations. A typical measurement sequence

[10] doi.org/10.1107/S0021889812042720
[11] doi.org/10.1002/batt.202100126

consists of XANES/EXAFS measurements on one or several absorption edges to track the oxidation states and changes to the coordination sphere around the absorbing atom due to ion-migrations, as well as one or more XRD patterns to allow identification of different phases and accurate estimation of lattice parameters at different stages of the charging cycle. For slow cycling experiments (with charge-discharge rates of 1 C or below), one can perform measurements on many cells simultaneously with sufficient data points during every cycle. Hence, users are both encouraged and provided support to design holders for cycling multiple devices synchronously (Figure 49).

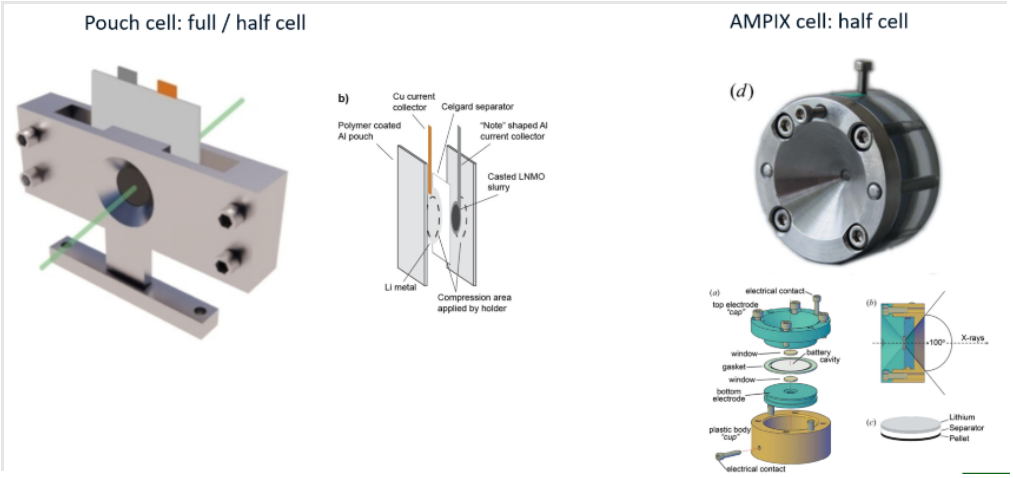

Figure 48. Setups used for operando battery cycling measurements at Balder.

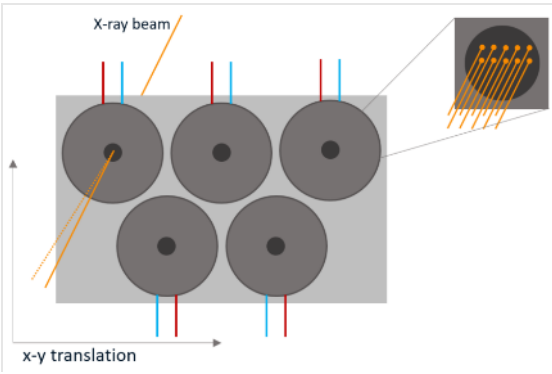

Charge / discharge rate	Number of devices	measurements per cycle
0.1 C	1	15.000-36.000
	5	2.900-7.200
1 C	1	1500-3600
	5	290-720
10 C	1	150-360
	5	29-72

Figure 49. Schematic representation of a holder for performing simultaneous measurements on up to 5 cells. The table shows the typical range of the number of measurements that can be carried out per charge-discharge cycle for different cycling rates.

In-FORM

The in-FORM platform was developed within a recently concluded project and is now available to users. It enables in-situ measurements of XAS, XRD and X-excited optical luminescence during solution-to-solid-state reactions after thin film deposition, as employed in the fabrication of perovskites for photovoltaics or deposition of battery electrode materials. The in-FORM platform is essentially an in-situ robotic slot die coating device which is integrated into the Balder beamline, as depicted in Figure 50. It is comprised of a basic roll-to-roll architecture with 30 m of substrate, allowing for up to 300 individual coating processes in one run. For easy adaption to different material systems and process designs, it is comprised of modular components for deposition, solvent extraction, and two zone annealing (up to 350°C), which can be arranged flexibly and allow for in-situ X-ray characterization at every processing step. The system is equipped with an advanced self

cleaning mechanism to automatically clean the slot-die coating head and tubing system assuring uncontaminated processes, even when changing the composition of the ink. A separated ink-feed and mixing system allows the mixing of up to two precursor systems for performing combinatorial experiments on an automated base. The whole system is placed in two small footprint controlled environment boxes to perform synthesis processes under the exclusion of oxygen and moisture, as necessary for many state-of-the-art battery and photovoltaic synthesis processes.

The coating system is fully remotely controllable and can perform up to hundreds of coatings under different parameters without direct manual intervention. This is an important prerequisite for enabling X-ray measurements at a beamline where no experimentalist can be present during actual experiments, considering the high radiation dose in the experimental hutch. The internal instrument communication is handled via CAN-Bus. We developed a python based integrated command based control system for user operation: It exhibits low level commands for motion or ink-feed, e.g. mvr band 20 (for performing 20 cm of band motion) or inject 1,10,1 (for 10 µl ink feed from syringe 1 with 1 µl/s) as well as high level commands for processes and cleaning, e.g. experiment (0.5,1,0.3) (to perform a full experiment with coating, solvent extraction and annealing with a coating speed of 0.5 cm/s, an ink feed of 1 µl per cm substrate at a coating head distance of 0.3 mm. A benchmarking of the coating system by means of film homogeneity of the as-coated and annealed film (Figure 51) demonstrates exceptional control for an in-situ device. For mitigating beam induced effects in the hard X-ray based characterization, we implemented direct communication with the beamline control system for controlled material renewal at the measurement position. The above described instrumentation is unique worldwide in terms of (i) high-throughput and automation, (ii) the combination of X-ray spectroscopy and diffraction techniques and (iii) its performance in terms of precise control of synthesis conditions for such a small footprint system. Experimental data from this system can be found in the in-house research section of this document.

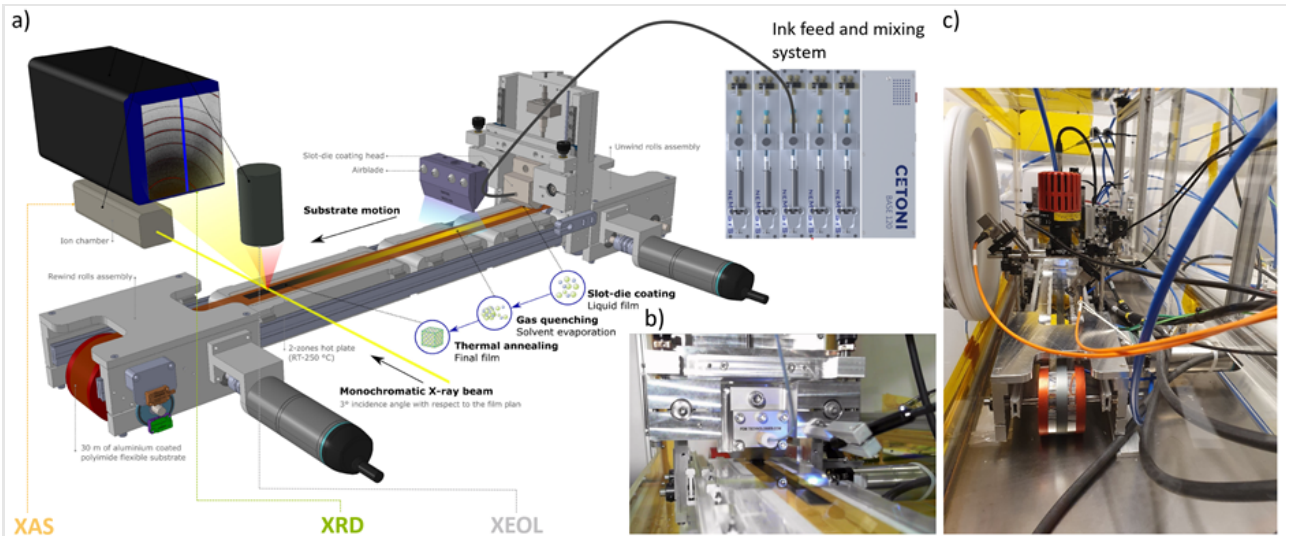

Figure 50. a) Technical 3D rendering of the as-developed robotic slot-die coating system with in-situ measurement capabilities for XAS, XRD and XEOL. b) Roll-to-roll coating tests of the as built system c) longitudinal view into the in-FORM instrumentation equipped with in-situ optical probes and enclosed in a controlled environment box.

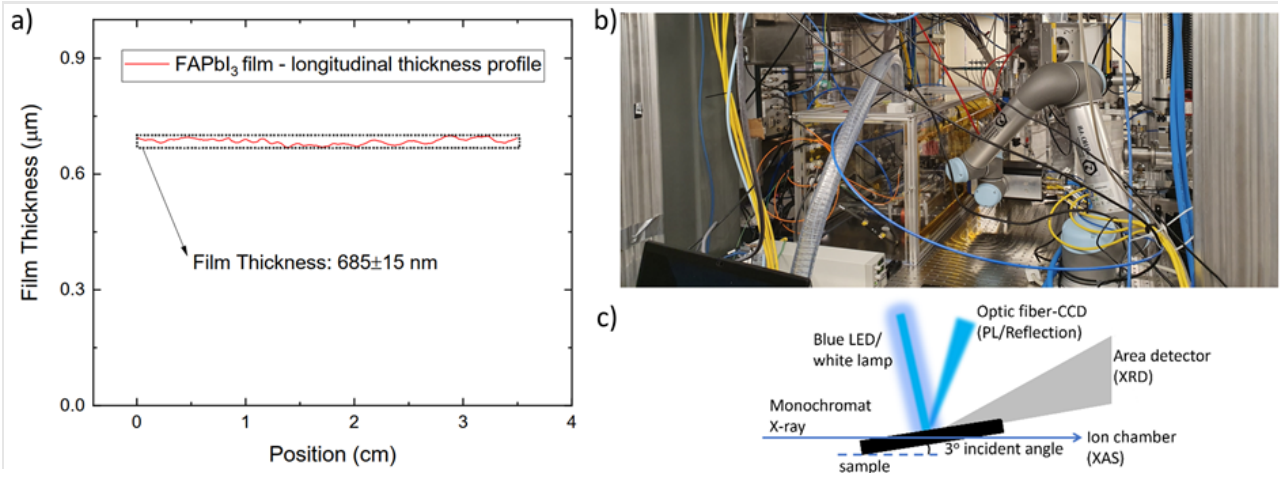

Figure 51. a) Measured film uniformity by means of X-ray absorption for an as coated film in the developed in-FORM coating system. b) Picture of the beamline-integrated setup c) Schematic of the beam and measurement arrangement for in-situ measurements during coating, solvent extraction or annealing within the in-FORM setup.

2.5 Experimental infrastructure

2.5.1 Gas system (including IC filling)

The *ion chamber gas filling* system is currently being updated (Figure 52). This includes the assembly of new hardware and integration of software and PLC control into the beamline control system. From early 2024, this will enable staff and users to reliably adjust the ion chamber gas filling to experimental requirements.

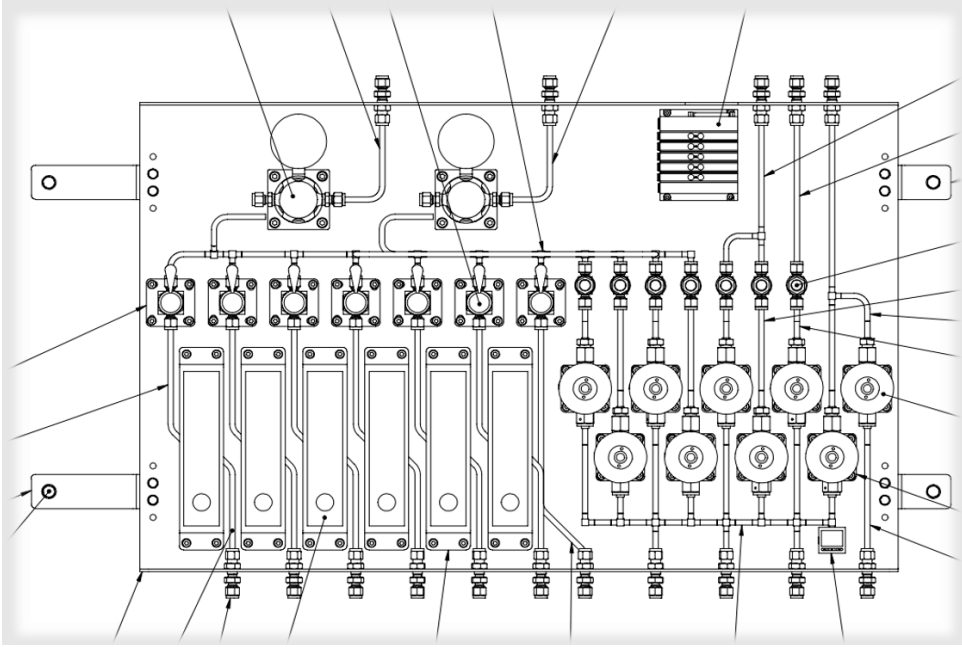

Figure 52. IC filling panel for automatic filling of ionization chambers (N_2, He, Ar, Kr) and dosing of inert gases for cryostat (He) and Eiger detectors (N_2).

The major *Balder gas system* will support dosing and mixing of gases at pressures up to 40 bar and with gas flows up to 100 ml/min. The system is designed to handle the following gas types: He, N_2, Ar, Kr, O_2, Air, CO_2, NO, NO_2, SO_2, H_2, CO, C_xH_y, SYNGAS, NH_3, and H_2S. Gas cylinders for flammable gases are separately stored in

an ATEX/Ex classed storage room and the rest of the gases are installed in a second gas-storage room (Figure 53). Sulphur-containing gases are stored in two gas cabinets located inside the experiment hutch. From the gas-storage rooms and cabinets gases are passed to the gas-mixing system through orbital-welded stainless tubing. Gases passing through the mixing system is then led to the experiment (reactor) through stainless-steel capillary tubing and continues after the experiment through heated tubing to mass spectrometers and exhaust ventilation.

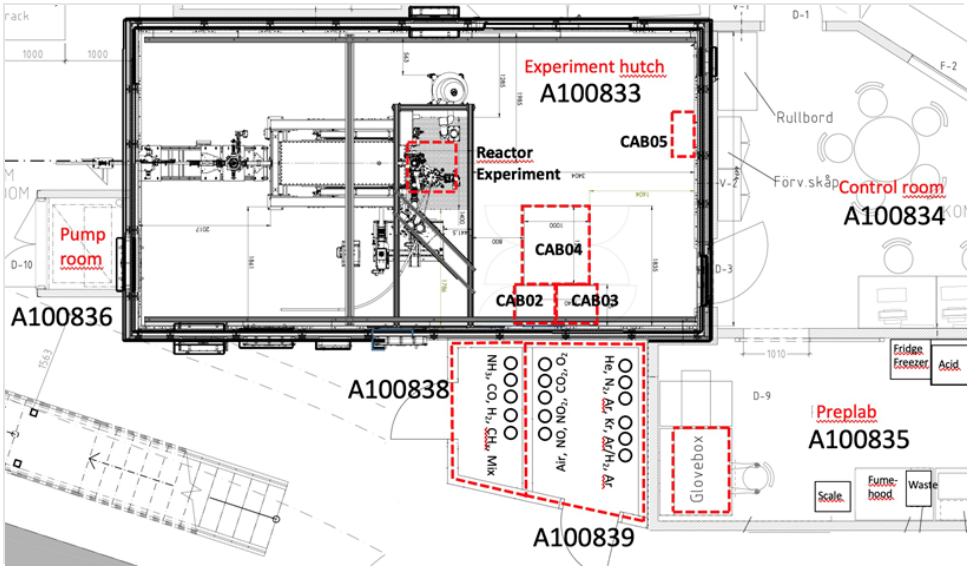

Figure 53. Balder floorplan. A100838: Storage room for flammable gases. A100839: Storage room for non-flammable gases.CAB02: Cabinet for H_2S cylinder. CAB03: Cabinet for SO_2 cylinder. CAB04: Gas-mixing cabinet. CAB05: PLC cabinet for the gas-mix system.

The gas-system project managed by the Central Project Office (CPO) is complex with dependencies on the overall MAX IV ventilation system and strict safety regulations, such as ATEX/Ex and gas detection/alarm systems. The project status is given in Table 2. Completion of the gas-system project is expected in 2024/2025, date pending rework of all beamline ventilation. Forsee full user operation in 2026 (7.2).

Table 2. The status for the different parts of the gas-system project.

Installation	***Status***	***Remaining work***
Gas storage	Installed and pressure tested	ventilation and gas alarms
Inert gas supply, detectors	BPAG project, in construction	Construction
Inert gas supply to glove box	Installed and pressure tested	Glovebox
Gas-mixing system	Installed	Pressure test
Gas analysing, mass spectrometers	Installed	Control system
Ventilation of exhaust gas	Partly complete	Installation
Pumping system	To be purchased	Purchase and installation
Gas detection for safety system	Ongoing installation	Installation and tests
PLC system control	Ongoing PLC programming	Programming and tests
Tango user interface	Planning stage	Programming and tests

2.5.2 Balder chemistry lab

Adjacent to the control room and experimental hutch is Balder's own chemistry laboratory with equipment available for modest wet chemistry and sample preparation, including a glovebox and a fume hood (Figure 54). This lab is available for users during their beamtime. The list of specialized equipment is listed below (Table 3). For more vigorous sample manipulation and/or laboratory needs prior to beamtime, users are directed to book the Hard X-ray Biology and Chemical labs. Numerous chemicals are stored and available to users in the ventilated storage cabinets for corrosive, acid and base, and flammable compounds. Chemicals frequently used at the Balder lab are diluents (boron nitride, cellulose, polyethylene). High purity commercial compounds are mostly available for the development of the reference standard library SpecTable, see 2.5.3. Users highly appreciate that anaerobic sample manipulations inside the dry glovebox can be performed near the experimental hutch.

Table 3. List of equipment in Balder lab.

Equipment	Description
Balance	Sartorius, 0.001g
Fridge	ATEX/EX classed
Fume hood	
Glove box	MBraun Labstar, Ar atmosphere, including O_2 and H_2O analyzers, balance (0.001 g), pellet press, video microscope
Heating cabinet	Binder 28 L, 230°C
Microscope	Leica Zoom 2000, 45X
Pellet press	Specac 10 ton press, 5 and 13 mm diameter pellets
pH meter	Hanna 212
Centrifuge	Eppendorf 5804 R, -9 – 40°C, 0.2 – 250 ml tubes
Ultra-pure water	Millipore, Direct-Q 5, Type 1 water

Figure 54. A user preparing samples for an in-situ experiment at Balder chemistry lab.

2.5.3 SpecTable - Reference and Standard Library

Balder has invested in a series of chemical compounds for preparation of an online absorption spectral library of model compounds titled SpecTable (Figure 55). In collaboration with MAXESS industry arena (via MAX IV industry office), access to the SpecTable library is intended to be available online for use by the broader user community. Raw data of model spectra will be progressively uploaded by beamline staff as measurements have been collected. Web visitors are able to search and filter queries to selected spectra. Visitors will also be able to download spectra and data files with original metadata.

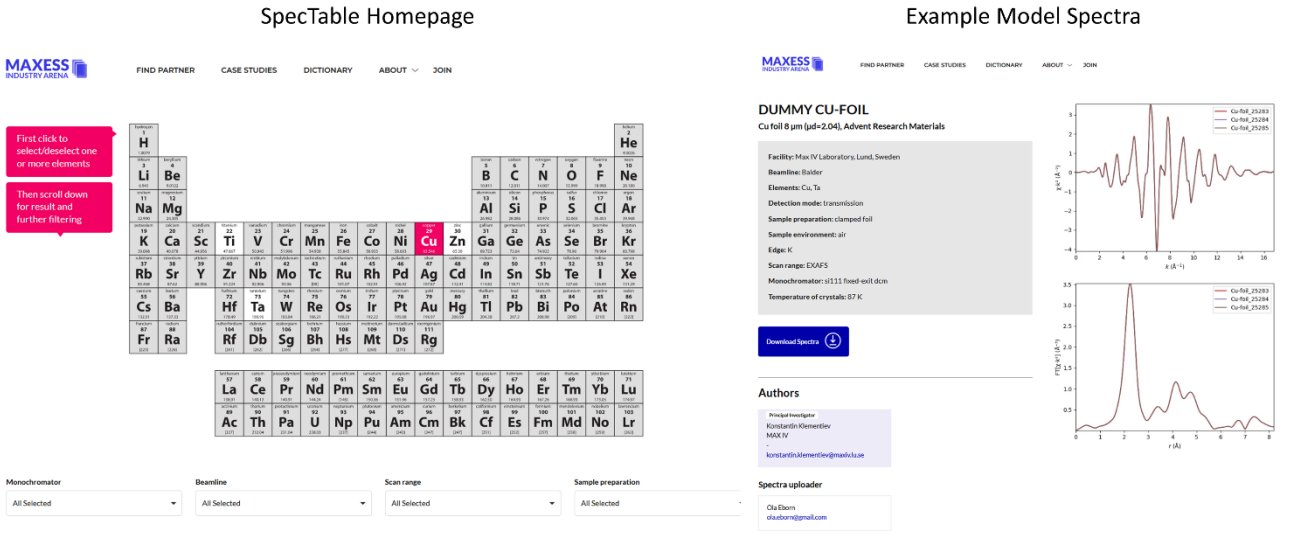

Figure 55. Homepage for SpecTable and example model spectra. (currently under construction)

2.6 User interface & Data pipeline

User interface to Sample viewing

Both the ambient sample stage and the cryostat have borescope, a macro camera with a working distance ~4 cm that views the sample at ~45° angle. The camera also has 4 illumination LEDs. Based on this camera, we have created a widget *OrthoView* that internally transforms the image scene distorted by the off-axis viewing to an orthogonal view where physically horizontal and vertical lines appear horizontal and vertical on the image, see Figure 56. After this transformation, one can command x and y motions by simply clicking to a point on the image. This point will move to the previously calibrated beam position on the image.

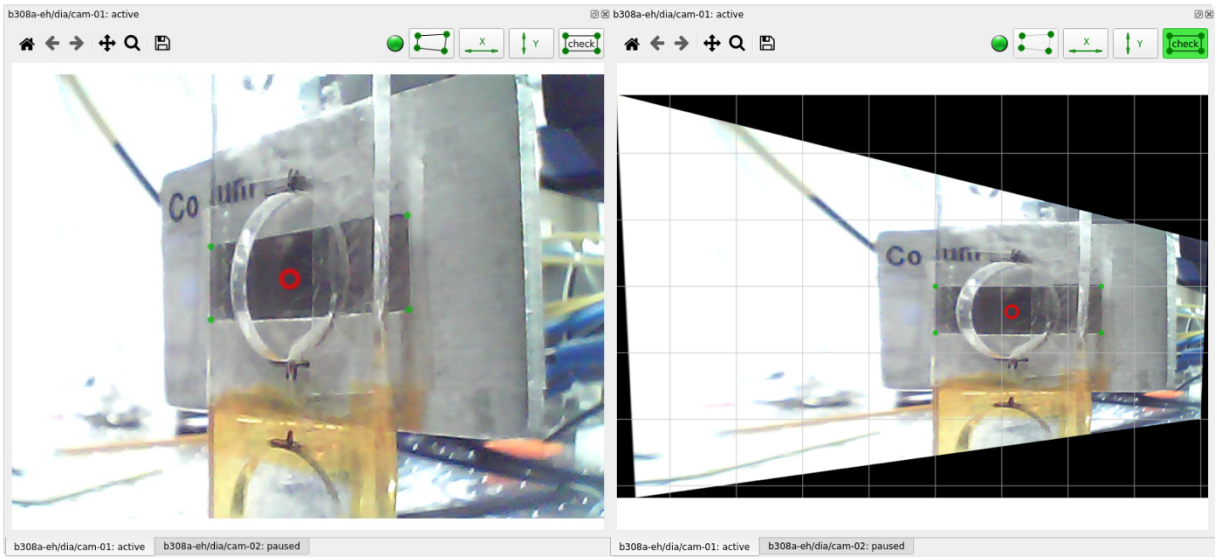

Figure 56. Balder's OrthoView widget. Left: the original view as seen by the camera. The user defines 4 corners of a rectangle with horizontal and vertical sides and specifies its sizes. Right: the verification view that demonstrates the orthogonalization transformation. The red mark encircles the beam position that was defined there by means of visualizing the beam with a fluorescence screen.

User Interface to Scans

General scanning facilities are provided by the control system Sardana, which is a software system built over the device managing system Tango. The required scan parameters (range, step size, dwell time, number of repeats) are typically set from a python script edited by the user. Using scripts, rather than a GUI, allows greater flexibility to interface with any device defined in Tango.

The scan visualization at Balder was specifically built for the needs of XAS (see Figure 57). The user can see the resulting EXAFS spectrum in real time, both in *k* and Fourier transformed space.

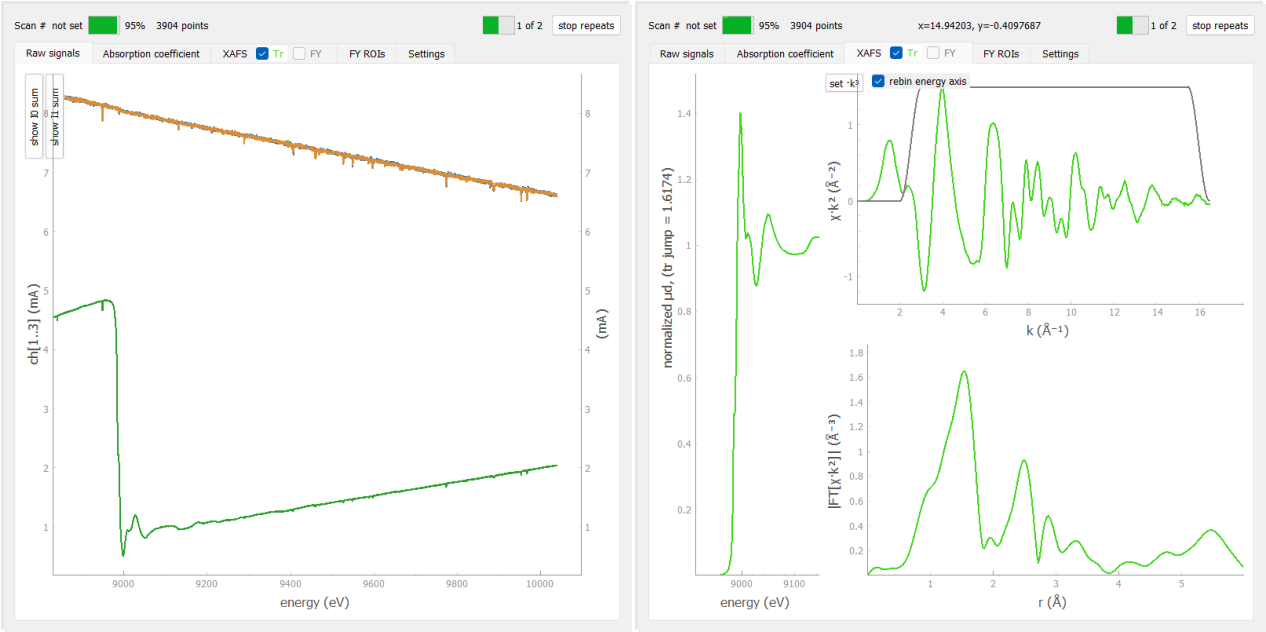

Figure 57. (animated in gui-EXAFS.gif) Raw signals (left) and XANES and EXAFS parts of the absorption coefficient (right). The top and bottom parts of I0 signal (orange and blue) are dynamically kept equal by MoCo, see section 2.1.1; the actual I0 is obtained as the sum of them.

XAS Data Analysis Pipeline

All measured scans are saved by Sardana to a large hdf5 file. XAS scans are additionally saved to separate column text files with user-defined file names that are suffixed by system-unique scan IDs. These ascii files are compatible for analysis in common EXAFS analysis programs. We also offer an analysis pipeline *ParSeq – XAS*[12] that can automatically load scans upon completion of data collection and display them side by side in various plots to comparatively check data quality and reproducibility, see Figure 58.

[12] github.com/kklmn/ParSeq, github.com/kklmn/ParSeq-XAS

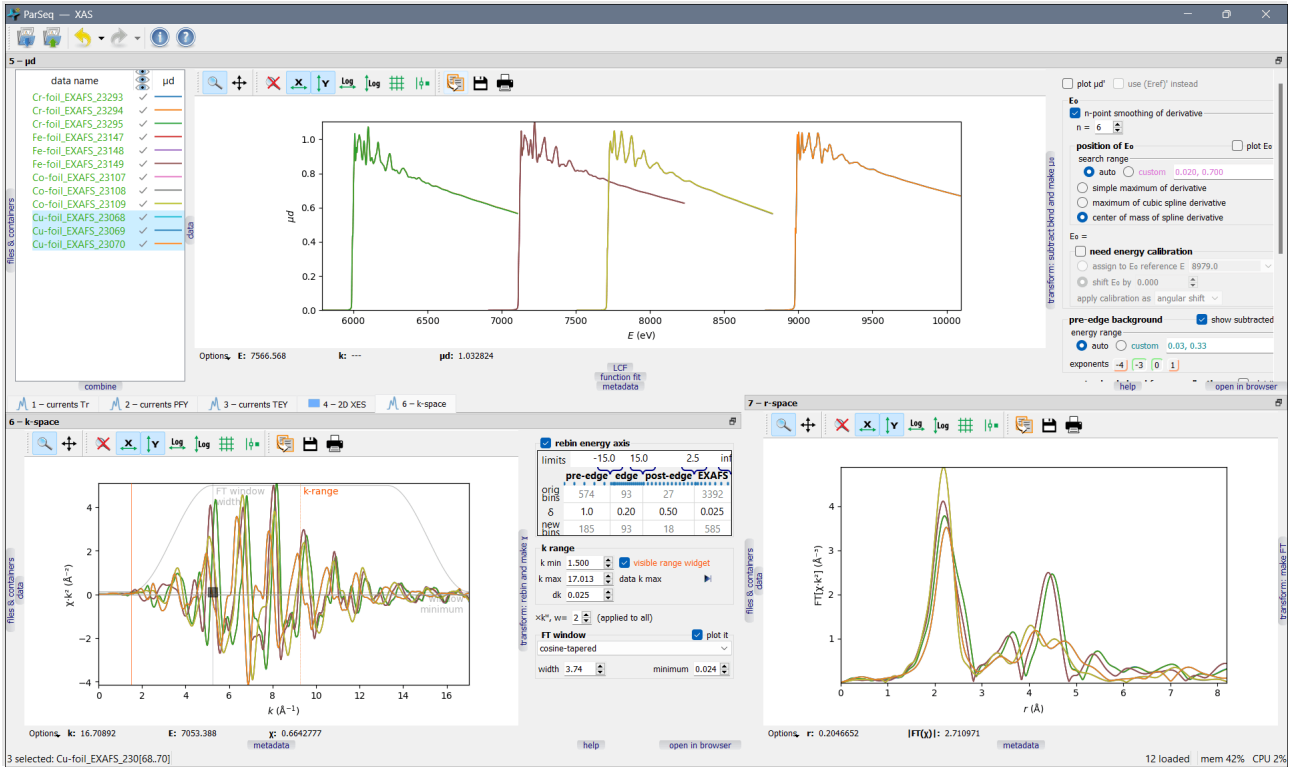

Figure 58. ParSeq – XAS analysis pipeline displaying four metal foil spectra, each measured with three repeats. The curve colors are common in all plots.

Live-view MCA spectrum/map XRF

Live viewing of 2D mapping can be set up with user-defined elements of interest or total ICR (incoming count rates) (Figure 59). Users can select single or sum multiple detector elements depending on the detector chosen and elements available. Each pixel contains x and y motor positions in order to set up subsequent scans. Based on the Silx viewer[13], line integration and masking operations are also available.

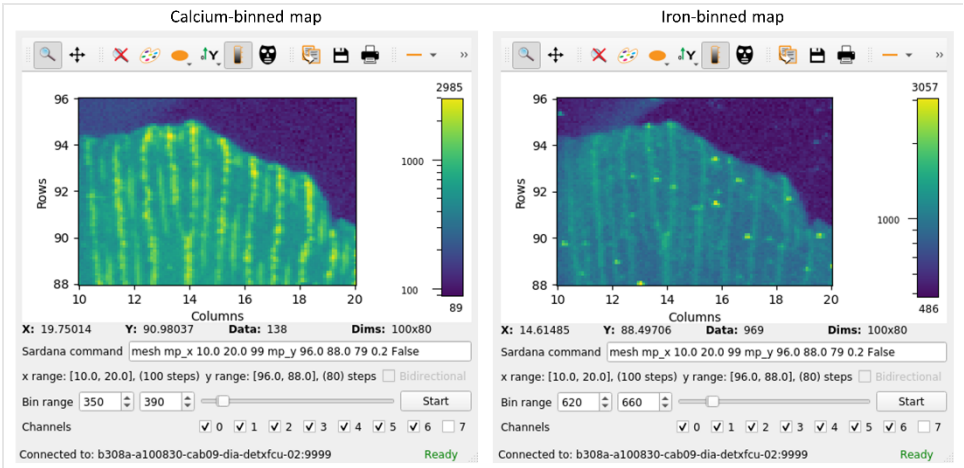

Figure 59. XRF live viewer.

[13] http://www.silx.org/

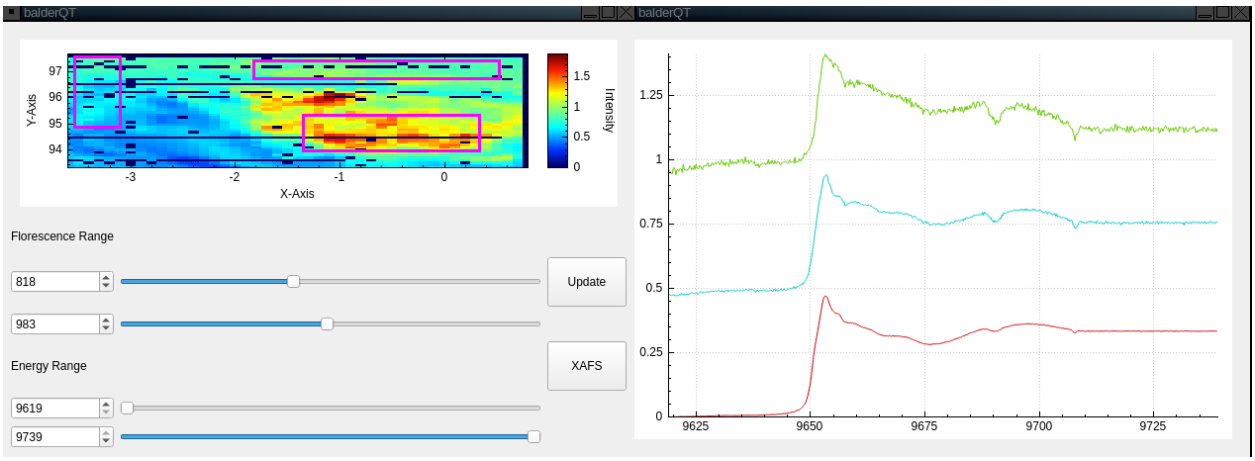

Figure 60. A new program to extract XRF maps and "region XANES" from our new "rapid XANES mapping" strategy in development.

A fast map-XFS slicer and viewer (Figure 60) for integrating regions of the XRF-maps within any region of interest (not just the range specified during the user experiment) displays the EXAFS data from any number of geometric regions, and comparison with the fluorescence intensity of other elements in the sample. This can be achieved with typically 1-2 second response time.

Live-view and azint pipeline for XRD

During XRD acquisition, live 2D data is streamed out of the EIGER detector and can be viewed on a simple image viewer (Figure 61). The viewer enables the user to define a mask to blank out the *hot pixels* either via a static or a dynamic mask threshold value. Even though only the reduced data is used for quantitative analysis, 2D diffraction images provide valuable information regarding the sample morphology, grain size and texture.

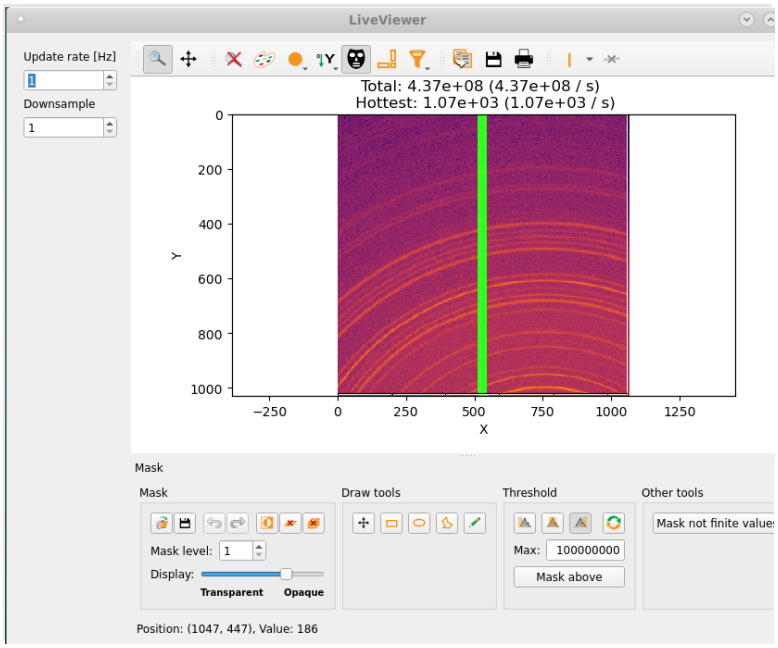

Figure 61. The XRD live viewer showing the 2D diffraction image following a simple mask operation.

Azimuthal integration can be done either live via a dedicated pipeline, or offline on the MAX IV cluster or local machine, based on needs of the experiment (Figure 62). A pipeline has been developed at Balder which performs real-time data reduction on the MAX IV DAQ cluster to produce one dimensional curves of I vs q (or

2θ) using information from the PONI file provided by the user. This is especially useful to monitor, in real time with a 1 to 5 Hz display, the progress of a reaction during an in-situ process where sequential XAS-XRD measurements are carried out with a time sub-second resolution.

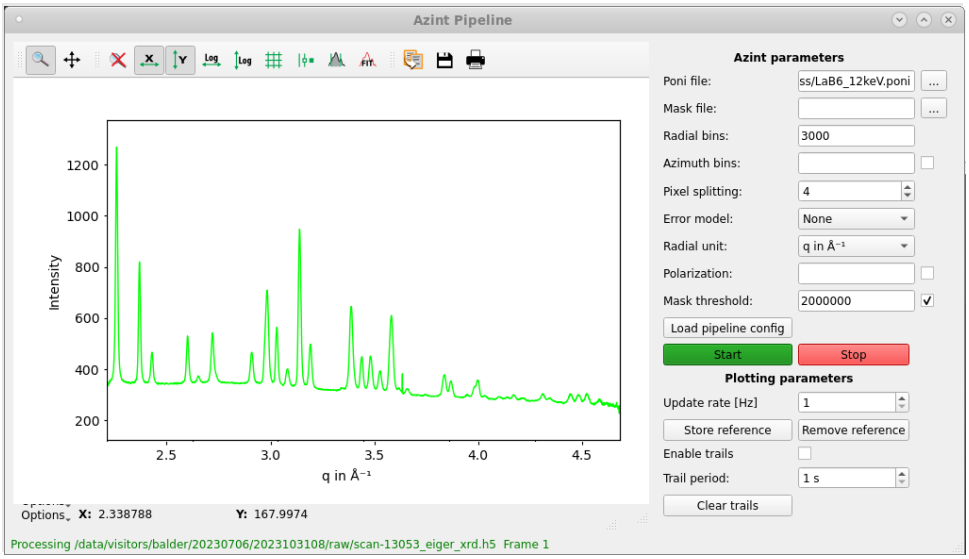

Figure 62. The azimuthal integration pipeline showing integrated 1D data.

XES data analysis pipeline

The XES scans (rocking curves from the analysers) can be viewed by the analysis pipeline *ParSeq – XES scan*[14] that can load available scans and display them side by side in various plots to comparatively check data quality and reproducibility, see Figure 63.

[14] github.com/kklmn/ParSeq, github.com/kklmn/ParSeq-XES-scan

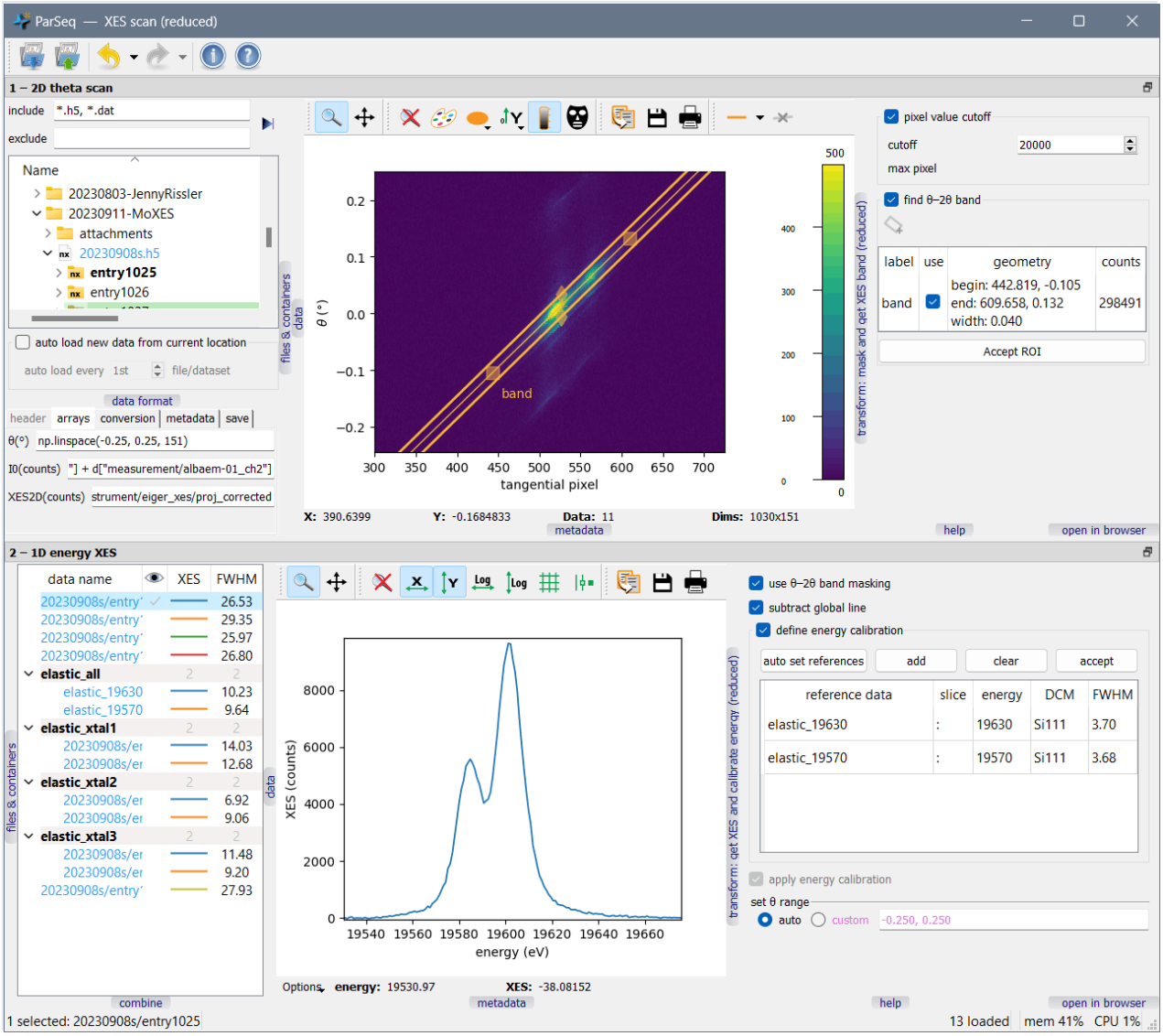

Figure 63. XESSCAN. The XES data analysis pipeline. The top plot stacks the reduced Eiger images (2D to 1D) into a 2D plot with the ordinate being the scanning axis. One defines a θ-2θ band that after energy calibration by means of elastic scans yields the XES spectrum seen on the bottom plot.

Jupyter Notebooks

While the pipelines provide a real-time data visualization, they are often not useful for detailed data analysis. A typical example is an in-situ experiment where multiple elemental edges and XRD patterns are measured in a repeated sequence. In this case, XAFS at each edge needs to be analyzed separately and compared with one another and with XRD. For this purpose, Jupyter Notebooks with interactive widgets have been developed where users can perform custom analysis and plotting (Figure 64).

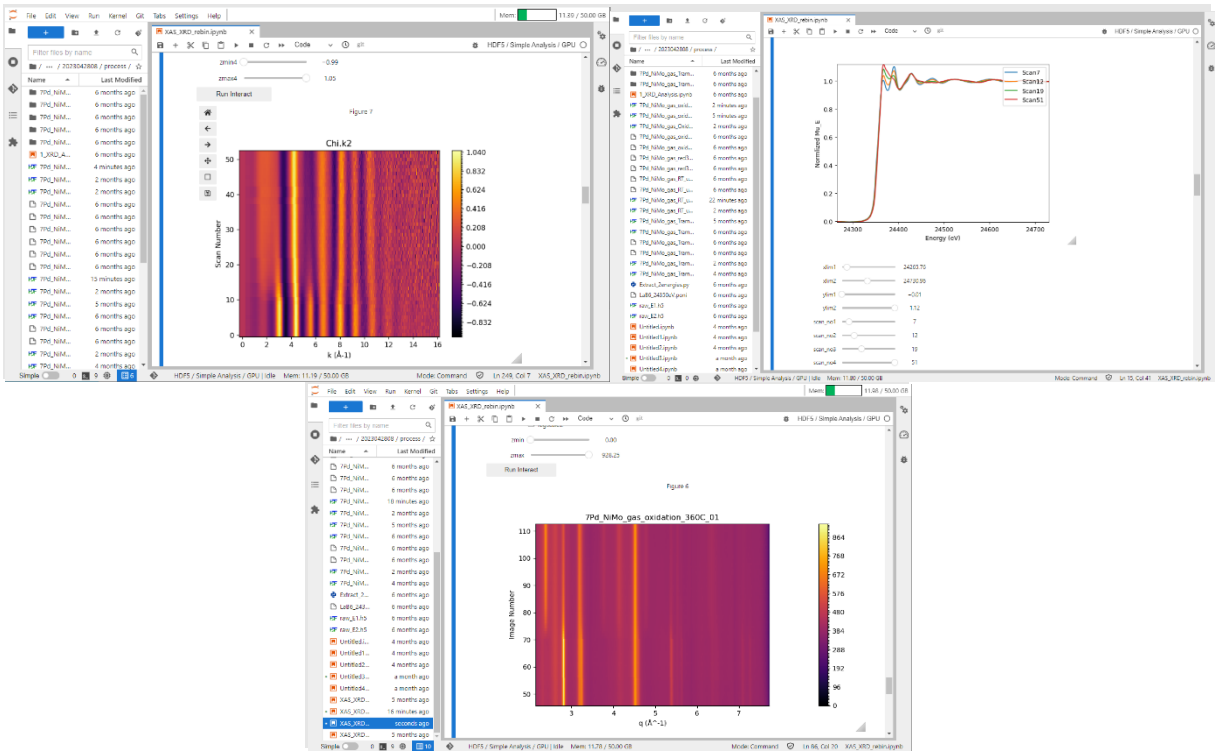

Figure 64. Screenshots of interactive widgets on Jupyter showing changes during an in-situ reaction: 2D map of EXAFS (top-left), azimuthal integrated XRD (bottom) and 1D XANES (top-right).

Moreover, these notebooks can be accessed by users after their beamtime using the MAX IV VPN, thereby making it easier to perform post-analyses without the need for downloading large chunks of raw data (especially when XRD is used) to their local machines.

2.7 Beamline documentation

Communication and documentation are carried out through multiple channels (Table 4).

Table 4. Summary of communication channels used by the beamline.

Platform	Purpose
Microsoft Teams	Microsoft Teams is presently used to reach everyone in the beamline team at the same time. We share a team and work on 8 different channels focused on particular areas: General, Balder beamline meetings, Balder projects, Balder status, Beamtime related, Cryostat meeting, (Journal club), KITS communication and SCANIA-2D. Documents are mainly shared in files under the General channel.
Elogy	This is a web-based logbook available on the MAX IV network, is used for error logs at the beamline, experimental parameter setup, and some “how to” procedures. Users are welcome to use this platform for detailed lab notes.
Wiki	MAX IV Wiki is used to document “how to” procedures such as troubleshooting solutions. The content should be reviewed twice a year to ensure the information is up to date.

Pidgin	Pidgin is a chat room to communicate with other R3 ring beamlines and machine operators.
Balder web page	The Balder web page is used for communication with users and external research community. This is updated before every proposal-call with the correct information. Has a potential to be used more for “highlights”. This is the only information available externally to MAX IV, i.e. without registering for a MAX IV account.
Sphinx	For documentation of the beamline as an ultimate user guide. However, this has just started and needs to be filled with content. Can in the future replace the wiki page for users at the beamline (available through V).

3 Beamline operation

3.1 Modes of operation and statistics

Beamtime allocation of the total available beam shifts follows the 75% to user and 25% to in-house activity share. As an example, in Fall 2023 (present cycle) this corresponds to 468 shifts of 624 to users (a shift is 4 hours). The in-house share includes commissioning activities, regular maintenance, in-house experiments, and will be discussed further in chapter 4. In the user share, different access modes are included. The access modes available at Balder are: Standard Access (59.7%), Fast Access (SMS and SF, 5.2%), Proprietary Access (5.2%), Training & Education (2.6%) and new for this year Guaranteed Access Time (2.6%). The percentages given in parentheses reflect the Spring 2024 call cycle.

Standard access mode has a new call every half year. The spring call reaches from March to June (13 weeks), and the fall call give you beamtime in September to February (18 weeks). Submitted proposals are evaluated by the Balder team for technical feasibility and by PAC (proposal advisory committee) for scientific excellence. Proposals are either accepted, refused or put on a reserve list.

Balder is a highly demanded beamline with typically 40 - 50 standard access proposals/cycle (Figure 65). This makes Balder one of the most popular beamlines at MAX IV and has for the last years had an oversubscription rate between 4.6 and 2.5 (higher on the shorter spring cycle) (Figure 66). For the last two years, the oversubscription rate was 3.6 on average over the spring and fall cycles. During the pandemic 2020 – 2021, the statistics are skewed as the more “complicated” proposals from VT20 (Spring 2020) that could not be measured by remote mail-in service were postponed and instead were measured during fall 2020 and 2021 period (Jan-May 2021 MAX IV had a Covid-19 motivated warm shutdown). Therefore, only a few new proposals were accepted from the merged 2021 cycle. The discrepancy between “accepted and finished” in Figure 65, depicted in the standard proposal calls over the years 2019 - 2023, is due to executing proposals from the reserve list.

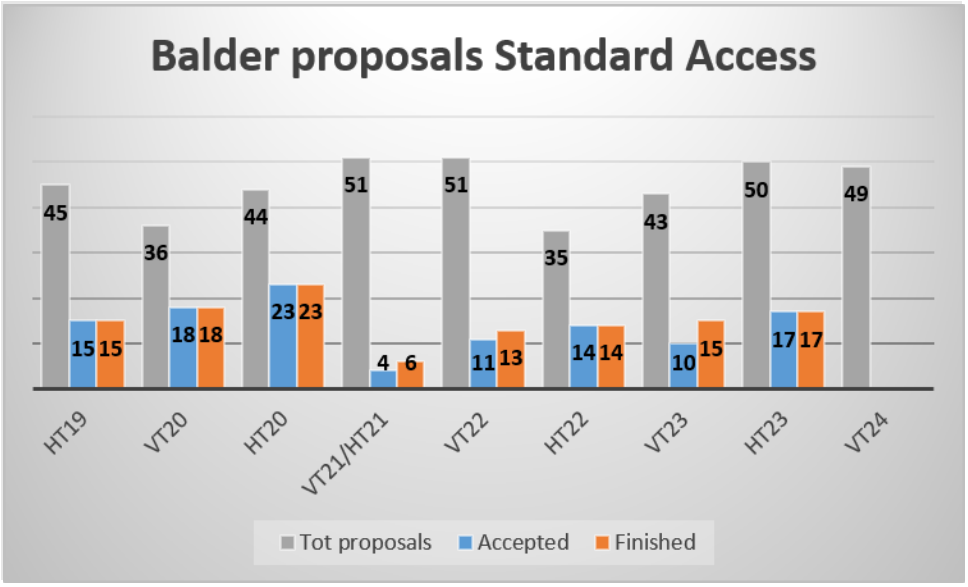

Figure 65. Standard Access proposals for each call period (HT = fall, VT = spring), total number submitted (grey bar), accepted by PAC (blue bar) and finished measured proposals (orange bar) which could include proposals from the reserve list

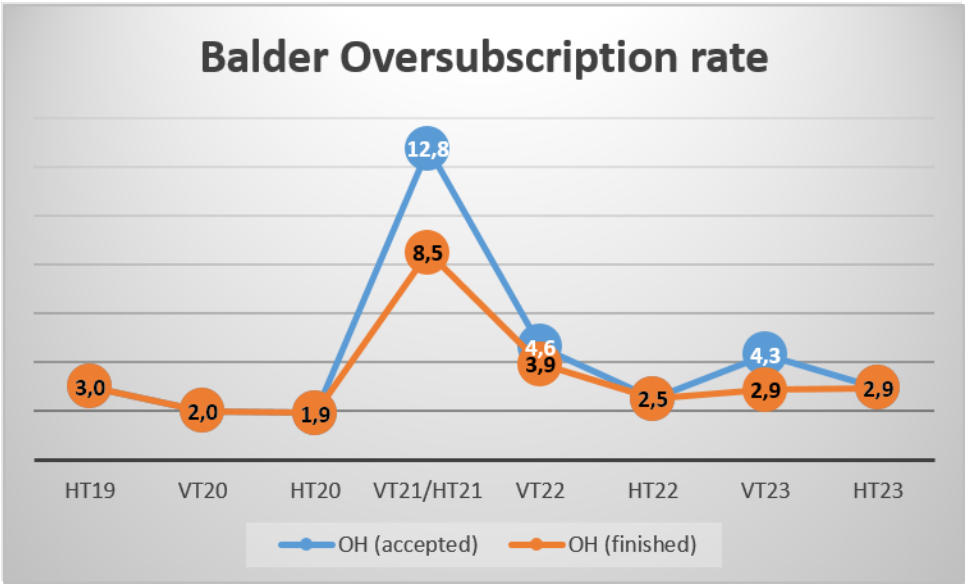

Figure 66. The oversubscription rate at Balder per call period (HT = fall, VT = spring). In blue are the accepted proposals and in orange are all the finished proposals included (reserve list).

The quality of the proposals is, in general, high (e.g. above a ranking of 3.5 (max 5.0)). To be awarded beamtime at Balder you need a score above 4.2 and in the last year even higher (Figure 67). This will lead to dissatisfaction within the user community if excellent proposals are still unable to get beamtime.

A standard proposal is as short as 6 shifts (24 h) and longest 36 shifts (6 days). The median length is 12-18 shifts. The shifts are scheduled in a row or broken up to chunks on the demand of the user. The *in-situ* proposals with gases are typically longest with the need for buildup and sample incubation/reaction time, even if the data collection is fast to perform.

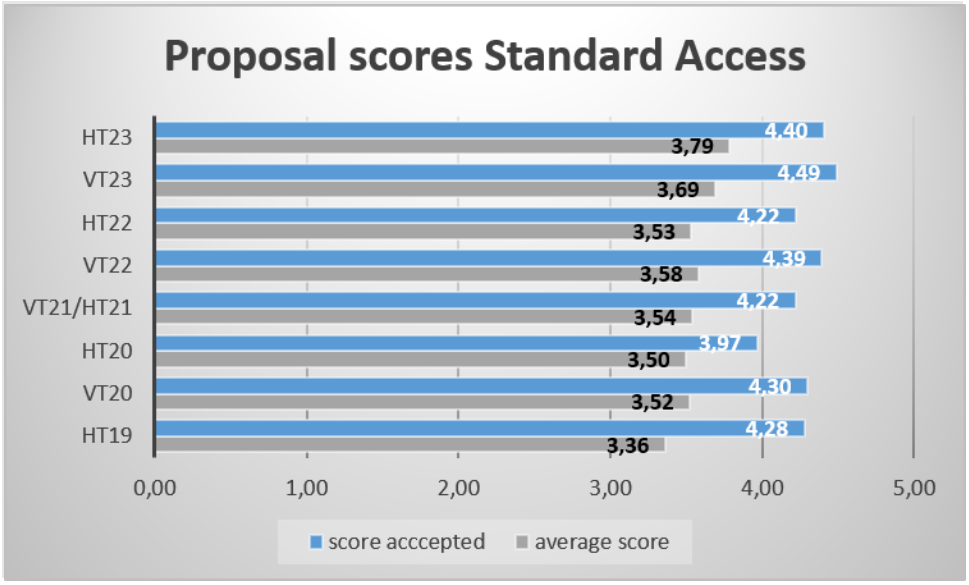

Figure 67. The proposal scores; average of all submitted proposals (grey) and all accepted proposals (blue) per call period (HT = fall, VT = spring).

Fast Access mode (FA) was introduced in 2022 to boost the beamline productivity and quality of the experiments. Users can ask during cycles for 1-2 shifts (4-8 h) of FA and after evaluation for feasibility (by the beamline) are scheduled on a "first come first served" basis, fitting into the beamline scheduled "FA reserved days". Balder offers two modes: Sample Feasibility (SF) and Standard Measurement Service (SMS). SF is aimed at users with new types of samples or cells to test feasibility and the correct measurement condition for a full proposal/beamtime. SMS is aimed at user with only standard samples and too few for a full standard proposal (min 6 shifts). It could be a reference sample missing for data analysis or a few samples to complete a publication. A standard sample is defined as a sample that can be measured at our ambient sample stage or in the cryostat in the standard holders (2.4.1). Samples are made by the users and mailed-in to be measured by staff (users sometimes come to the beamline as well). We have reserved 1-2 days/month for FA and proprietary access. Typically users are notified if they have been granted FA beamtime within 3 weeks and are scheduled upon short notice.

Training & Education (T & E) access mode is today offered upon request to the beamline (in sync with scheduling of the call). We reserve 2 % of the available shifts for this activity. This fall we have already had two educational beamtimes via courses arranged by the LINXS themes (Nordic Lights on Food theme and Heritage theme). Between cycles fall 2021 and spring 2023 T& E was part of the normal call with proposals coming in and being evaluated by a special PAC, however, this didn't work well in practice, and this fall we adhere to the process described above.

Proprietary access mode is available for paying customers from industry (or elsewhere) (Figure 68). The proprietary user owns their data and do not need to publish. The industry liaison office handles the contract and purchase of beamtime per hour (typically 1 shift). The beamline is involved in feasibility questions and acts as local contacts for the proprietary beamtime. Scheduling can be done on short notice, with days reserved every month in the cycle schedule. After BioMAX, Balder is the beamline with most proprietary hours to industry. In the figure, right panel, you can see that Vinnova funded projects were the major financer of the proprietary beamtimes. Vinnova is Sweden's innovation agency that fund projects stimulating collaborations between companies, researchers, and public sector in direction of a sustainble future (vinnova.se). Many of the Vinnova funded projects asked questions about chemical speciation of elements in industrial sidestream materials (ashes, steel slag) that can be toxic to the enviroment. To further promote proprietary use at Balder, staff has recently presented to both process industry, mining and battery

communities on events mainly organised by the industry office. Proprietary beamtime is easy to get, with access within two to three weeks. Another venue for industry to access the facility is via collaborations with academic groups. At the proposal submission, users get the question if they have industry connection. In Figure 68, left panel, you can see how many users answered yes (dark green) per year (= 2 cycles) and how many of those that were accepted (light green). In 2022 and 2023 the industry-connected proposals did on average better (a lower oversubscription rate (OSR)) than all proposals together (compare 2022 OSR 2.7 vs 3.55, 2023 OSR 1.9 vs 3.6).

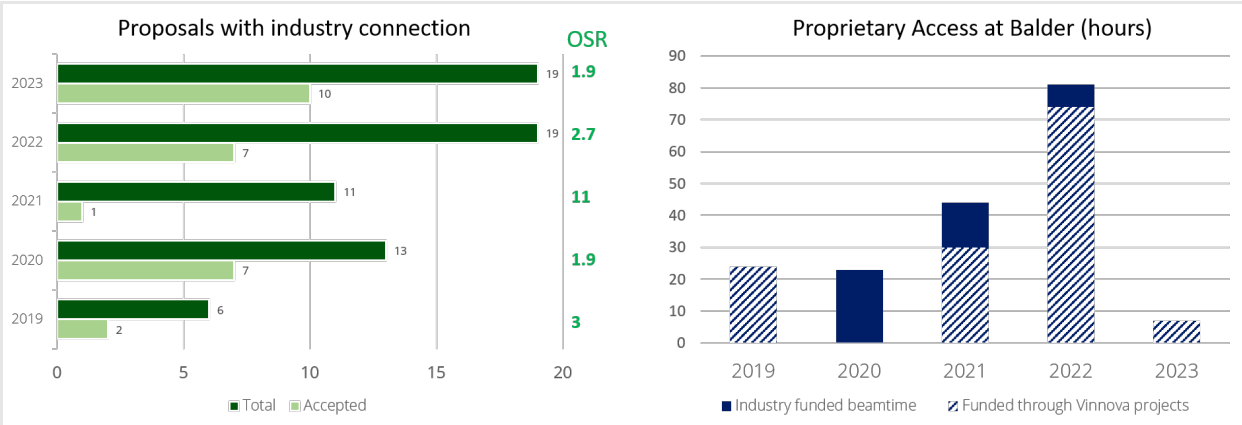

Figure 68. Industry access to Balder. Left panel, General proposals with industry collaboration total submitted (dark green) and accepted (light green) indicated, OSR in green number. Right panel, proprietary access hours sold at Balder per year. Funding indicated, Vinnova projects (striped bars) and industry funding (full bars).

To summarize, Vinnova funded industry beamtime was used extensively in 2022. The end of funding has resulted in fewer proprietary proposals; however, an increasing part of the accepted standard proposals have industry connection (Figure 68, left).

Guaranteed Access Time is a mode connected to MAX IV obligations in different external access programs. In the case of Balder, the program is called REMADE@ARI and is an EU funded program for access to multiple infrastructures via a science proposal in the sustainability area. MAX IV are obliged to provide 36 shifts/year for three years divided between two beamlines Balder and ForMAX. The first call is served this fall with one proposal at ForMAX, in the spring cycle we have set aside 12 shifts at Balder for potential REMADE projects. Many new projects have been submitted for feasibility at Balder, most of them are in situ catalyst proposals (4-6 days) and don't fit the reserved 12 shifts. To solve this, we will probably serve a longer proposal in fall. Scheduling of this "special access" is challenging since it is not coordinated with MAX IV call cycle.

In Figure 69, you can see the number of proposals (= number of experiments) for each access mode that have been executed at Balder between the start in 2019 and today. FA has really increased the productivity and quality of the experiments. As an example, the very productive May 19th 2022 with two FA users scheduled the same day and they both published their results in 2023.[15,16] The time between beamtime and publication is typically two-three years and FA seems to speed this up.

[15] doi.org/10.1016/j.molliq.2023.122233
[16] doi.org/10.1007/s11664-023-10434-6

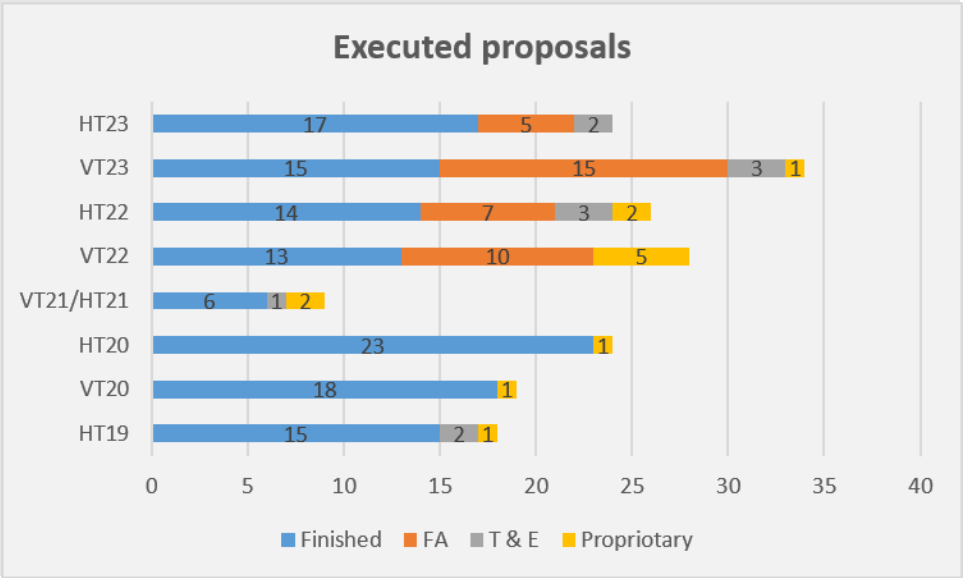

Figure 69. Number of executed proposal (experiments) of the different access modes all part of the user allocated beamtime share (75% of all available shifts). Finished (blue) refers to all general access experiments, FA (orange), T&E (grey) and proprietary (yellow).

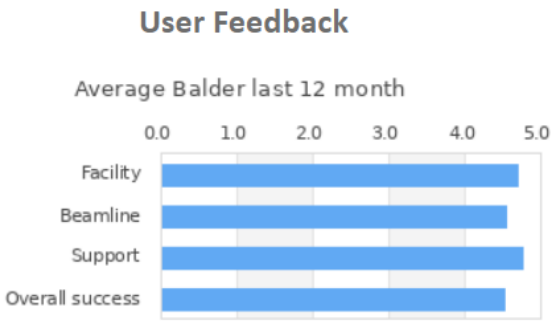

Figure 70. User feedback statistics from DUO, based on the end of beamtime feedback form the last 12 months. Max grade is 5.0.

In general, the users are very satisfied with MAX IV, the beamline and the support (Figure 70). Their experiments are overall very successful. However, the beamline also has improvements to make. Selected negative comments from users: User complaints about the stability of the control system (occurred more often in 2023 than in previous years and most significantly from in situ user groups). Users would like to have a canteen at MAX IV (or very close by). Positive comments: User really like the scan gui (live plotting) and extremely helpful Balder staff who do everything in their power to make the experiments work.

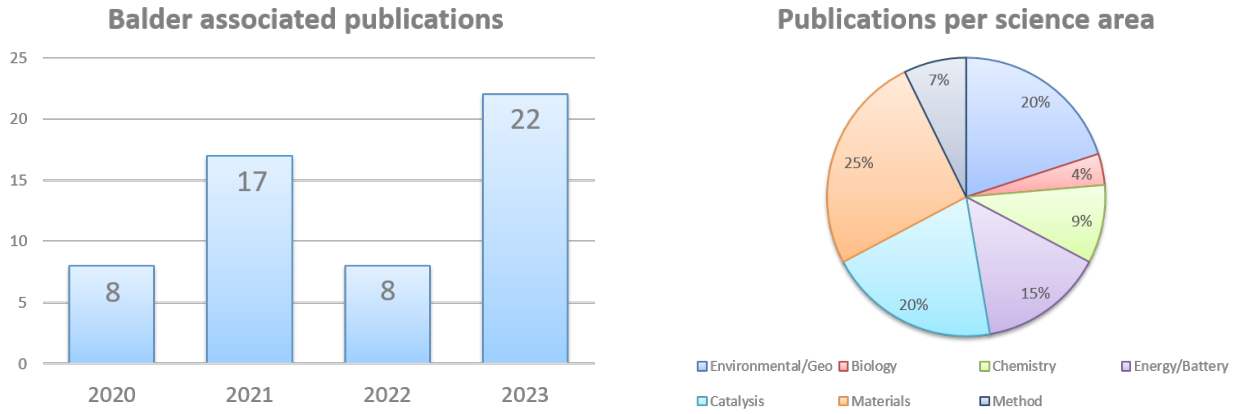

Figure 71. Left panel, number of publications using the Balder beamline, in total 55, found by searching DUO portal as well as google scholar (search XAS/Balder, XANES/Balder, EXAFS/Balder). Right panel, all 55 publications divided into science areas; Environment/Geology (blue), Biology (red), Chemistry (green), Energy & Battery (purple), Catalysis (cyan blue), Materials (orange) and Methods development (grey).

The number of publications associated with Balder are increasing rapidly this year and we have in total 55 publications (as of 1 November 2023, Figure 71, see a full list of all publications in appendix 1). There is a two(-to-three)-year delay between experiment and publication. Visible in the very low number of publications last year as an effect of fewer experiments being performed during the pandemic 2020. The higher number in 2021 fits with start of user operation in fall 2019 and time for users to write during the second pandemic year. Balder users publish in diverse science fields including Environment/Geology, Biology, Chemistry, Energy & Battery, Catalysis, Materials and Methods development, with percentages of published papers from the different fields reflecting well the split for accepted proposals. Methods development is an outlier which is more related to the in-house activities like commissioning and in-house experiments. The materials category has the largest share in the pie diagram; here was a mix of applications but with the common aim of the proposals to characterize and understand materials. The publications in highest impact journals are mainly from Environment/Geology area (Journal of Hazardous materials 14.22, Science of the total Environment 10.75, Water research 12.8, Chemical Enginnering Journal 16.74). Three higher impact publications in other areas; one in Science (30.26, Catalysis), one in Light Science & Applications (19.4, Biology) and one in Advanced Energy Materials (29.69, Energy/Battery). The number of publications are still rather low compared to other similar beamlines (see 5.3), but expected to grow significantly the coming years with the two(-to-three)-year delay between experiment and publication in mind.

3.1.1 KPI

Key performance indicators (KPI) showing that a beamline's impact and success are, for example, the number of user experiments, the number of publications and high impact publications. Another important factor for a healthy beamline is contributions to the new generation of scientists. This can be directed training courses as well submitted PhD theses based on data from Balder.

In 2023 Balder has had:

- 58 user experiments (32 Standard Access (SA), 20 FA, 1 Proprietary Access (PA) and 5 T&E)
- 22 publications
- 4 publications with impact factor > 7
- Average h-index of PI and main proposer 26.6 (32.7 in 2022)

- 6 PhD thesis based on Balder data

Since start of user operation (fall 2019) Balder has had:

- 404 Standard proposals submitted
- 112 Accepted standard proposals and 121 finished standard proposal (including reserve list) experiments.
- Oversubscription rate of 3.6 for accepted proposals and 3.3 including executed reserve list proposals.
- Total 190 experiments by users (121 SA, 47 FA, 13 PA and 9 T&E)
- 55 publications
- 12 Swedish PhD thesis based on Balder data and 4 Master thesis (associated with MAX IV)

Short term goal KPI:

- Number of user experiments: 40+ / year
- Number of publications: 20+ / year
- A few publications each year in journals with high impact factor > 7

Mid-term goal KPI:

- Number of user experiments with industrial participation: 5+ / year
- Number of publications: 30+ / year
- Several publications each year in journals with high impact factor > 7

As can be seen, Balder is already achieving its short term goal.

3.2 Staffing

Together Balder staff have broad technical and scientific expertise to cover the needs of the beamline (Table 5).

Table 5. List of current beamline staff with specified expertise.

Team member	Role	Expertise
Kajsa Sigfridsson Clauss	Beamline scientist, manager	XAS, XES, XRF, life sciences, liquids
Konstantin Klementiev	Beamline scientist	XAS, XES, beamline optics, analysis tools
Justus Just	Beamline scientist	XAS, XRD, time resolved in situ materials research
Susan Nehzati	Postdoc/researcher	XAS, XES, XRF, paleo-biogeochemistry
Mahesh Ramakrishnan	Postdoc	XRD, XAS, in situ materials research
Dörthe Haase	Engineer 50%	Sample environments

Permanent staff

Konstantin Klementiev, beamline scientist (100%), started in 2013. Conceptual Designer of the Balder optics (CDR) and of the SCANIA-2D XES spectrometer. He also created the new ionization chambers together with design office. Develops analysis tools and guis for the Balder users.

Kajsa Sigfridsson Clauss, beamline manager and scientist (100%), started at MAX IV in 2012 (postdoc at I811) and as scientist at Balder 2016. Took over the budget responsibility after project manager Katarina Norén left the project 2018. Develops sample environments for sensitive samples; in house designed cryostat and PI of the microfluidics project, AdaptoCell. Developed together with design office the standard sample holders and the ambient stage.

Justus Just, beamline scientist (100%,- parental leave 25%), started in 2018, first as XRD postdoc and later the same year as scientist. He drives the implementation of new motion controller and hardware based scanning and builds sample environments for in situ users (capillary reactor and in-FORM project).

Dörthe Haase, research engineer works as shared technician with DanMAX (50%). She started at MAX-lab in 2008 (at 1711). Has previously worked in the SEDS (sample environment and detector support) team and as team lead of experimental safety. Started August 2023 at Balder and DanMAX, to work with sample environments, technical solutions and maintenance at the beamlines.

Vacant, engineering/technical position (100%) was filled from 2020.05-2023.08, but the person has recently left for a position in industry. This position will not be filled until the recruitment freeze is lifted. The impact of lack of technical staff is that the scientists have to do a lot of technician work at the expense of beamline development, user support and data analysis and driving science at Balder.

Temporary staff

Susan Nehzati, postdoc/researcher, started 2019 and will finish 2023 Dec. 50% beamline operation and 50% external funded science (Per Persson/LU and Vivi Vajda/NRM). She is driving XRF and XANES mapping.

Mahesh Ramakrishnan, postdoc, started 2020 as the XRD postdoc (funded by Chalmers) taking over the operational position after Susan for 2024. He is driving the XRD project.

Associated staff

Stuart Ansell, scientist in scientific data, started 2018 at Balder as research engineer/scientist, moved over to radiation safety team to calculate radiation permits (for Balder and other beamlines). Moved to scientific data 2022, today part of the local contact pool (<10%).

Yang Chen, support lab manager, started at MAX IV 2019 as biolab manager. Supports BioXAS users together with Kajsa, training to become part of the local contact pool.

Two resource teams have dedicated beamline contacts: Software beamline contact – Vanessa Silva, Electronics beamline contact – Marcelo Alcocer

Alumni

Katarina Norén, Balder Project manager 2011 to 2018.
Iulian Preda, Manufactured optics, crystals for SCANIA-2D and HRM
Juliano Murari, software engineer first hired by Balder 2017 moved over to IT
Lindsay Merte, postdoc 2017-2018
Svetolik Ivanovic, Balder engineer/technical position 2020.05-2023.08
Pushparani Micheal Raj, postdoc AdaptoCell 2019-2021
Matteo Ciambezi, postdoc in-FORM 2020-2022
Jiatu Liu, postdoc in-FORM 2021-2023

Local contact (LC) pool

The LC pool at Balder is currently composed of Kajsa, Justus, Konstantin, Susan, Mahesh and occasionally Stuart. Last year, a second local contact was informally introduced on all standard experiments to support the first LC during setting up (and in case of illness take over). Local contacting is labor intense at Balder, especially for in-situ beamtimes. All users come with different needs (energies, sample environments) and level of experience (beginners to advanced level). The most demanding experiments are those when the users are inexperienced and highly understaffed to cover all their shifts. Our aim is to always try to deliver the most out of the instrument for the user satisfaction. With the FA beamtimes (mail-in samples) we are putting extra strain on the LC pool. It is very difficult to complete the beamtime schedule to fulfill the employment legislation on hours of rest. Increasing the local contact pool would help. However, a high level of expertise is needed to fulfill the duty. Second local contacting is the perfect opportunity for the training. For example, support lab manager Yang is participating in such local contacting training as time permits.

Support from resource teams

The resource groups at MAX IV support the beamline operation and projects with their expertise and are today organized in the technical division; Infrastructure, Software, Electronics, Scientific data, Central project office, Engineering I (Survey, alignment & mechanical stability, Vacuum, Mechanical Design, Mechanical Workshop) and Engineering II (Electrical & power supply systems, Automation, Technical infrastructure, Logistics and Technical services). Operational support is provided by on-call functions from key resource groups. Regular support is especially important from software team, organized in KITOS (control IT operational support) together with electronics, infrastructure and scientific data (17-23 workday, 08-20 weekend). The 24/7 on-call groups for emergencies are; PLC (Automation), water/ O_2 alarm/ cryo/ gas (technical infrastructure), electrical and radiation safety. Floor coordinators are always present at the facility to assist in varying tasks.

Safety has its own organization: Radiation safety, General safety and Experimental safety. The experimental safety team assesses the safety aspects of the experiments to ensure safe execution together with the users and the beamline local contact.

Central Project office (CPO) works together with the beamlines to provide professional help in project management of (larger) projects, plan resources and pulse their timeline every week. Beamline office (BO) helps with planning and execution of smaller projects (BPAG) involving one or two resource groups. Running Balder projects see Table 6.

Table 6. Currently running Balder projects. *(DO= mechanical design office, WS = workshop, SW = software, El = electronics/electricians, SD = scientific data, PLC = Automation, TI= tecnical infrastructure (water, gas, cryo), BO= beamline office)*

Running projects	Type	Resources
XES spectrometer	CPO	DO, WS, SW, El, PLC
XRD	CPO	PLC, El, SW, DO, WS
DAQ	CPO	SW, SD
IC filling	BPAG	DO, TI, El, PLC
Chiller move	BPAG	TI, El
SCANIA-2D upgrade window	BPAG	DO, WS
Replace MaxiGauge	BPAG	PLC
Antivibration cryolines	BPAG	BO, TI, DO

3.3 Typical beamtime process

A typical beamtime process begins with the submission of a proposal by the user, or, more typically at Balder, initial discussions between prospective users with the beamline staff regarding a possible experiment at Balder. This sets in motion a series of steps for different stakeholders which are summarized in the flowchart Figure 72:

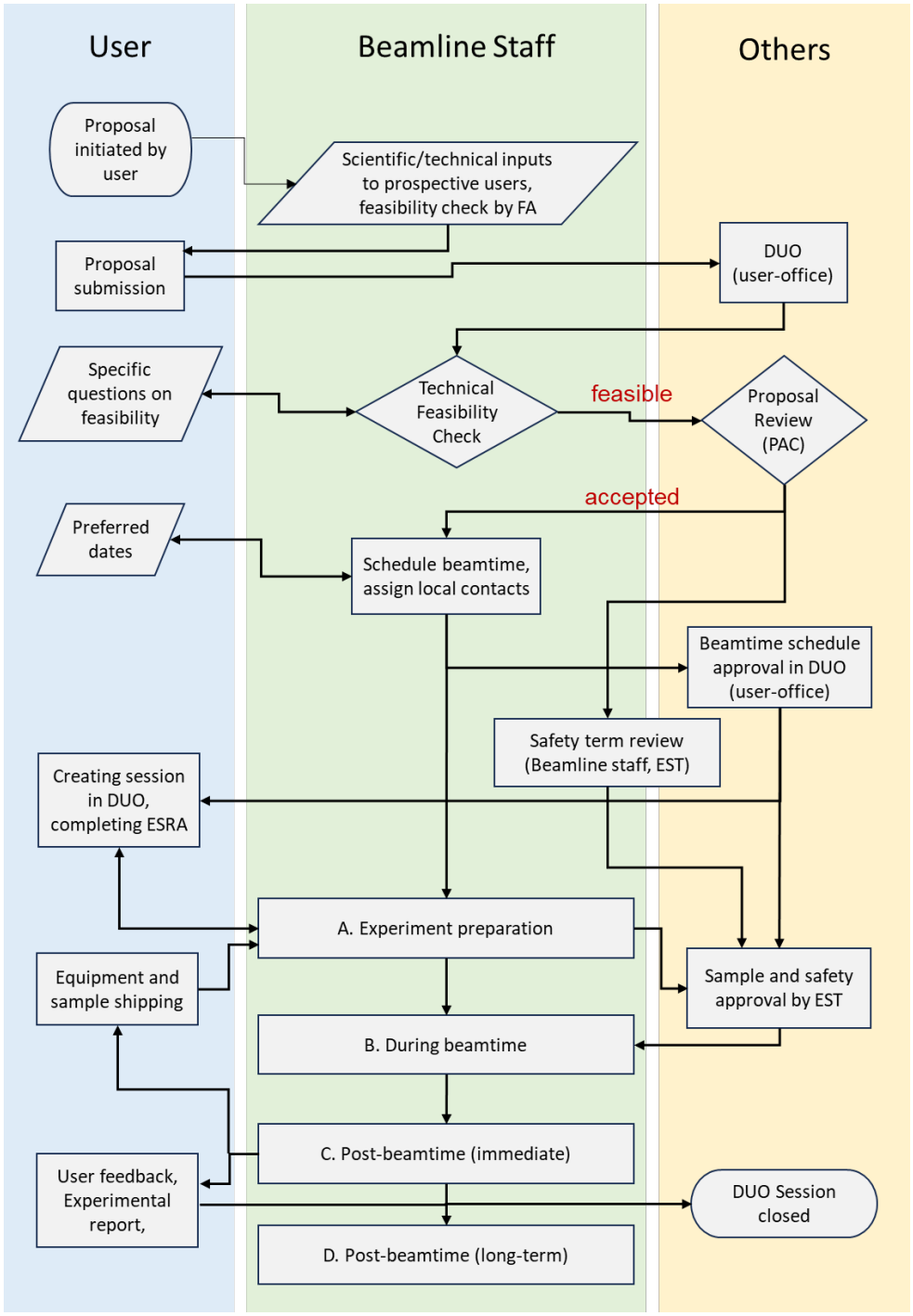

Figure 72. Typical beamtime process at Balder. (Abbreviations- DUO: digital user office, PAC: proposal advisory committee, EST: experimental safety team, ESRA: experimental safety risk assessment).

Once a proposal is awarded beamtime by the PAC, the beamline staff, in discussion with the user, schedule the beamtime. For most experiments at Balder, typically, two local contacts are assigned (see LC pool 3.2). The primary contact coordinates the communication with the users and the support groups while the secondary contact helps during the initial days of the actual beamtime. The main duties of the local contacts are elaborated below:

Table 7. Outline of local contact duties per beamtime experiment.

Experiment preparation	i) Prepare experimental plan with user ii) Order gases, chemicals, consumables iii) Equipment testing and commissioning including modifications to sample-environments (such as in-situ cells, sample delivery systems) iv) Provide guidance on safety protocols, risks and mitigation, booking labs etc. v) Provide help navigating through administrative procedures (DUO, ESRA) vi) Actively involve in discussions with experimental safety team vii) Organize engineering and electronics support personnel for installation of gas delivery systems, user motors etc. viii) Help users organize shipping equipment, samples
During beamtime	i) General introduction to the beamline infrastructure and radiation safety training ii) Coordinate equipment installation and sample-environment setup, safety gatekeeping iii) Setup beamline, control system, measurement protocols iv) Help users build in-situ setups v) Setup pipelines/scripts to perform basic data analysis real-time during the experiment vi) Train users on handling basic operations with the beamline control system, sample environment and detectors specific to the experiment. vii) Train (inexperienced) users to perform data handling viii) Introduce users to basic troubleshooting protocols, available online documentation and support and emergency contact information. ix) Providing on-call support x) Monitor status of inert gases, chemicals and other consumables (esp. for in-situ beamtimes). Replenish as and when needed. xi) Logging beamline settings, changes, technical issues
Post-beamtime (immediate)	i) Bring beamline back to standard state including optics, X-ray guides, sample environment and detectors ii) Scientific evaluation of the beamtime and discussions with users, introduce the users to Balder-specific analysis tools available for offline data treatment iii) Ensure user equipment and custom temporary constructions, wiring, cabling and gas connections at the experimental hutch are removed, return equipment borrowed from pool iv) Organize shipping of user samples and equipment v) Clear remaining user-samples, sort and dispose chemical wastes

	vi) vii) viii) ix)	Reporting of technical difficulties, follow-up with support groups Share experience with beamline team, update documentation on changes, new knowledge and troubleshooting methods Procuring and replacing depleted consumables Obtain direct feedback from the users on various aspects surrounding their beamtime.
Post-beamtime (long-term)	i) ii) iii) iv)	Provide support in data analysis (scientific and technical inputs) Follow-up on progress of data evaluation Motivate publication, support manuscript preparation Discuss merits for follow-up experiments and future scientific collaborations

3.4 Community outreach and training

The status of beamline capabilities are updated on the Balder webpage[17] before every proposal call is opened. There, users can see what is available in terms of energy range, techniques, detectors, sample environments, chemistry lab, sample holders and find contact to the beamline staff. Under the heading "Science at Balder" you can read about developments at the beamline and see examples of experimental data of the different techniques offered to users (XAS, XES, XRF, XRD).

Outreach to potential new users is achieved through giving invited talks, conference and workshop attendance in the immediate region and abroad. For example, Balder has been presented by staff and users at the SWEPROT conference each year for the protein science community. The MAX IV user meeting is also an opportunity well used to show case the beamline on posters and presentations and a few times via a special session called "Balder meets Users". Balder is presented and shown to visiting groups to MAX IV (politicians, scientist and funders) on a routine basis. Balder was also advertised via targeted presentations to interest groups from, for example, the mining industry, and life science visiting MAX IV or via visits to, for example, Alfa Laval and AstraZeneca. By engaging and presenting to the LINXS (institute of advanced neutron and X-ray science) themes, several new communities have been made aware of science opportunities with X-ray spectroscopy at Balder (Imaging, Dynamics, Nordic Lights on Food, New materials, Heritage, Chemistry of Life, Environment and Climate). Balder is also often asked to contribute and provide information/give talks to other networks not directly involved at Balder, for example, talks and training days for the Vinnova-funded NextBioForm network.

A number of Training and Education beamtime has been organized with participants from a wide field of research (Table 8). Up to 40 participants registered in each short course. Modules included both lectures on the Theory of XAS and hands-on experience at the Balder beamline. Beamtime modules were intended to train future users in preparing and running effective measurements. Topics included sample preparation,

[17] https://www.maxiv.lu.se/beamlines-accelerators/beamlines/balder/

various data acquisition strategies, and data analysis. On occasion, participants enrolled in post-educational programs which could gain university credits. In addition to the short courses, Balder will soon host five PRISMAS PhD projects (EU-COFUND) affiliated with universities across Sweden from Malmö to Umeå; see Table 9, with ongoing recruitments. During their programs, students will spend a minimum of three months at Balder working towards their dissertations.

Table 8. Course with practical exercise at Balder beamline.

Date	Co-organizers	University credit
June 19, 2019	Technical University of Denmark (DTU)	Yes
September 26, 2019	Swedish Agricultural University (SLU)	Yes
November 4, 2021	LINXS – New Materials Theme (LU)	Yes
March 16, 2023	MATRAC 1 School (RÅC)	No
March 22, 2023	LINXS – New Materials Theme (LU)	Yes
May 10, 2023	Malmö University	Yes
August 31, 2023	LINXS – Northern Lights on Food Theme	No
Oct 6, 2023	LINXS – Heritage Science Theme	No

Table 9. PRISMAS PhD student program with secondment at Balder beamline.

Science area	PI	Project title	University
Healthy planet	M. Högbom	Spectroscopic and geometric characterization of high-valent dinuclear metalloprotein intermediates	Stockholm University
Healthy planet	N. Skoglund	How could oxidation state and local structure of chromium affect strategies for phosphorus recovery?	Umeå University
Healthy planet	J. Rissler	Closing the Loop: Chemical Speciation using XAS a Key for Safe Secondary Use of Materials	Lund University
Clean Energy	L. Merte	Combining spectroscopy and diffraction for operando studies of complex oxide	Malmö University
Clean Energy & Beamline technology	P. Wernet	Bridging the gap between ultrafast and steady-state: Nanosecond optical pump and X-ray probe spectroscopy for chemical, bio-inorganic and materials sciences	Uppsala University

4 User community and in-house research

4.1 User community

Balder users exist in all science areas exploiting synchrotron radiation. The beamline was originally designed with strong use cases in environmental science and catalysis. Influenced by beamline staff and user interests, the capabilities have diverged into expertise in more areas. Balder is affected by being a true multipurpose beamline with consequences that goes with that: the good (learning from each other) and the bad (little time to focus). In Figure 73, you see all accepted and submitted proposals (2019-2023) divided into six science areas. The user community can be divided in two larger sub-populations where Materials, Catalysis and Energy/battery account for just under 2/3, and Environmental/Geo, Biology and Chemistry for approximately 1/3, of all accepted (and submitted) proposal.

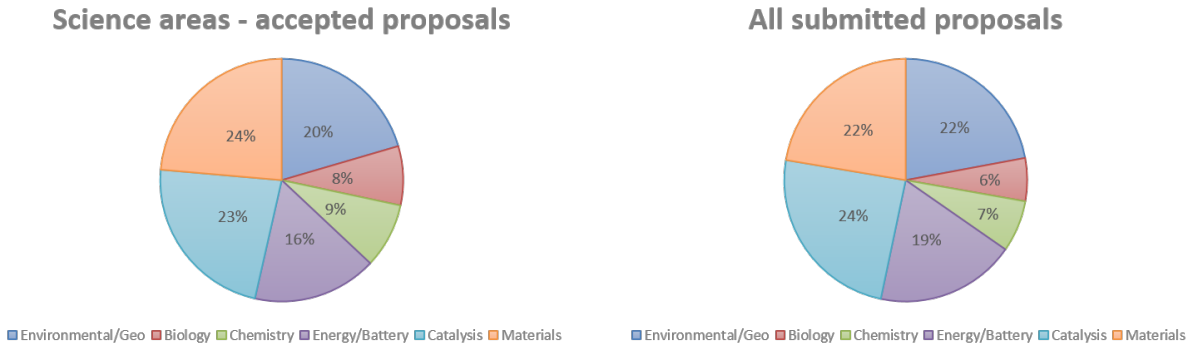

Figure 73. All accepted and submitted proposals (2019-2023) divided into science areas; (Environment/Geology (blue), Biology (red), Chemistry (green), Energy & Battery (purple), Catalysis (cyan blue), Materials (orange).

Chemistry PAC	Expertise
G. George	Life, environment and health sciences
B. Ravel	Physics, perovskites, XAS analysis
A. Puig Molina	Catalysis, power-to-X, ceramic materials
J. van Bokhoven	Heterogeneous catalysis
G. Vankó	Chemical physics, ultrafast dynamics, RIXS
A. Voegelin	Environmental biogeochemistry, trace elements

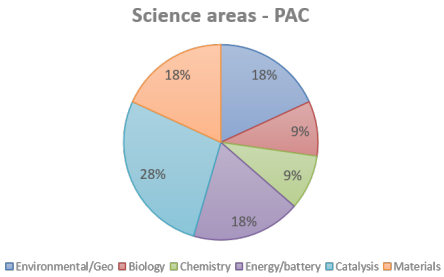

Figure 74. The members of the Chemistry PAC and their expertise. Pie diagram showing the share of their expertise divided into the science areas; (Environment/Geology (blue), Biology (red), Chemistry (green), Energy & Battery (purple), Catalysis (cyan blue), Materials (orange). Each PAC member can have expertise in more than one area.

The same share is reflected in the competence and interest of the Chemistry PAC, see Figure 74. The relationship between submitted user proposals from different science areas, the Chemistry PAC composition and the outcome from the PAC seems to be well balanced. In Figure 75, you can see that the home institutes of the Balder users are mixed; with one third Swedish, one third other Nordic and one third international (Fall 2023). There was a variation of more or less international versus Swedish during the past two years but overall is balanced.

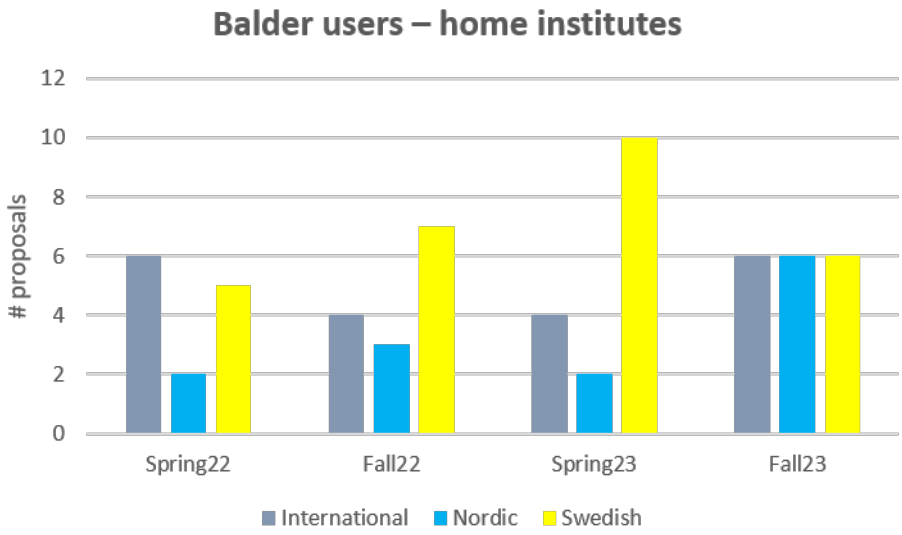

Figure 75. Balder users (Standard Access) come from a wide mix of countries, here number of proposals are divided in Swedish (yellow), Nordic (blue) and international (grey) from year 2022-23.

4.1.1 User highlights

Three recent publications from Balder where XAS data has been instrumental to the understanding, and one very high impact publication where EXAFS was part of a larger tool kit.

Environment:

K Wang et al. (2023) Molecular-scale characterization of groundwater treatment sludge from around the world: Implications for potential arsenic recovery, **Water research**[18]

Sludge from As-rich groundwater treatment plants were comprehensively characterized by combining a suite of macroscopic measurements, including XAS. The Fe K-edge XAS data revealed that all samples consisted of nanoscale Fe(III) precipitates with less structural order than ferrihydrite. The As K-edge XAS data indicated As was present in all samples predominantly as As(V) bound to Fe(III) precipitates in the binuclear-corner sharing (2C) geometry.

[18] doi.org/10.1016/j.watres.2023.120561

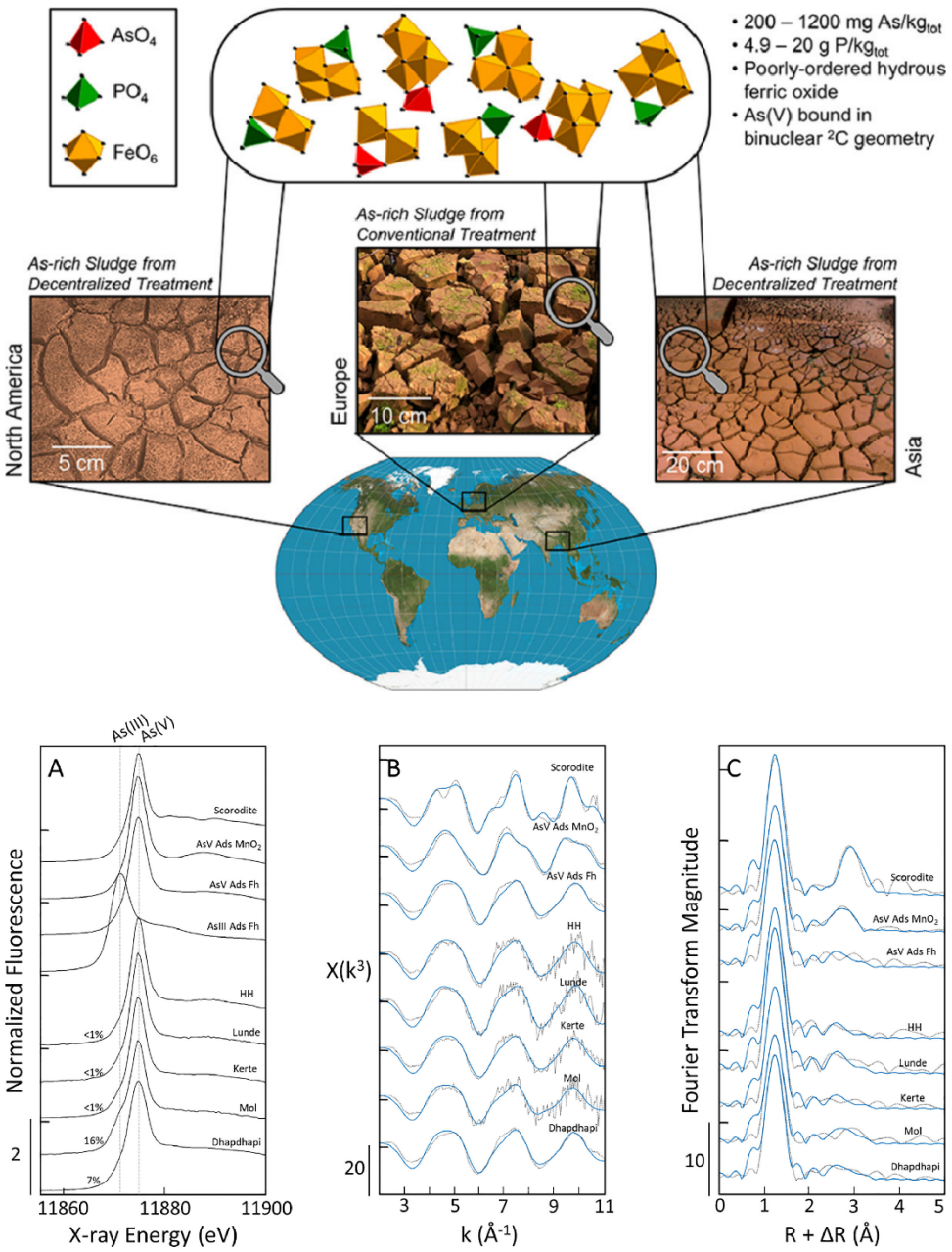

TA Formentini et al. (2024) Immobilizing arsenic in contaminated anoxic aquifer sediment using sulfidated and uncoated zero-valent iron (ZVI), **Journal of Hazardous Materials**[19]

The immobilization of As by four commercial zero-valent iron (ZVI) particles was investigated with the help of XAS.

[19] doi.org/10.1016/j.jhazmat.2023.132743

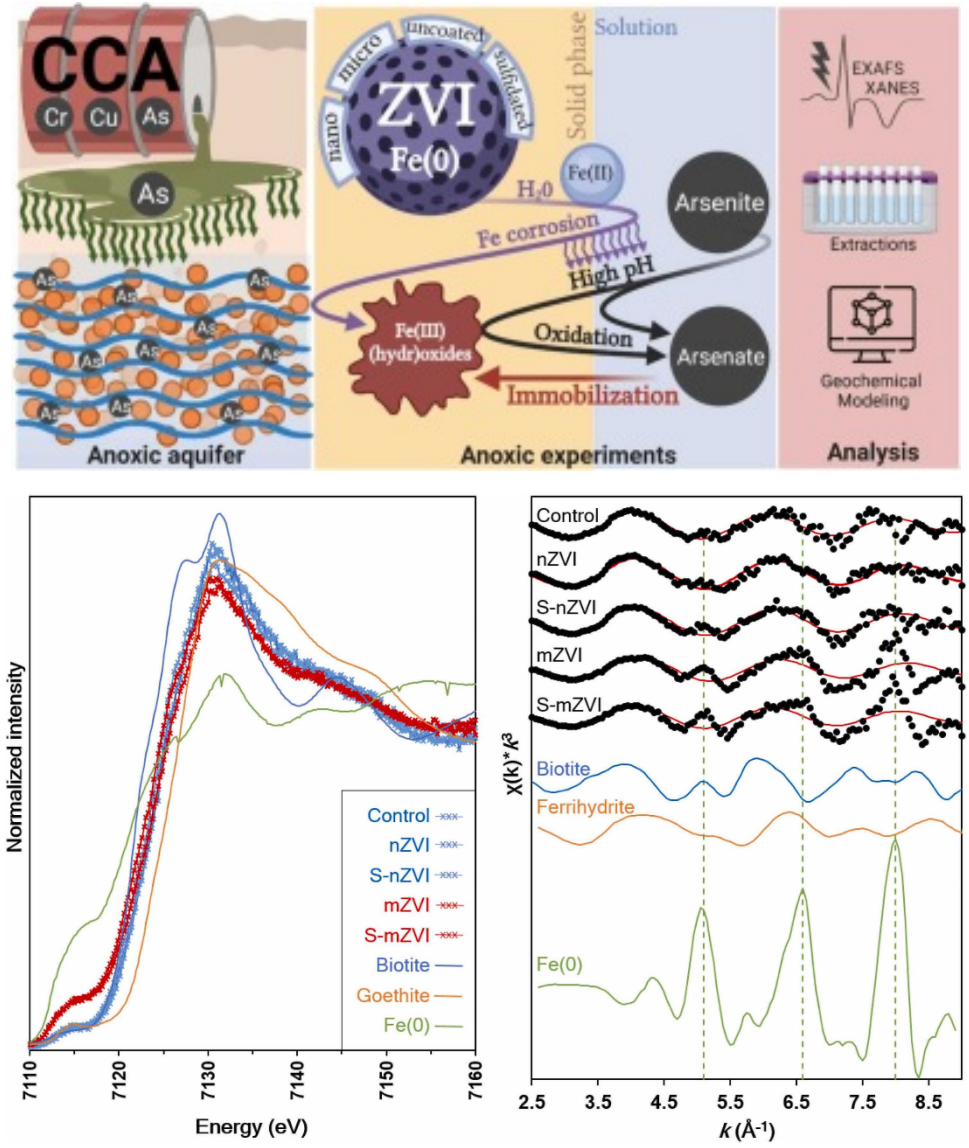

Materials:

L Rogström et al. (2023) Structural changes in Ti1-xAlxN coatings during turning: A XANES and EXAFS study of worn tools, **Applied Surface Science**[20]

Structural changes in Ti1-xAlxN coated tool inserts were investigated by XANES, EXAFS, EDS, and STEM. The Ti K, Cr K and Fe XANES reveal that structural and valence changes.

[20] doi.org/10.1016/j.apsusc.2022.155907

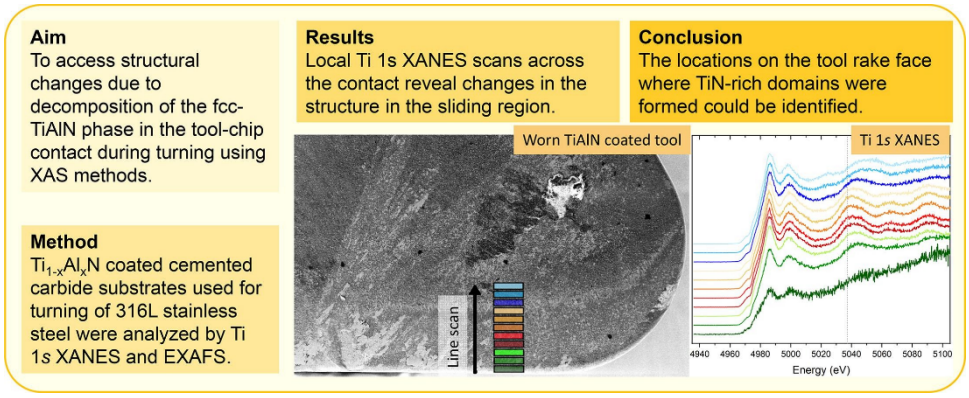

Catalysis:

V Muravev et al. (2023) Cat, Size of cerium dioxide support nanocrystals dictates reactivity of highly dispersed palladium catalysts, **Science**[21]

Detailed spectroscopic investigations, including the Pd K EXAFS, reveal that the size of the support of cerium oxide nanoparticles changes the reactivity of highly dispersed palladium catalysts for low-temperature carbon monoxide oxidation.

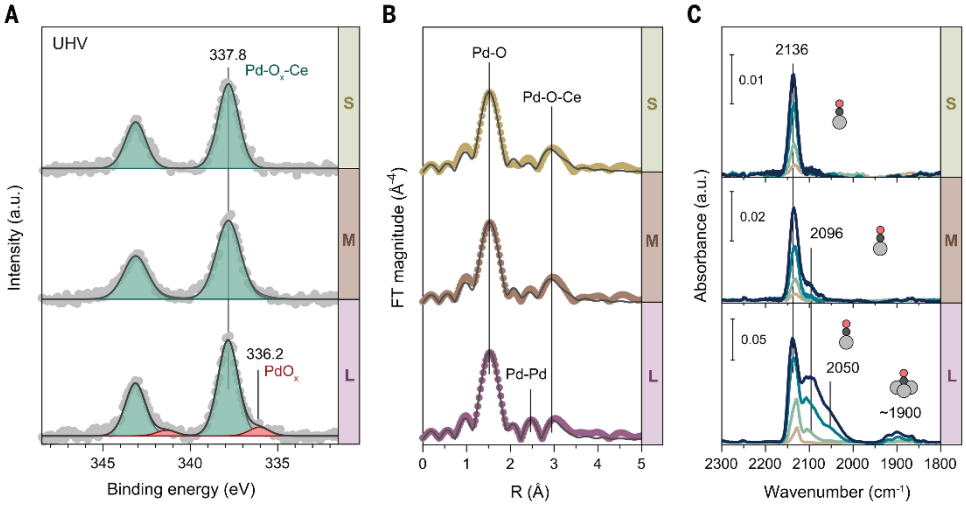

4.2 In-house program

Via the in-house science program, every Balder staff member, doing local contacting, gets 6 shifts of beamtime per cycle. Postdocs on external grants without beamline duties are awarded 3 shifts/cycle. Exactly what each person does during in-house beamtime is driven by their own science interest, grants and collaborations. In the examples below you will see the wide science application and development of the Balder instrumentation reflected in the in-house activities with lead investigator in parentheses. In-house beamtime also covers any technical development and commissioning activities of new equipment and capabilities and is planned as a team or sub-teams; for example, SCANIA-2D XES spectrometer, XRD, XRF and sample environments.

[21] doi.org/10.1126/science.adf9082

Environmental research - past and present (S.N.)

The past: The history of the Earth is chronicled in the sedimentary record providing a wealth of information on past environmental processes. The sediment facies preserve environmental factors that have occurred, and the fossils therein may hold clues to what they have endured. Of the multiple crises that have threatened the past biodiversity on Earth, five mass extinction events stand out with the largest decline of biodiversity. Of the five, only the end-Cretaceous extinction, which led to the estimated loss of 75% of species, is generally thought to have been triggered by a large asteroid impact. The overall theme of this research is to investigate the geochemical and biochemical record to identify triggers and changes to past environmental climates surrounding these in order to better understand the main drivers of the decrease of biodiversity. As an example, we investigated the strata spanning the end-Permian extinction bed and identified a drastic Fe redox-shift situated right at the "death horizon" (Figure 76, A). When compared to model Fe compounds, we identified in the oxidized sediment immediately following the extinction event, a large component of iron complexed with dissolved organic matter present.

The present: The Boreal Zone, also known as the taiga, is the largest land biome on Earth located in the northern hemispheres just below the Arctic Circle. In recent decades, the browning of freshwaters in these areas, caused by the increasing exports of iron (Fe) and dissolved organic carbon (DOC) have been concerning due to the consequent deterioration of water quality and risk to the health of aquatic ecosystems. Using XAS we can investigate the iron phases and environmental trends to better understand the process of Fe mobilization. We investigated Fe speciation in forested field sites and catchment areas across Sweden and results show that afforestation and riparian catchment sites can be major contributors to the increased Fe concentrations found in freshwater. The dominant chemical species found in these areas were identified as Fe(III)-OM (iron complexed with organic matter) modelled after Fe(III) complexed with fulvic acid – a byproduct of plant and animal break down (Figure 76, B).

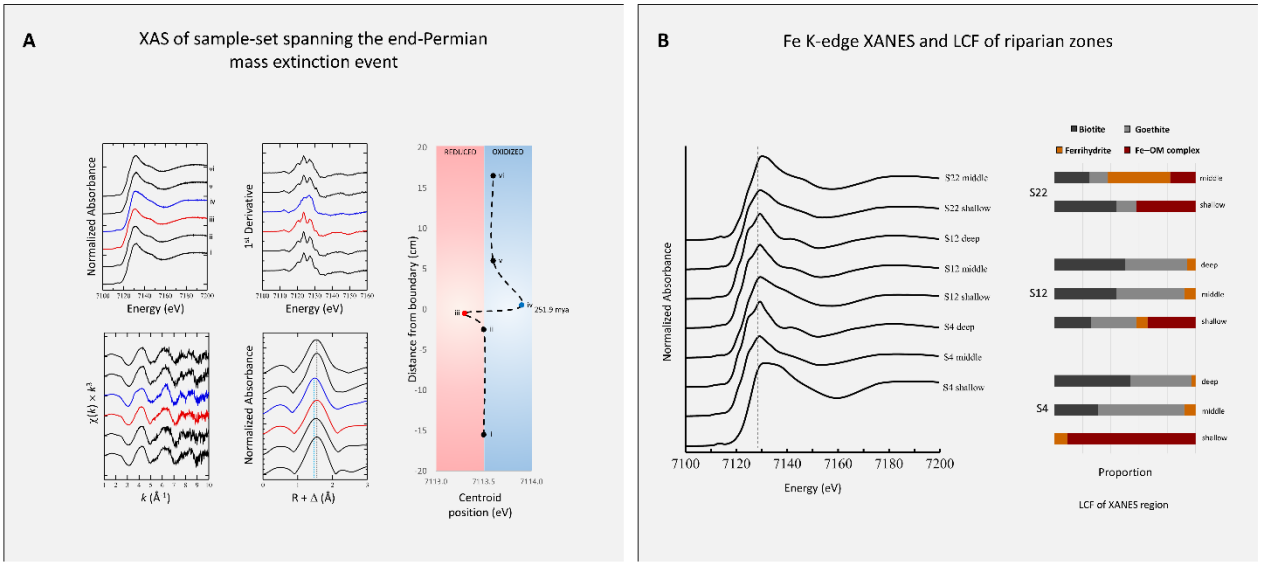

Figure 76. A: Fe K-edge XAS of strata spanning the end-Permian extinction bed. B: Fe K-edge XANES and LCF fit of riparian zones in northern Sweden.

Advanced XES applications (K.K.)

After finishing the three technical upgrades of the Balder's XES spectrometer (see section 2.2.3), its conceptual development is expected in two main directions: (a) achieving "super-resolution" and (b) implementing scan-less energy dispersing acquisition by moving the Rowland circle towards the sample. In both cases, the XES spectrum is obtained by projection onto a basis set of response spectra (elastically scattered bands of finely spaced variable DCM energies). The fundamental difficulty in utilizing elastic scattering for obtaining the spectrometer's response function comes from the difference in polarization: emission is unpolarized whereas elastic scattering preserves the horizontal polarization of incoming X-rays. The conceptual development of an X-ray depolarizer is expected to happen within in-house research activities.

The XES technique has a great potential of achieving site selectivity, i.e. separate spectroscopic response for atoms of the same chemical element but of different valence state or atomic environment. Conceptually this is enabled by chemical shift of emission lines and technically achieved by integrating them in certain energy ranges. Valence-to-core (VtC) emission band, that is situated right below the corresponding absorption edge, is expected to have the strongest effect on the chemical shift. An addition of simultaneous VtC spectroscopy to a combined XAS+XRD catalysis project is also expected to happen within in-house research activities.

5 Balder in the landscape

5.1 Balder through the years

The first ideas of a new hard X-ray XAS beamline at the new MAX IV facility originate from 2009. Driving was the Swedish user community of the I811 beamline, XAFS beamline at MAX-lab. The project was chosen as one of the first seven beamlines funded by Knut and Alice Wallenberg foundation. With the recruitment of Konstantin in 2013, the scope was updated to include XES and Sulphur K-edge. Balder had first monochromatic light in the optical hutch early 2017. Two major delays stopped us from bringing light to a sample. Delay 1, the beam transfer pipe send to Innospec for lead shielding got lost/displaced for a year and arrived at last for Christmas 2017. Delay 2, was waiting for a radiation permit from SSM (Svenska Strålskyddsmydigheten), due to missing capacity in the radiation safety team. Balder was granted a permit for the entire beamline in September 2018, with first light on sample in the experimental hutch in October 2018. Commissioning of baseline XAS with the first commissioning expert users in April 2019. Regular XAS user operation started in September 2019. To further advance the capabilities, user operation was mixed with commissioning activities, see the timeline in Table 10. The share of 75 –25% User-to-In-house has been the rule since 2019 with extra commissioning shifts the first years (2019-20). User operation of XES started in 2023 with first regular users in June.

Table 10. Timeline over past activities, milestones and major events from 2017 to today showing the mix of operation and commissioning.

Milestones /Activities	Q1	Q2	Q3	Q4
2017	First light in Optics hutch (OH)	First Cu XANES in OH	Delay 1 – beam transfer pipe	
2018	Installation of beam transfer pipe	Delay 2 – radiation permit	Granted radiation permit (Sept)	Commissioning with X-rays
2019	Comm XAS	Expert users XAS	Installation of XES spectrometer User operation XAS starts (Sept)	XAS users Comm XES Comm XRD
2020	XAS users	*Pandemic* – only local users or mail-in. Installation cryostat Expert users XRD	Comm XES	XAS User operation on site again Installation HRM
2021	*Pandemic* - Warm shutdown (SD)	SD until May Cryostat users	Normal XAS user operation Comm XRD	SDD Be window broke
2022	Mono motion control upgrade	Expert users XES Comm XRF Comm XRD	Comm XES XRD user operation	Starting FA Comm XES
2023	Comm HRM	XES user operation	Comm DAQ	Beamline review

5.2 SWOT analysis of Balder today

As preparatory work for the beamline review, the Balder team started with a SWOT analysis of the beamline to build the basis of the review. It is by no means complete in its execution but provides an inside perspective.

References within the review to "Strengths" can be found in sections 1, 3.2, 2.1, 2.2.1, 2.6, 2.4 and 5.3. References to "Weaknesses" can be found in points of concern 6, and sections 3.2, 2.7. References to "Opportunities" can be found in sections 3.4, 2.1.2, 2.6, 2.4.5, 2.4.6 and 3.4. References to "Threats" can be found in in points of concern 6 and sections 3.2, 3.3, and 3.1.

5.3 Benchmarking

To compare technical specifications and performance, a short list of similar European XAS beamlines is listed below. They are chosen because the user communities of these beamlines partly overlap with Balder user community.

Table 11. Comparison with other European XAS beamlines.

	Balder (MAXIV)	SuperXAS (SLS)	Core-EXAFS (Diamond)	BM 23 (ESRF)	P64/65 (DESY)	SAMBA/ ROCK (Soleil)
Operation started	2019	2008	2010	2011	2017	2010/2016
Num of publications in 2020–2022	33	185	262	–	134/142	143/98
Flux (ph/s)	$5\times10^{12(typ)}$	1×10^{12}	5×10^{11}		1×10^{13}	3×10^{11} / 2×10^{12}
Spot size – focused (μm^2)	70×70	100×100	200×250	3×3	150×50	~300×300

Spot size – defocused (µm²)	500×2000	5000×500		13000× 1000	2000× 1000	5000× 2000
Time resolution	Sub second	10 ms			20-100 ms	min / 50ms
Energy range [keV]	4 – 40 (event. 2.4-)	4.5 - 35	2.05 - 35	5 - 75	4 – 44	4.2 - 40
Techniques offered	XAS, XES, qEXAFS, XRD, XRF	XAS, qEXAFS, XES	XAS, XRD	XAS, XRD, XRF, XMLD	XAS, XES, qEXAFS	XAS / qXAFS

Status: Balder is a multimodal beamline dedicated to hard X-ray spectroscopy (XAS; XES), with XRD and XRF as secondary techniques with a good time resolution. Interchangeable sample environments; in operando cells with gases, liquid cells, cryostat, furnaces, etc. Balder took first light 2017 and has been in regular user operation (for simple EXAFS) since September 2019.

Comparisons: The beam properties at Balder compare well with benchmarked beamlines (that have been in operation for a while) with an exceptionally high stability.

6 Points of concern

Reflected in Weaknesses and Threats in the SWOT section 5.2. Here divided in topics:

Technical and Beamline

- The main technical concern is the *beamline's control system*. It is still, after years of operation, unstable and quite pre-mature. Control system issues in terms of reliability and error reporting cause still significant trouble. Centrally provided (Taurus based) GUIs appear in general slow and unstable. The operation of the beamline requires a high flexibility of hardware used (different stages, detectors, etc.), while disconnection of single devices still causes the whole control system to break. Our hope is that the ongoing developments of hardware orchestrated scanning will lead to improvements in the reliability of scanning. We would suggest that a direct coupling of support personnel, especially software developers, into the beamline core team, in opposition to the current organizational structure, would result in a much higher efficiency for software developments and problem fixing.

- Despite the above presented achievements in scan speed and *spectral quality* of XAS spectra, Balder could do even better. We identified the following two aspects to limit the quality of measured XAS spectra: **I)** As described in 2.1, the spectral and lateral distribution of X-ray intensity from our *wiggler* is not flat but exhibits a clear oscillatory behavior (Figure 3). While for homogenous samples, these beam inhomogeneities cancel out properly in normalization with the incident beam, they impact spectral quality dramatically for inhomogeneous samples or in case of non-linear detectors (e.g. fluorescence detection with higher count rates) and can even result in distorted spectra. The oscillatory part of these artefacts can even wrongly be interpreted as EXAFS oscillations. Despite the measures we are already implementing to reduce these distortions to the best extent possible (electron beam inclinations), only downgrading the magnetic uniformity, in reality a replacement of our insertion device would really be able to solve this problem. **II)** Residual *beam vibrations* at the sample, in conjunction with slight sample inhomogeneities often introduce noise into the spectra. As described in section 2.1 (Heat load & cooling) these vibrations originate from the direct coupling of the cryogenic cooling lines to the monochromator crystals, as well as from non-ideal performance of

our fast feedback beam height regulation. Both shortcomings are identified and can be mitigated with decent effort, which will be done within the coming year.

- We have identified a rather low level of *documentation* at the beamline, even though excellent plans exists (Sphinx, section 2.7), the dynamic changes in control system and new developments have made documention quickly obsolet. Propper time needs to be dedicated to complete the documentation and establish update rutines.

Staffing

Even though it might look like a comparably good staff situation at our beamline, the workload for the beamline staff and local contacts is quite high for the following reasons:

- Due to the hiring freeze for the beamline engineer, the scientific staff performs currently most of the technical work.
- Especially for complex in-situ / operando experiments, which include actually majority of experiments at Balder, the planning, build-up and conduction of the experiments demands a high level of involvement of the local contacts.
- Local contact efforts often require deep involvment to support users measuring at Balder to both plan and prepare pre-beamtime and teach the users during beamtime as well as helping out post processing after the run.
- Fast access proposals are more difficult to schedule in advance and come then on top of the already assigned duties.
- The high workload among the beamline staff, delays further developments, improvements and scientific engagement.
- An identified concern is that expertise knowledge sometimes is isolated with a key staff member. To the point that certain experiments must be supported by this key person.

Education of user community

The level of experience and competence varies among the users from true beginners to super-user groups. However, our experience is that even supposedly experienced groups send just their students to the beamtime to be trained by the beamline personnel. In fact, we often put a lot of time into helping the users prepare good samples, optimize data collection (our job) and explaining/helping with post processing. Regular accessible training is needed. We have, together with LINXS theme “New Materials” (Jens Uhlig, LU), arranged a deeper training course for PhD students, postdocs and alike to master XANES/EXAFS analysis in 2021 and 2023. This was following in the footsteps of the popular EXAFS course that was a regular item at the old MAX-lab given by Ingmar Persson, SLU (Swedish Agricultural University). The majority of the user community at I811, predecessor of Balder at MAX-lab, had taken this training course and all had a good level of understanding of the technique to make the most out of the beamtime. Ingmar gave it once at Balder before his retirement (2019). We would benefit from (again) having a more regular training course available for our users. In addition, we also see that people from different scientific disciplines might need more tailored courses to fully thrive.

Budget

- The large uncertainty with the MAX IV budget situation for anything outside bare operation might completely freeze further development at the beamline, with the risk of falling behind international fellow XAS/XES beamlines. Worse if MAX IV not even can afford repairs and necessary maintenance to stay operational.
- Another concern is the limited travel budget for beamline staff (this year 20 kSEK (~1700 €) per FTE), which can be used for conferences, travel to collaborators, beamtime at other facilities. It will most

likely become even more restricted next year. For postdocs, senior management are considering reducing this amount further and in general permitting only one MAX IV representative per conference/workshop. It is barely possible to perform adequate representation on international conferences, which limits the possibility to keep up with the state of the art of other beamlines and user needs as well as to attract new research to Balder.

- A third budget related concern is that the direction of beamline developments and activities can be forced by "others" granted funding. Grants, where the beamline has not been involved in planning nor asked to participate. One similar example is topical guarantee access time programs committing beamtime.

7 Developments: ongoing, planned, and possible

MAX IV's Strategic plan 2023-2032[22] highlights six transformative science areas that are priorities for long-term development. The versatility of research capabilities at Balder enables investigations that directly impact five of the six areas: Life and biomedical science, Energy materials and technologies, Tackling Environmental Challenges, Quantum materials and device technologies, and Atomic, molecular and optical science. Prevalent elements include realistic measurement conditions covering both temporal and spatial requirements, multi-modal capabilities for complex materials, and high-quality spectral resolution to discriminate subtle chemical characteristics. Detailed plans at Balder in line with MAX IV's strategic goals are described below.

Roadmap process at MAX IV

To execute the MAX IV long-term strategy a roadmap is developed at the facility, a living document to be updated yearly and that this should guide the budget process and future new projects at the beamline. All the information you see below is included in the first version of the Balder roadmap contribution.

High-level roadmap

We have identified domains where Balder excels or have potential to do so in the future.

Wide energy range readily accessible due to broad wiggler light source and easy to exchange optics. This allows probing lighter to heavy elements in the same beamtime and even same sample with ***fast energy changes***. Reaching energies down to the Sulphur K-edge will significantly broaden the application range.

High quality EXAFS, design goal of Balder, is achieved with a stable beam and fast sub-second scanning on homogenous samples. Cryogenic conditions increases the signal-to-noise ratio. However, for highly dilute or natural samples, further competitive detectors and smoothing of the wiggler background would be needed to excel. We aim to provide the full range of detection techniques including RefleXAFS and total electron yield for getting surface information complementing bulk.

The ***XES high resolution spectrometer*** SCANIA-2D gives access to detailed electronic structure providing rich chemical information complementary to XAS. In particular, we can reach low energy absorption edges with hard X-rays. The back scattering geometry can be combined with any sample environment. Increased detection limit can be reached with reduced background counts.

[22] https://www.maxiv.lu.se/about-us/max-iv-strategy-2023-2032/

Deeper scientific knowledge can be reached with ***combined methods*** like XAS-XRD, XAS-XES, XAS-XRF, visible light spectroscopy, electrochemistry, and mass spectrometry simultaneous under same conditions.

Balder can provide all techniques above together with ***specialized sample environments*** to study chemical systems under ***in situ/operando*** conditions. An extensive gas mixing system is tailored to catalysis research. We will continue to develop sample environments for ***time resolved*** sub-second experiments, like flow cells, liquid jets and reaction cells probing chemistry in diverse fields together with users.

The fast energy scanning allows combination of the above techniques with spatial scanning. Which is particularly important to probe ***complex heterogeneous materials at realistic conditions***, highly relevant in research tackling environmental challenges.

For increased beamline impact on the scientific communities, we constantly aim to educate users by training and outreaching.

7.1 Missing design capabilities

Wide energy range is readily accessible due to broad wiggler light source and easy to exchange optics. Balder was designed for the energy range from 2.4 (Sulphur K-edge) up to 40 keV. Reaching energies down to the Sulphur K-edge will significantly broaden the application range and satisfy a waiting user community. Tasks are; 1) provide sample environments (He or vacuum), 2) start operating the harmonic rejecting mirrors (HRM), 3) changing to thinner windows on ICs and 4) replacing I_0 function with the DiSC (diagnostic scattering chamber).

7.2 Short-term and middle-term developments

In order to maintain and strengthen Balder as a highly productive work horse beamline for the Swedish community and simultaneously develop world leading spectroscopy we foresee the following activities (required resources and unfunded costs stated in parenthesis, underlined is top three prioritized and listed in order):

Short-term planning (1-2 years)

- Improving quality by hardware orchestrated scanning (SW, SD, DAQ project - *ongoing (section 2.1.2*)), by removing vibrations in mono cooling cryo-lines (BO, 300 kSEK - *started*)
- Sulphur K-edge spectroscopy delivered to users (DO, WS, 250 kSEK) - *partly started (section 7.1)*
- SCANIA-2D spectrometer for natural low concentration samples (background reduction solutions, DO, WS, *ongoing (section 2.2.3*)) including flyscans for XES (SD, SW) (100 kSEK)
- Simultaneous XAS-XRD: sustainable integration of new XRD robot (Chalmers) – *started (section 2.2.5)*
- Spatial probe inhomogeneity of chemical state, 2D XANES mapping. (SD) - *started (section 2.2.4)*
- Heating and cooling sample environment with electron yield (DO, WS, El, SW, PLC, 1 MSEK external grant needed) *(section 2.4.3*)
- Reflection XAS for surface science (60 kSEK) - (*section 2.2.6*)

Mid-term planning (3-4 years)

- Fully developed SCANIA-2D (adding second branchline, funding required)

- Automatic sample change by robotic arm at ambient and cryo conditions for higher throughput of standard samples (SW, PLC *(section 2.4.1*)
- Upgrade of BPM (beam position monitors) (BO *(section 2.1*)
- Improved data live view for XES and other multimodal techniques, including streamlined data reduction and processing (SD)
- Operando experiments with own gas mixing system in user operation. - *ongoing (section 2.5.1)*
- Multimodal spectroscopy, adding secondary IR and Raman, XEOL, UV-vis spectroscopy
- In-situ/operando site selective spectroscopy (XES, DAFS, XEOL)

(DO= design office, WS = workshop, SW = software, El = electronics, SD = scientific data, PLC = Automation, BO= beamline office)

7.3 Major development possibilities

Long-term planning (> 4 years)
Considerable costs:

- Fully developed SCANIA-2D by adding second branchline
- Improve Wiggler magnetic structure (smooth energy spectrum) - new Wiggler
- New generation fluorescence detectors

Requires resource time:

- Anchoring science hubs at Balder
- Increased user support pre-, during, post-beamtime for less experienced user groups
- Increased automation (of today manual tasks)
- New developments determined together with the user community.

7.4 Prioritization of the development projects

The number one prioritized ongoing project is the DAQ, hardware orchestrated scanning to deliver sub-sec EXAFS, fly-scanning with weighted acquisition to minimize deadtime of measurements benefitting all users, section 2.1.2.

Number two and the primary focus of 2024 is to deliver the missing capability of Sulphur K-edge to users.

Number three, during the next two years (2024-25) bring SCANIA-2D XES spectrometer to full use for natural low concentration samples which involves decreasing absorption and background scattering.

Number four, with increasing demand for combined XAS-XRD capability from the user community, realizing the new XRD detector positioning system described in section 2.2.5 is aimed for user operation end 2025.

8 Charge questions

MAX IV asks the review committee to evaluate the material presented in the written report and the oral presentations and discussions and address the following charge questions:

1) Technical realization of the beamline:

   a. Does the beamline provide adequate capabilities, and does the beamline team address areas of necessary improvement?
   b. Does the beamline offer unique capabilities to the user community?
   c. How does the beamline compare to leading beamlines in its field worldwide?
2) User communities, science program, and impact:
   a. Is the beamline attracting and supporting the relevant user communities?
   b. Is there sufficient focus between the different activities?
   c. Do the capabilities meet the needs of the relevant scientific communities (as laid out in the original science case)?
   d. Are the staff research and development projects of appropriate quality and in line with the current and future direction of the science program at the beamline?
   e. Are user and in-house science programs productive and making a sufficient impact in their science fields?
   f. Is the beamline missing opportunities regarding user communities, science programs, or research directions?
   g. Does the beamline / MAX IV employ an adequate outreach and training program?
3) Beamline operation:
   a. Is the user support at the beamline of high quality and allowing for a productive user program with high impact?
   b. Is the beamline or the facility missing out on opportunities for further improving user productivity?
   c. Are sufficient support labs and related facilities available to enable high-quality research at the beamline?
   d. Is the facility setting the right priorities in providing high-quality supporting infrastructure, services, and procedures?
4) Future directions:
   a. Does the beamline have a well-laid-out and actionable development plan?
   b. With the user community and national and international developments in mind, are the right priorities set out for these developments?
   c. Is the beamline / MAX IV having an adequate funding strategy and making use of funding opportunities?
   d. Are there additional opportunities (funding, development, science directions) that the beamline or the facility should take into account?
   e. Are the (envisioned) operation and science programs at the beamline well-adjusted?